UNIVERSITY OF CALIFORNIA SAN DIEGO

Overcoming Epigenetic-mediated Immune Evasion in Pancreatic Cancer

A Dissertation submitted in partial satisfaction of the requirements
for the degree Doctor of Philosophy

in

Biology

by

Yuwenbin Li

Committee in charge:

Professor Ronald M. Evans, Chair
Professor Christopher K. Glass
Professor Stephen M. Hedrick
Professor Anthony R. Hunter
Professor Cornelis Murre

2024

The Dissertation of Yuwenbin Li is approved, and it is acceptable in quality and form for publication on microfilm and electronically.

University of California San Diego

2024

DEDICATION

To my beloved parents, Xiaomei Wang and Qiang Li, whose unwavering love, sacrifice, support and belief in my research potential have been my greatest sources of strength.

To my collaborator, mentor, and friend, Morgan Truitt, your constant encouragement and inspiring suggestions have been a guiding light throughout this academic endeavor.

To my esteemed advisor, Ronald Evans, I express my deepest gratitude for your wholehearted support and invaluable guidance, shaping the trajectory of my research journey.

I also extend heartfelt thanks to my other mentors, Michael Downes, Annette Atkins, and Ruth Yu, whose guidance and expertise have profoundly shaped my intellectual growth and perspective on research.

To the members of our lab's management team, Lita Ong and Christi Brondos, your organizational prowess has created an environment conducive to my scholarly excellence.

To my exceptional labmates, Ting Fu, Gaoyang Liang, Weiwei Fan, Sihao Liu, Nanhai He, Zong Wei, Hunter Wang, Ling-Wa Chong, Yang Dai and Hongru Yu, your enthusiasm, collaboration, and knowledge have not only contributed to the advancement of my projects but have also sustained my passion for science.

Lastly, to my dearest schoolmates and friends, Yingcong Li, Yue Sun, Shijia Liu, Jiayi Dong, Yang Chen, Zhaoren He, Xiangyu Ren, Jingtian Zhou, Hanqing Liu, Xiaochun Cai, and Zhaoning Wang, your companionship, laughter, and moral support have made this academic undertaking a joyful and fulfilling experience.

This work is a reflection of the collective contributions of those around me, and for that, I am profoundly grateful.

TABLE OF CONTENTS

LIST OF FIGURES

ACKNOWLEDGEMENTS

I would like to acknowledge Professor Ronald Evans, Professor Christopher Glass, Professor Anthony Hunter, Professor Cornelis Murre and Professor Stephen Hedrick for their support and guidance as my committee members.

Chapter 1, in full, is unpublished material. The dissertation author was the primary author of this chapter. This chapter was written under the guidance of Morgan Truitt, Michael Downes, Annette Atkins, Ruth Yu and Ronald Evans.

Chapter 2, in full, is currently being prepared for submission for publication of the material. Work in this chapter was done in collaboration with Morgan Truitt, who helped with experiments, and Tae Gyu Oh, who helped with bioinformatic analysis of scRNA-seq data. Senada Bashi, Hanna Dhiyebi, Mariel Burquez and Yang Dai provided technical support. The dissertation author was the primary researcher and author of this material. This chapter was written under the guidance of Morgan Truitt, Michael Downes, Annette Atkins, Ruth Yu and Ronald Evans.

Chapter 3, in full, is currently being prepared for submission for publication of the material. Work in this chapter was done in collaboration with Morgan Truitt, who helped with experiments, and Hung VanThanh Nguyen, who helped with BPD-OTX production. Senada Bashi, Hanna Dhiyebi and Mariel Burquez provided technical support. The dissertation author was the primary researcher and author of this material. This chapter was written under the guidance of Morgan Truitt, Michael Downes, Annette Atkins, Ruth Yu and Ronald Evans.

Chapter 4, in full, is currently being prepared for submission for publication of the material. Work in this chapter was done in collaboration with Morgan Truitt, who helped with experimental design and data analysis. Hanna Dhiyebi, Mariel Burquez, Daniel Cao and

Christopher Liddle provided technical support. The dissertation author was the primary researcher and author of this material. This chapter was written under the guidance of Morgan Truitt, Michael Downes, Annette Atkins, Ruth Yu and Ronald Evans.

VITA

2016 Bachelor of Science in Biology Base Class, Wuhan University

2024 Doctor of Philosophy in Biology, University of California San Diego

PUBLICATIONS

Y. Li, M. L. Truitt, M. Burquez, D. Cao, H. Dhiyebi, C. Liddle, R. T. Yu, A. R. Atkins, T. Hunter, M. Downes and R. M. Evans, "TIF-induced immune evasion of pancreatic cancer driven by tumor-intrinsic LIF signaling", currently in preparation.

M. L. Truitt, **Y. Li**, T. Oh, H. V. Nguyen, S. Bashi, H. Dhiyebi, M. Burquez, Y. Dai, R. T. Yu, A. R. Atkins, J. A. Johnson, M. Downes and R. M. Evans, "BET inhibitors reshape immunosuppressive microenvironment and sensitize pancreatic cancer to immunotherapy", currently in preparation.

Dong, X., M. Qi, C. Cai, Y. Zhu, **Y. Li**, S. Coulter, F. Sun, C. Liddle, N. V. Uboha, R. Halberg, W. Xu, P. Marker and T. Fu (2024). "Farnesoid X receptor mediates macrophage-intrinsic responses to suppress colitis-induced colon cancer progression." JCI Insight 9(2).

Liang, G., T. G. Oh, N. Hah, H. Tiriac, Y. Shi, M. L. Truitt, C. E. Antal, A. R. Atkins, **Y. Li**, C. Fraser, S. Ng, A. F. M. Pinto, D. C. Nelson, G. Estepa, S. Bashi, E. Banayo, Y. Dai, C. Liddle, R. T. Yu, T. Hunter, D. D. Engle, H. Han, D. D. Von Hoff, M. Downes and R. M. Evans (2023). "Inhibiting stromal Class I HDACs curbs pancreatic cancer progression." Nat Commun 14(1): 7791.

Fu, T., **Y. Li**, T. G. Oh, F. Cayabyab, N. He, Q. Tang, S. Coulter, M. Truitt, P. Medina, M. He, R. T. Yu, A. Atkins, Y. Zheng, C. Liddle, M. Downes and R. M. Evans (2022). "FXR mediates ILC-intrinsic responses to intestinal inflammation." Proc Natl Acad Sci U S A 119(51): e2213041119.

Wang, W., **Y. Li,** Y. Wang, C. Shi, C. Li, Q. Li and R. J. Linhardt (2018). "Bacteriophage T7 transcription system: an enabling tool in synthetic biology." Biotechnol Adv 36(8): 2129-2137.

Wang, Y., L. Cao, C. Y. Lee, T. Matsuo, K. Wu, G. Asher, L. Tang, T. Saitoh, J. Russell, D. Klewe-Nebenius, L. Wang, S. Soya, E. Hasegawa, Y. Cherasse, J. Zhou, **Y. Li**, T. Wang, X. Zhan, C. Miyoshi, Y. Irukayama, J. Cao, J. P. Meeks, L. Gautron, Z. Wang, K. Sakurai, H. Funato, T. Sakurai, M. Yanagisawa, H. Nagase, R. Kobayakawa, K. Kobayakawa, B. Beutler and Q. Liu (2018). "Large-scale forward genetics screening identifies Trpa1 as a chemosensor for predator odor-evoked innate fear behaviors." Nat Commun 9(1): 2041.

ABSTRACT OF THE DISSERTATION

Overcoming Epigenetic-mediated Immune Evasion in Pancreatic Cancer

by

Yuwenbin Li

Doctor of Philosophy in Biology

University of California San Diego, 2024

Professor Ronald M. Evans, Chair

Pancreatic ductal adenocarcinoma (PDAC) presents a formidable challenge as a highly lethal malignancy, anticipated to rise to the rank of second-leading cause of cancer-related mortality by 2030. Despite this alarming trend, effective treatment options for PDAC remain elusive. Surgical resection, the primary curative intervention for PDAC, is only feasible in ~20%

of patients and has a high recurrence rate. Traditional cancer therapies, such as chemotherapy and radiation therapy, have demonstrated limited efficacy against PDAC.

In recent years, immunotherapies have shown promise in various cancer types. However, their effectiveness as standalone treatments for PDAC has been hindered by the desmoplastic stromal response characteristic of PDAC tumors. This stromal reaction involves a complex interplay between tumor cells and various stromal cell types, creating an immunosuppressive tumor microenvironment (iTME) that excludes cytotoxic T cells and inhibits anti-tumor immune responses. The complexity of the stromal compartment in PDAC remains inadequately understood, encompassing questions regarding its diverse composition, intricate interplay between stromal compartments, functional implications in fostering immunotherapy resistance, and the underlying mechanistic regulation within PDAC. Thus, a comprehensive dissection of stromal composition, function, and regulation is imperative.

To address the questions raised above, this study aimed to elucidate the role of epigenetic regulation in shaping the iTME of PDAC. Using single-cell sequencing techniques, we identified distinct populations of tumor-associated macrophages (TAMs), myeloid-derived suppressor cells (MDSCs), and cancer-associated fibroblasts (CAFs) with immunosuppressive potential and demonstrated that their immunosuppressive functions were disrupted by pharmacological BET inhibitors (BETi), which preferentially block super enhancer driven gene expression. Moreover, by disrupting the immunosuppressive TME, we found that BETi could enhance the efficacy of immune checkpoint blockade, promoting anti-tumor T cell responses mediated by the IFNγ-CXCL9/10 axis. This discovery laid the groundwork for our development of a novel therapeutic strategy utilizing nanoparticle-conjugated BETi to improve tumor drug delivery and reduce systemic toxicity.

Furthermore, our investigations into the immunosuppressive mechanisms of the TME unveiled the ability of stromal signals to reprogram tumor cells and promote their resistance to T cell-mediated cytotoxicity. By developing an antigen-specific tumor killing platform, we demonstrated that soluble factors present in tumor interstitial fluid (TIF) could induce a transcriptional profile associated with immune evasion in tumor cells. This transcriptional program is regulated, in part, by stroma-induced NFκB activation. *In vivo* studies targeting NFκB-regulated immunosuppressive genes, including COX2 and LIF, suggest that disrupting this pathway could be a promising avenue for enhancing immunotherapy responses in PDAC driven by antigen-specific T cell killing, such as CAR-T cell therapy.

In summary, this study not only facilitates a deeper comprehension of the underlying causes of current therapeutic shortcomings in PDAC, but also paves the way for the development of innovative strategies aimed at targeting immune resistance mechanisms and sensitizing PDAC to immunotherapies.

Chapter 1 Decoding Pancreatic Cancer: Challenges, Complexity, and Therapeutic Perspectives

1.1 Pancreatic cancer general facts and statistics

Pancreatic cancer, sometimes referred to as the “king of carcinomas”, stands out as a particularly aggressive and formidable type of malignancy originating in the pancreatic tissue. Data from the American Cancer Society reveal that in 2023, pancreatic cancer accounts for 8.3% of all cancer-related deaths in the United States, despite comprising only 3.3% of all cancer diagnoses. Forecasts suggest that by 2030, pancreatic cancer is poised to overtake colorectal cancer as the second leading cause of cancer-related deaths in the country, with a five-year survival rate of only 12%. This alarming discrepancy between its relatively low incidence and high mortality rate not only highlights the current gaps in our understanding of pancreatic cancer pathogenesis, but also emphasizes the urgency for innovative approaches to better combat this lethal disease.

Despite decades of research in the field of pancreatic cancer, significant challenges remain that hinder progress in combating this deadly disease. One major obstacle is its tendency to be diagnosed at an advanced stage, as it often remains asymptomatic early on or presents with nonspecific symptoms that can easily be mistaken for less severe conditions such as biliary stricture, irritable bowel syndrome, or pancreatitis. This is exacerbated by pancreatic cancer’s aggressive nature. Unlike more indolent forms of cancer, such as skin or testicular cancer, pancreatic cancer rapidly grows and invades nearby organs and tissues, often leading to local invasion and early metastasis. Consequently, many patients are diagnosed only after the cancer has metastasized to the liver, peritoneum, diaphragm, lungs, and lymph nodes, making them ineligible for a potentially curative surgical resection. Ultimately, fewer than 20% of patients are candidates for surgical resection.

Importantly, pancreatic cancer's aggressiveness not only complicates early detection but also makes recurrence common among patients who undergo surgical resection. These patients are instead dependent on therapeutic interventions. Unfortunately, pancreatic cancer is remarkably resistant to most standard therapies. Indeed, advanced cases are typically unresponsive to a wide array of chemotherapies, radiation therapies, targeted therapies, and immunotherapies. While these treatments may occasionally slow tumor progression, they rarely achieve a cure, underscoring the urgent need for innovative therapeutic strategies in the battle against pancreatic cancer.

1.2 Pancreatic cancer classification

In addition to the challenges posed by pancreatic cancer's poor prognosis, aggressiveness, and therapy resistance, its complex classification further complicates efforts to understand and develop treatments for these multifaceted malignancies. Pancreatic cancer encompasses two primary types based on the tissue origin: exocrine pancreatic cancer, which arises from exocrine cells comprising the pancreas's acinar and ductal components and represents approximately 95% of pancreatic cancer cases, and neuroendocrine pancreatic cancer, which accounts for the remaining 5% and originates from the pancreas's endocrine gland responsible for hormone production and blood sugar regulation. Within exocrine pancreatic cancer, pancreatic ductal adenocarcinoma (PDAC) is the most prevalent form, constituting around 90% of all cases. Initially believed to originate solely from ductal cells, recent discoveries of acinar-to-ductal transformation (ADM) during PDAC formation suggest acinar cells as another significant source (Storz 2017). Other rare types of exocrine pancreatic cancer include acinar cell carcinoma (~1-2%), squamous cell carcinoma (<1%), adenosquamous carcinoma (~1-4%), and colloid carcinoma (~1-3%). Given PDAC's prevalence and aggressiveness compared to other types, it is the primary focus of research

for developing pancreatic cancer therapy strategies and will be prominently discussed throughout this thesis.

A deeper exploration of the genetic, molecular, and cellular features of PDAC allows for further classification into basal or classical subtypes (Moffitt, Marayati et al. 2015), each exhibiting distinct characteristics that profoundly influence the disease's behavior and response to treatment. The basal subtype of PDAC, characterized by a high frequency of TP53 and KDM6A mutations, is associated with: 1. a higher proportion of grade 3 lesions, 2. aggressive phenotypes marked by rapid proliferation, dysregulated cell cycle control, and defective DNA repair mechanisms, 3. increased resistance to drug therapies, 4. a more pronounced desmoplastic stromal response, and 5. a correlation with poor patient prognosis. In contrast, the classical subtype of PDAC, identified by the expression of pancreatic progenitor markers and regulated by GATA6, exhibits: 1. a higher prevalence of grade 1 and 2 lesions, 2. more stable and controlled phenotypes, 3. heightened sensitivity to drug therapies, 4. a more regulated stromal response, and 5. a correlation with improved patient survival (Moffitt, Marayati et al. 2015) (Chan-Seng-Yue, Kim et al. 2020) (O'Kane, Grunwald et al. 2020).

During that period, several studies employed distinct classification strategies to further categorize PDAC into more detailed subtypes (Collisson, Sadanandam et al. 2011) (Bailey, Chang et al. 2016). However, the overarching division of PDAC into basal-like versus classical subtypes has gained widespread recognition and reference. More recently, comprehensive multi-platform analyses integrating genomic, transcriptomic, and proteomic profiling have reaffirmed the existence of basal and classical features within PDAC. Taking into account microenvironment gene expression characteristics, this binary classification has evolved into five distinct subgroups: 1. pure basal-like, 2. stroma activated, 3. desmoplastic, 4. pure classical, and 5. immune classical

(Puleo, Nicolle et al. 2018). Notably, recent advancements in PDAC subtype research have revealed that while bulk RNA-seq analysis is adequate for dichotomously classifying PDAC into basal and classical subtypes, single-cell RNA sequencing analysis has unveiled the presence of both classical and basal cancer populations within the same tumor (Lee, Bernard et al. 2021). Moreover, populations containing both classical and basal features have been simultaneously identified in certain PDAC tumors (Raghavan, Winter et al. 2021). This intra-tumoral subtype heterogeneity, alongside inter-tumoral subtype heterogeneity, may account for the varied responses to therapy observed among individuals with PDAC and could contribute to resistance to therapeutic strategies targeting specific subtypes of the disease.

1.3 Genetic mutations in PDAC

PDAC presents a diverse array of subtypes throughout its development, yet a consensus emerges in the form of genetic mutations and alterations prevalent within the majority of PDAC tumor cells. These mutations and alterations confer upon tumor cells the capability to evade intrinsic constraints such as cell cycle regulation, DNA repair mechanisms, chromatin stability maintenance, and apoptosis induction. Additionally, they grant tumor cells independence from extrinsic constraints such as regulation by cytokines and growth factors, nutrient scarcity, and immune surveillance. The selection and enrichment of these genetic changes occur not only across different stages of PDAC tumor development but also within unique tumor microenvironments (TMEs) that vary from one individual to another. Consequently, comprehending the commonalities and heterogeneities of genetic mutations and alterations in PDAC tumors is imperative for elucidating tumor evolution and devising targeted therapies for PDAC treatment.

Advanced exome and copy number variation analyses have provided insights into the mutational landscape of PDAC tumors (Jones, Zhang et al. 2008) (Biankin, Waddell et al. 2012) (Waddell, Pajic et al. 2015). Key recurrently mutated or altered genes in PDAC include the oncogene KRAS (activated in ~95% of PDAC cases), the tumor suppressor TP53 (inactivated in ~74% of PDAC cases), the tumor suppressor CDKN2A (also known as P16, inactivated in ~35% of PDAC cases) and the tumor suppressor SMAD4 (inactivated in ~31% of PDAC cases) (Waddell, Pajic et al. 2015). Aberrant KRAS activation stands out as the most pervasive mutation in PDAC, leading to sustained activation of cellular pathways such as RAF/MEK/ERK and PI3K/AKT/MTOR. These pathways drive uncontrolled cell division and facilitate tumor progression. Conversely, loss of TP53, a crucial tumor suppressor gene involved in regulating cell growth and DNA repair, enables cancer cells to evade growth control mechanisms and fosters their survival and evolution. CDKN2A, another tumor suppressor gene, plays a role in inhibiting cell division and maintaining orderly cell cycle progression. Meanwhile, SMAD4 is integral to the transforming growth factor-beta (TGF-β) signaling pathway; its absence disrupts normal cell growth and differentiation processes, contributing to cancer expansion.

It is important to recognize that the frequently mutated signature genes in PDAC do not arise simultaneously within cancer cells during tumor initiation, nor do they appear randomly as the tumor progresses. Instead, these gene mutations tend to emerge at various stages of tumor progression to facilitate the evolution of tumor cells from one stage to the next. According to the classical progression model for PDAC, KRAS activation serves as the initiating event during the formation of neoplastic lesions, followed by the loss of CDKN2A, which is more likely to occur during aberrant clone expansion stages. The loss of TP53 and SMAD4, however, typically occurs at later stages to promote the progression of pancreatic neoplasia to a higher dysplastic stage

(Hruban, Goggins et al. 2000). Interestingly, while KRAS activation is indispensable for the formation of most PDAC cases, not all of the aforementioned tumor suppressors are simultaneously required to drive tumor formation. Using genetic mouse models, independent studies have demonstrated that KRAS activation, combined with either CDKN2A (Aguirre, Bardeesy et al. 2003), TP53 (Hingorani, Wang et al. 2005) or SMAD4 (Bardeesy, Cheng et al. 2006) loss of function, is sufficient to induce PDAC formation.

In addition to the four gene mutations mentioned earlier, numerous other recurrently mutated genes accumulate among smaller clusters of PDAC patients. These genes participate in various cellular activities and responses, including chromatin modification (ARID1A, KMT2D/2C, KDM6A), DNA damage repair (BRACA1/2, PALB2), growth factor signaling (TGFBR2, FGFR1), and others (ROBO1/2, MUC16, RNF43, TTN, GNAS, BRAF, MYC, etc) (Waddell, Pajic et al. 2015) (Cancer Genome Atlas Research Network. Electronic address and Cancer Genome Atlas Research 2017). This diverse mutational signature appears to be a significant contributor to intertumoral heterogeneity and plays a role in therapy resistance.

1.4 Cell of origin impacts PDAC subtype

Despite the pancreas's relatively simple structural composition, the cell of origin in PDAC formation has long been a subject of controversy. As previously mentioned, PDAC primarily arises in the exocrine part of the pancreas. Structurally, this exocrine system comprises two major epithelial cell types: acinar cells, responsible for producing and secreting digestive enzymes, and ductal cells, which form branched tubes for draining these enzymes into the duodenum. Historically, it was believed that PDAC originates directly from pancreatic ductal cells, given that most observed PDAC tumor cells resembled ductal cells morphologically and expressed ductal

biomarkers. Consequently, this disease type was termed "ductal adenocarcinoma." However, accumulating evidence from mouse models of PDAC has identified both acinar cells and ductal cells as capable of giving rise to PDAC tumors.

Central to the theory that acinar cells can initiate PDAC is the observation that both tissue injury (induced by pancreatic ductal ligation or repeated caerulein administration in mouse models) (Strobel, Dor et al. 2007) (Pinho, Rooman et al. 2011) and KRAS activation (G12D mutation) (De La, Emerson et al. 2008) (Habbe, Shi et al. 2008) (Kopp, von Figura et al. 2012) can prompt the trans-differentiation of acinar cells into ductal cells, a process termed acinar-to-ductal transformation (ADM). During this process, these cells undergo metaplasia and express ductal cell-specific markers such as Sox9, Hnf1β, and Krt9 (Pinho, Rooman et al. 2011), which ultimately replace the normal acinar-forming tubular structures (Pinho, Rooman et al. 2011). Under specific genetic conditions, these cells have the potential to progress into Pancreatic Intraepithelial Neoplasia (PanIN), a major precursor lesion of PDAC (Chuvin, Vincent et al. 2017). Importantly, the acinar cell-specific (Ptf1a-driven) expression of $Kras^{G12D}$ alone or in combination with $Trp53^{null}$ (or loss-of-function mutation $Trp53^{R172H}$) can induce PDAC formation at different ages in mice, confirming acinar cells as one origin of PDAC (Flowers, Xu et al. 2021). However, recent literature suggests that certain progenitor-like subpopulations of acinar cells may be more susceptible to genetic mutations that trigger PDAC formation than other acinar cells (Gopalan, Singh et al. 2021) (Neuhofer, Roake et al. 2021), adding another layer of complexity to the cell origin of PDAC.

Meanwhile, numerous studies have confirmed that genetic mutations in ductal cells can lead to PDAC formation in ductal-cell-specific (Hnf1β, CK19, or Sox9 driven) mouse models (von Figura, Fukuda et al. 2014) (Bailey, Hendley et al. 2016) (Ferreira, Sancho et al. 2017) (Lee,

Dubois et al. 2019). However, unlike in acinar cells where KRAS activation alone is sufficient to drive cancer, mutant KRAS in ductal cells alone is inadequate to induce tumors. Instead, it must be combined with inactivation of tumor suppressor genes such as Trp53 or Fbw7. But even with these additional mutations, the tumor progression rate is slower compared to that in acinar cells (Flowers, Xu et al. 2021). In addition, ductal cells predominantly develop tumors through the formation of Intraductal Papillary Mucinous Neoplasm (IPMN), unlike the more frequently observed PanIN formation in tumors originating from acinar cells (von Figura, Fukuda et al. 2014) (Kopp, Dubois et al. 2018).

Central to understanding the cell origin of PDAC is the inquiry into whether different origins account for the classification of various PDAC subtypes and their distinct responses to treatments. Integrating cell-type-specific PDAC mouse models with gene expression signatures of different PDAC subtypes has revealed that tumors derived from acinar cells exhibit similarities to the classical subtype of PDAC (characterized by less aggressiveness and better prognosis) in human patients, whereas tumors originating from ductal cells resemble the basal subtype of PDAC (associated with greater aggressiveness and poorer prognosis) (Ferreira, Sancho et al. 2017) (Flowers, Xu et al. 2021). These findings underscore the utility of dissecting tumor subtypes using cell-specific genetic mouse models of PDAC, providing valuable insights for early detection, risk assessment, and the development of targeted therapies for different PDAC subtypes.

1.5 Current paradigms for PDAC treatment

Therapeutic options for PDAC remain significantly limited despite ongoing efforts. Surgical resection stands as the most effective and sole curative treatment. However, the lack of early symptoms and limited screening strategies result in up to 80% of PDAC patients presenting

with advanced or metastatic disease at initial diagnosis, precluding them from surgical resection (Li, Xie et al. 2004). Based on metastatic features and resectability, PDAC is clinically classified into four stages: resectable pancreatic cancer (RPC), borderline resectable pancreatic cancer (BRPC), unresectable/local advanced pancreatic cancer (ULAPC), and metastatic pancreatic cancer (MPC). The standard of care for RPC involves upfront surgical resection followed by six months of adjuvant chemotherapy, such as mFOLFIRINOX (modified fluorouracil, irinotecan, and oxaliplatin), gemcitabine+capecitabine (Gem/Cap), gemcitabine+nab-paclitaxel (Gem/nabP), or gemcitabine (Gem) alone (Jiang and Sohal 2023).

For BRPC and ULAPC, no established standard-of-care recommendations currently exist. Neoadjuvant treatments, including induction chemotherapy, preoperative chemoradiation, or stereotactic body radiation therapy, can be considered, followed by a re-evaluation of resectability (Jiang and Sohal 2023). In cases of MPC, first-line treatment typically involves FOLFIRINOX or Gem/nabP. Second-line treatment may involve testing for druggable genomic alterations to identify patients eligible for targeted therapy. For example, patients harboring NTRK fusions should receive tropomyosin kinase receptor inhibitors (larotrectinib or entrectinib), those with mismatch repair deficiency or microsatellite instability high should be treated with PD1 inhibitors (pembrolizumab), and patients with germline BRCA1 or BRCA2 mutations, sensitive to platinum-based chemotherapy, should be treated with continued chemotherapy or PARP inhibitors (olaparib). Patients not eligible for targeted therapy options may consider second-line chemotherapies such as Gem/nabP, fluorouracil+nanoliposomal irinotecan, or fluorouracil+oxaliplatin (Sohal, Kennedy et al. 2020). It is essential to note, however, that while these chemotherapy strategies may extend lifespan in some cases, they rarely result in a cure for patients with PDAC due to long-term toxicity issues and treatment resistance.

1.6 Stromal response in PDAC

In contrast to many other cancer types, PDAC exhibits notable resistance to various therapeutic approaches, including chemotherapy, radiation therapy, and immunotherapy. This inherent resistance is largely attributed to the unique TME of PDAC characterized by a desmoplastic stromal response (Iacobuzio-Donahue, Ryu et al. 2002). Remarkably, up to 80% of the PDAC tumor volume is occupied by a dense fibrotic stroma (Erkan, Michalski et al. 2008). Beyond its extracellular matrix (ECM) components, the PDAC stroma comprises diverse somatic cell types, including cancer-associated fibroblasts (CAFs), endothelial cells, pericytes, neurons, and infiltrating immune cells (Hosein, Brekken et al. 2020). These stromal cells get hijacked by signals emanating from tumor cells, leading them to physically interact with and support tumor cell growth, while also shielding them from the anti-tumorigenic effects of drugs, cytokines, growth factors, and metabolites.

As the most prevalent stromal cell type within PDAC, CAFs exhibit remarkable heterogeneity and diverse functionalities, largely attributed to their varied origins (Ohlund, Elyada et al. 2014). CAFs can arise from tissue-resident fibroblasts (Arina, Idel et al. 2016), pancreatic stellate cells (Neuzillet, Tijeras-Raballand et al. 2019), differentiated mesenchymal stem cells (Miyazaki, Oda et al. 2021), or trans-differentiated non-fibroblastic lineage such as epithelial cells (Rhim, Mirek et al. 2012), endothelial cells (Zeisberg, Potenta et al. 2007) and bone marrow-derived macrophages (Iwamoto, Ohuchida et al. 2021). Upon activation by signaling pathways including TGFβ, Sonic hedgehog (SHH), TNFα, IL-1, IL-6, or IL-10 (von Ahrens, Bhagat et al. 2017), CAFs contribute to ECM deposition by producing collagen, hyaluronan (HA), and proteoglycans (Vaish, Jain et al. 2021), providing structural support and shielding tumor cells.

Additionally, CAFs secrete various growth factors (PDGF, CTGF, and EGF), cytokines (IL-6, LIF, and IL-11), and chemokines (CXCL1, CXCL5, CXCL7, CXCL8, CXCL12, and CCL12) to promote tumor cell proliferation, angiogenesis, and the recruitment of pro-tumorigenic immune cells into the stroma (Zhang, Ren et al. 2022). Furthermore, CAFs have been implicated in fostering reciprocal signaling cascades, amplifying autonomous KRAS signaling in tumor cells (Tape, Ling et al. 2016).

Interestingly, CAFs exhibit paradoxical roles, as their depletion or disruption of activating signaling leads to a more aggressive PDAC phenotype (Ozdemir, Pentcheva-Hoang et al. 2014) (Rhim, Oberstein et al. 2014). This complexity is further underscored by the discovery of distinct CAF subpopulations, including inflammatory CAFs (iCAFs), myofibroblastic CAFs (myCAFs), and antigen-presenting CAFs (apCAFs), each exerting differential impacts on PDAC tumorigenesis (Ohlund, Handly-Santana et al. 2017) (Elyada, Bolisetty et al. 2019). myCAFs, characterized by αSMA expression and close proximity to tumor cells, primarily restrain tumor growth, thus exhibiting an anti-tumorigenic role. Conversely, iCAFs promote tumorigenesis through the expression of IL-6 and CXCL12, often located distantly from tumor cells (Ohlund, Handly-Santana et al. 2017). In line with these findings, an increased myCAF-to-iCAF ratio in PDAC tumors correlates with a better prognosis (Biffi, Oni et al. 2019). Additionally, apCAFs, identified by their expression of MHC class II genes, were initially believed to be anti-tumorigenic by facilitating antigen presentation-mediated effector T cell activation (Elyada, Bolisetty et al. 2019). However, recent studies have revealed a nuanced role for apCAFs, as they can induce the differentiation of naïve CD4 T cells into regulatory T cells (Tregs) in an antigen-specific manner (Huang, Wang et al. 2022). The heterogeneity and complex functions of CAFs in PDAC development underscore the necessity for a deeper understanding of this stromal cell subtype to

selectively target pro-tumorigenic aspects, thereby facilitating more effective PDAC therapy development.

Myeloid cell populations, particularly tumor-associated macrophages (TAMs) and myeloid-derived suppressor cells (MDSCs), constitute the predominant immune cell cohort within the PDAC stroma. Notably, depletion of myeloid cells retards PDAC tumor progression and triggers T-cell mediated anti-tumor responses (Zhang, Velez-Delgado et al. 2017), underscoring their pivotal pro-tumorigenic roles. TAMs are recruited by tumor cell-produced GM-CSF (Bayne, Beatty et al. 2012), and can accrue within the tumor during its early developmental stages (Liu, Li et al. 2016). Functionally, they impede anti-tumor immune responses by secreting immunosuppressive cytokines such as IL-6, IL-10, and TGF-β, while also upregulating inhibitory factors like PD-L1 and Arg1 (Yang, Liu et al. 2020). Moreover, TAMs bolster tumor progression and metastasis through the secretion of factors like TNF-α, CCL5, CCL18, and CCL20 (Ye, Zhou et al. 2018) (Liu, Jia et al. 2016) (Liou, Doppler et al. 2013).

Macrophages exhibit phenotypic and functional diversity through a process termed macrophage polarization. While traditionally believed to polarize into either a pro-inflammatory state (M1) driven by IFN-γ/LPS or an anti-inflammatory state (M2) driven by IL-4/IL-10/TLR agonists (Abdelaziz, Abdelwahab et al. 2020) (Martinez, Sica et al. 2008), TAMs within PDAC tumors often display a hybrid of M1-like and M2-like characteristics, defying straightforward categorization (Poh and Ernst 2021). Alternatively, TAMs can be classified into two major subsets based on their distinct origins: tissue-resident macrophages and circulating monocytes (Zhu, Herndon et al. 2017). Although recent studies have identified multiple TAM clusters using single-cell RNA sequencing (scRNA-seq) techniques in PDAC tumors (Werba, Weissinger et al. 2023) (Oh, Yoo et al. 2023) (Chen, Wang et al. 2021), the full scope of their functions and contributions

to PDAC tumor progression and therapy resistance remains incompletely elucidated. Importantly, the spatial distribution of different TAM subsets within tumors has been shown to correlate with survival prognosis in PDAC patients (Vayrynen, Zhang et al. 2021), highlighting the significance of unraveling TAM subset behaviors and their interactions with tumor cells and other stromal cell types in PDAC.

On the contrary, MDSCs in PDAC can be categorized into two primary subtypes: polymorphonuclear/granulocytic MDSCs (gMDSCs) and mononuclear MDSCs (mMDSCs) (Bronte, Brandau et al. 2016). Depletion of Ly6G+ gMDSCs has been shown to enhance anti-tumor T cell responses in mouse models of PDAC (Stromnes, Brockenbrough et al. 2014), while mMDSCs exhibit a STAT3-mediated immunosuppressive function (Trovato, Fiore et al. 2019). Although both MDSC subtypes can suppress T cell functions via the overexpression of Arg1 (Raber, Ochoa et al. 2012), their mechanisms of immunosuppression may differ at other levels (Youn, Nagaraj et al. 2008), highlighting the need for further investigation into this population in PDAC.

In summary, within the PDAC TME, stromal cells such as CAFs, TAMs and MDSCs are abnormally recruited and activated in response to tumor intrinsic signaling. Working in concert, they establish an immunosuppressive milieu that results in the exclusion of immune cell types capable of combating cancer cells, including cytotoxic T cells, natural killer cells, and dendritic cells. A comprehensive exploration of stromal cell heterogeneity in terms of both subtypes and functions is imperative for the development of therapeutic strategies aimed at remodeling the pro-tumorigenic TME and sensitizing PDAC to currently tolerated therapies.

1.7 Therapeutic resistance of PDAC

The unique and complex TME characterized by desmoplastic stromal responses described above, in combination with tumor cell intrinsic genetic and epigenetic adaptations, accounts for PDAC's resistance to multiple single-agent therapies, including chemotherapy, immunotherapy, and targeted therapy—approaches that have shown efficacy in the treatment of many other cancer types.

In the case of chemotherapy, agents like gemcitabine, when administered, are hampered by hypovascularization and high intra-tumoral pressure in PDAC stroma. This environment physically hinders drug access to tumor cells (Jacobetz, Chan et al. 2013). Furthermore, the stroma secretes various factors that induce intrinsic resistance in tumor cells, including the downregulation of drug transporters (Nordh, Ansari et al. 2014), upregulation of drug efflux pumps (Zinzi, Contino et al. 2014), and alterations in enzyme production that interfere with the drug's mechanism of action (Patzak, Kari et al. 2019) (Zhou, Oliveira et al. 2010) (Costantino, Witkiewicz et al. 2009). Additionally, PDAC stroma promotes tumor cell proliferation and inhibits apoptosis, counteracting the efficacy of cytotoxic drugs (Principe, Underwood et al. 2021) (Swayden, Iovanna et al. 2018).

The failure of immunotherapy, on the other hand, stems from the multi-level blockade of anti-tumor T cell responses imposed by the immunosuppressive PDAC stroma. This includes interference with T cell priming, prevention of T cell recruitment, escape from T cell recognition, and induction of T cell exhaustion, challenges not fully addressed by single immunotherapy agents (Schmiechen and Stromnes 2020). For instance, immune checkpoint inhibitors such as αPDL1 can overcome PD1 checkpoint-mediated T cell inactivation and exhaustion (Bian and Almhanna 2021) but cannot prevent immunosuppression imposed by stromal cells through mechanisms such as

macrophage-produced Arginase 1 (Menjivar, Nwosu et al. 2023), fibroblast-produced CXCL12 (Ene-Obong, Clear et al. 2013), and regulatory T cell (Treg)-presented CTLA-4 (Bengsch, Knoblock et al. 2017). Furthermore, issues like autophagy-induced downregulation of MHCI in tumor cells (Yamamoto, Venida et al. 2020), inactivated antigen presentation by stromal cells (Beatty, Chiorean et al. 2011) and engagement of other checkpoint-mediated inhibitory pathways in T cells (through Tim3, Lag3, and TIGIT) cannot be overcome with αPDL1 treatment alone. Alternatively, chimeric antigen receptor (CAR)-T cell therapy circumvents the naïve T cell priming process and enhances tumor cell targeting efficiency. However, this therapeutic approach encounters hurdles such as limited trafficking and infiltration into PDAC tumors, immunosuppressive signals emanating from stromal compartments, and tumor heterogeneity leading to the emergence of target-negative cells (Sterner and Sterner 2021).

Targeted therapies primarily interfere with dysregulated signaling pathways and components in tumors, including intrinsic targets in tumor cells, as well as pathways and factors present in stromal cells and the stromal matrix. Unfortunately, many of the previously developed targeted therapies, such as EGFR signaling inhibitors (Haas, Waldschmidt et al. 2021) (Philip, Benedetti et al. 2010), VEGF signaling inhibitors (Rougier, Riess et al. 2013), IGF signaling inhibitors (Kundranda, Gracian et al. 2020), MEK inhibitors (Bodoky, Timcheva et al. 2012), Hedgehog signaling (Catenacci, Junttila et al. 2015) and hyaluronan digestive enzymes (Van Cutsem, Tempero et al. 2020), have failed in PDAC clinical trials. Their failures can be attributed to multiple different reasons, such as inefficient drug delivery, imbalances of toxicity versus efficacy, or an unselected patient pool for specific molecular alterations. Despite ongoing development of novel targeted therapy drugs, they all face similar obstacles with PDAC at multiple different layers.

Conclusion and Perspectives

Despite its relatively low incidence rate among all cancer types, PDAC remains a highly lethal disease with limited treatment options. The diversity of PDAC subtypes, driven by differences in cell-of-origin and combinations of oncogenic and tumor suppressor genetic alterations, presents a formidable challenge in developing effective pan-PDAC therapeutic strategies. While personalized therapies hold promise for the future, understanding the underlying causes of therapy resistance is paramount. Recent insights suggest that the desmoplastic stromal response orchestrated by tumor cell intrinsic signaling not only fosters tumor progression but also establishes a protective and immunosuppressive TME, enabling resistance to various therapies. Successful treatment of PDAC necessitates a comprehensive understanding of the roles played by both stromal cells and cancer cells within the tumor and their intricate interplay. It is imperative to explore strategies that target the pro-tumorigenic functions of various intra-tumoral populations from diverse perspectives. Breakthroughs in treatment design may involve targeting multiple factors with a single agent or combining agents that target different factors synergistically. In the forthcoming chapters, we will delve deeper into efforts aimed at deciphering therapy resistance mechanisms and developing combination strategies to overcome them in PDAC.

Acknowledgements

Chapter 1, in full, is unpublished material. The dissertation author was the primary author of this chapter. This chapter was written under the guidance of Morgan Truitt, Michael Downes, Annette Atkins, Ruth Yu and Ronald Evans.

References

Abdelaziz, M. H., S. F. Abdelwahab, J. Wan, W. Cai, W. Huixuan, C. Jianjun, K. D. Kumar, A. Vasudevan, A. Sadek, Z. Su, S. Wang and H. Xu (2020). "Alternatively activated macrophages; a double-edged sword in allergic asthma." J Transl Med 18(1): 58.

Aguirre, A. J., N. Bardeesy, M. Sinha, L. Lopez, D. A. Tuveson, J. Horner, M. S. Redston and R. A. DePinho (2003). "Activated Kras and Ink4a/Arf deficiency cooperate to produce metastatic pancreatic ductal adenocarcinoma." Genes Dev 17(24): 3112-3126.

Arina, A., C. Idel, E. M. Hyjek, M. L. Alegre, Y. Wang, V. P. Bindokas, R. R. Weichselbaum and H. Schreiber (2016). "Tumor-associated fibroblasts predominantly come from local and not circulating precursors." Proc Natl Acad Sci U S A 113(27): 7551-7556.

Bailey, J. M., A. M. Hendley, K. J. Lafaro, M. A. Pruski, N. C. Jones, J. Alsina, M. Younes, A. Maitra, F. McAllister, C. A. Iacobuzio-Donahue and S. D. Leach (2016). "p53 mutations cooperate with oncogenic Kras to promote adenocarcinoma from pancreatic ductal cells." Oncogene 35(32): 4282-4288.

Bailey, P., D. K. Chang, K. Nones, A. L. Johns, A. M. Patch, M. C. Gingras, D. K. Miller, A. N. Christ, T. J. Bruxner, M. C. Quinn, C. Nourse, L. C. Murtaugh, I. Harliwong, S. Idrisoglu, S. Manning, E. Nourbakhsh, S. Wani, L. Fink, O. Holmes, V. Chin, M. J. Anderson, S. Kazakoff, C. Leonard, F. Newell, N. Waddell, S. Wood, Q. Xu, P. J. Wilson, N. Cloonan, K. S. Kassahn, D. Taylor, K. Quek, A. Robertson, L. Pantano, L. Mincarelli, L. N. Sanchez, L. Evers, J. Wu, M. Pinese, M. J. Cowley, M. D. Jones, E. K. Colvin, A. M. Nagrial, E. S. Humphrey, L. A. Chantrill, A. Mawson, J. Humphris, A. Chou, M. Pajic, C. J. Scarlett, A. V. Pinho, M. Giry-Laterriere, I. Rooman, J. S. Samra, J. G. Kench, J. A. Lovell, N. D. Merrett, C. W. Toon, K. Epari, N. Q. Nguyen, A. Barbour, N. Zeps, K. Moran-Jones, N. B. Jamieson, J. S. Graham, F. Duthie, K. Oien, J. Hair, R. Grutzmann, A. Maitra, C. A. Iacobuzio-Donahue, C. L. Wolfgang, R. A. Morgan, R. T. Lawlor, V. Corbo, C. Bassi, B. Rusev, P. Capelli, R. Salvia, G. Tortora, D. Mukhopadhyay, G. M. Petersen, I. Australian Pancreatic Cancer Genome, D. M. Munzy, W. E. Fisher, S. A. Karim, J. R. Eshleman, R. H. Hruban, C. Pilarsky, J. P. Morton, O. J. Sansom, A. Scarpa, E. A. Musgrove, U. M. Bailey, O. Hofmann, R. L. Sutherland, D. A. Wheeler, A. J. Gill, R. A. Gibbs, J. V. Pearson, N. Waddell, A. V. Biankin and S. M. Grimmond (2016). "Genomic analyses identify molecular subtypes of pancreatic cancer." Nature 531(7592): 47-52.

Bardeesy, N., K. H. Cheng, J. H. Berger, G. C. Chu, J. Pahler, P. Olson, A. F. Hezel, J. Horner, G. Y. Lauwers, D. Hanahan and R. A. DePinho (2006). "Smad4 is dispensable for normal pancreas development yet critical in progression and tumor biology of pancreas cancer." Genes Dev 20(22): 3130-3146.

Bayne, L. J., G. L. Beatty, N. Jhala, C. E. Clark, A. D. Rhim, B. Z. Stanger and R. H. Vonderheide (2012). "Tumor-derived granulocyte-macrophage colony-stimulating factor regulates myeloid inflammation and T cell immunity in pancreatic cancer." Cancer Cell 21(6): 822-835.

Beatty, G. L., E. G. Chiorean, M. P. Fishman, B. Saboury, U. R. Teitelbaum, W. Sun, R. D. Huhn, W. Song, D. Li, L. L. Sharp, D. A. Torigian, P. J. O'Dwyer and R. H. Vonderheide (2011). "CD40 agonists alter tumor stroma and show efficacy against pancreatic carcinoma in mice and humans." Science 331(6024): 1612-1616.

Bengsch, F., D. M. Knoblock, A. Liu, F. McAllister and G. L. Beatty (2017). "CTLA-4/CD80 pathway regulates T cell infiltration into pancreatic cancer." Cancer Immunol Immunother 66(12): 1609-1617.

Bian, J. and K. Almhanna (2021). "Pancreatic cancer and immune checkpoint inhibitors-still a long way to go." Transl Gastroenterol Hepatol 6: 6.

Biankin, A. V., N. Waddell, K. S. Kassahn, M. C. Gingras, L. B. Muthuswamy, A. L. Johns, D. K. Miller, P. J. Wilson, A. M. Patch, J. Wu, D. K. Chang, M. J. Cowley, B. B. Gardiner, S. Song, I. Harliwong, S. Idrisoglu, C. Nourse, E. Nourbakhsh, S. Manning, S. Wani, M. Gongora, M. Pajic, C. J. Scarlett, A. J. Gill, A. V. Pinho, I. Rooman, M. Anderson, O. Holmes, C. Leonard, D. Taylor, S. Wood, Q. Xu, K. Nones, J. L. Fink, A. Christ, T. Bruxner, N. Cloonan, G. Kolle, F. Newell, M. Pinese, R. S. Mead, J. L. Humphris, W. Kaplan, M. D. Jones, E. K. Colvin, A. M. Nagrial, E. S. Humphrey, A. Chou, V. T. Chin, L. A. Chantrill, A. Mawson, J. S. Samra, J. G. Kench, J. A. Lovell, R. J. Daly, N. D. Merrett, C. Toon, K. Epari, N. Q. Nguyen, A. Barbour, N. Zeps, I. Australian Pancreatic Cancer Genome, N. Kakkar, F. Zhao, Y. Q. Wu, M. Wang, D. M. Muzny, W. E. Fisher, F. C. Brunicardi, S. E. Hodges, J. G. Reid, J. Drummond, K. Chang, Y. Han, L. R. Lewis, H. Dinh, C. J. Buhay, T. Beck, L. Timms, M. Sam, K. Begley, A. Brown, D. Pai, A. Panchal, N. Buchner, R. De Borja, R. E. Denroche, C. K. Yung, S. Serra, N. Onetto, D. Mukhopadhyay, M. S. Tsao, P. A. Shaw, G. M. Petersen, S. Gallinger, R. H. Hruban, A. Maitra, C. A. Iacobuzio-Donahue, R. D. Schulick, C. L. Wolfgang, R. A. Morgan, R. T. Lawlor, P. Capelli, V. Corbo, M. Scardoni, G. Tortora, M. A. Tempero, K. M. Mann, N. A. Jenkins, P. A. Perez-Mancera, D. J. Adams, D. A. Largaespada, L. F. Wessels, A. G. Rust, L. D. Stein, D. A. Tuveson, N. G. Copeland, E. A. Musgrove, A. Scarpa, J. R. Eshleman, T. J. Hudson, R. L. Sutherland, D. A. Wheeler, J. V. Pearson, J. D. McPherson, R. A. Gibbs and S. M. Grimmond (2012). "Pancreatic cancer genomes reveal aberrations in axon guidance pathway genes." Nature 491(7424): 399-405.

Biffi, G., T. E. Oni, B. Spielman, Y. Hao, E. Elyada, Y. Park, J. Preall and D. A. Tuveson (2019). "IL1-Induced JAK/STAT Signaling Is Antagonized by TGFbeta to Shape CAF Heterogeneity in Pancreatic Ductal Adenocarcinoma." Cancer Discov 9(2): 282-301.

Bodoky, G., C. Timcheva, D. R. Spigel, P. J. La Stella, T. E. Ciuleanu, G. Pover and N. C. Tebbutt (2012). "A phase II open-label randomized study to assess the efficacy and safety of selumetinib (AZD6244 [ARRY-142886]) versus capecitabine in patients with advanced or metastatic pancreatic cancer who have failed first-line gemcitabine therapy." Invest New Drugs 30(3): 1216-1223.

Bronte, V., S. Brandau, S. H. Chen, M. P. Colombo, A. B. Frey, T. F. Greten, S. Mandruzzato, P. J. Murray, A. Ochoa, S. Ostrand-Rosenberg, P. C. Rodriguez, A. Sica, V. Umansky, R. H. Vonderheide and D. I. Gabrilovich (2016). "Recommendations for myeloid-derived suppressor cell nomenclature and characterization standards." Nat Commun 7: 12150.

Cancer Genome Atlas Research Network. Electronic address, a. a. d. h. e. and N. Cancer Genome Atlas Research (2017). "Integrated Genomic Characterization of Pancreatic Ductal Adenocarcinoma." Cancer Cell 32(2): 185-203 e113.

Catenacci, D. V., M. R. Junttila, T. Karrison, N. Bahary, M. N. Horiba, S. R. Nattam, R. Marsh, J. Wallace, M. Kozloff, L. Rajdev, D. Cohen, J. Wade, B. Sleckman, H. J. Lenz, P. Stiff, P. Kumar, P. Xu, L. Henderson, N. Takebe, R. Salgia, X. Wang, W. M. Stadler, F. J. de Sauvage and H. L. Kindler (2015). "Randomized Phase Ib/II Study of Gemcitabine Plus Placebo or Vismodegib, a Hedgehog Pathway Inhibitor, in Patients With Metastatic Pancreatic Cancer." J Clin Oncol 33(36): 4284-4292.

Chan-Seng-Yue, M., J. C. Kim, G. W. Wilson, K. Ng, E. F. Figueroa, G. M. O'Kane, A. A. Connor, R. E. Denroche, R. C. Grant, J. McLeod, J. M. Wilson, G. H. Jang, A. Zhang, A. Dodd, S. B. Liang, A. Borgida, D. Chadwick, S. Kalimuthu, I. Lungu, J. M. S. Bartlett, P. M. Krzyzanowski, V. Sandhu, H. Tiriac, F. E. M. Froeling, J. M. Karasinska, J. T. Topham, D. J. Renouf, D. F. Schaeffer, S. J. M. Jones, M. A. Marra, J. Laskin, R. Chetty, L. D. Stein, G. Zogopoulos, B. Haibe-Kains, P. J. Campbell, D. A. Tuveson, J. J. Knox, S. E. Fischer, S. Gallinger and F. Notta (2020). "Transcription phenotypes of pancreatic cancer are driven by genomic events during tumor evolution." Nat Genet 52(2): 231-240.

Chen, K., Q. Wang, M. Li, H. Guo, W. Liu, F. Wang, X. Tian and Y. Yang (2021). "Single-cell RNA-seq reveals dynamic change in tumor microenvironment during pancreatic ductal adenocarcinoma malignant progression." EBioMedicine 66: 103315.

Chuvin, N., D. F. Vincent, R. M. Pommier, L. B. Alcaraz, J. Gout, C. Caligaris, K. Yacoub, V. Cardot, E. Roger, B. Kaniewski, S. Martel, C. Cintas, S. Goddard-Leon, A. Colombe, J. Valantin, N. Gadot, E. Servoz, J. Morton, I. Goddard, A. Couvelard, V. Rebours, J. Guillermet, O. J. Sansom, I. Treilleux, U. Valcourt, S. Sentis, P. Dubus and L. Bartholin (2017). "Acinar-to-Ductal Metaplasia Induced by Transforming Growth Factor Beta Facilitates KRAS(G12D)-driven Pancreatic Tumorigenesis." Cell Mol Gastroenterol Hepatol 4(2): 263-282.

Collisson, E. A., A. Sadanandam, P. Olson, W. J. Gibb, M. Truitt, S. Gu, J. Cooc, J. Weinkle, G. E. Kim, L. Jakkula, H. S. Feiler, A. H. Ko, A. B. Olshen, K. L. Danenberg, M. A. Tempero, P. T. Spellman, D. Hanahan and J. W. Gray (2011). "Subtypes of pancreatic ductal adenocarcinoma and their differing responses to therapy." Nat Med 17(4): 500-503.

Costantino, C. L., A. K. Witkiewicz, Y. Kuwano, J. A. Cozzitorto, E. P. Kennedy, A. Dasgupta, J. C. Keen, C. J. Yeo, M. Gorospe and J. R. Brody (2009). "The role of HuR in gemcitabine efficacy in pancreatic cancer: HuR Up-regulates the expression of the gemcitabine metabolizing enzyme deoxycytidine kinase." Cancer Res 69(11): 4567-4572.

De La, O. J., L. L. Emerson, J. L. Goodman, S. C. Froebe, B. E. Illum, A. B. Curtis and L. C. Murtaugh (2008). "Notch and Kras reprogram pancreatic acinar cells to ductal intraepithelial neoplasia." Proc Natl Acad Sci U S A 105(48): 18907-18912.

Elyada, E., M. Bolisetty, P. Laise, W. F. Flynn, E. T. Courtois, R. A. Burkhart, J. A. Teinor, P. Belleau, G. Biffi, M. S. Lucito, S. Sivajothi, T. D. Armstrong, D. D. Engle, K. H. Yu, Y. Hao, C. L. Wolfgang, Y. Park, J. Preall, E. M. Jaffee, A. Califano, P. Robson and D. A. Tuveson (2019). "Cross-Species Single-Cell Analysis of Pancreatic Ductal Adenocarcinoma Reveals Antigen-Presenting Cancer-Associated Fibroblasts." Cancer Discov 9(8): 1102-1123.

Ene-Obong, A., A. J. Clear, J. Watt, J. Wang, R. Fatah, J. C. Riches, J. F. Marshall, J. Chin-Aleong, C. Chelala, J. G. Gribben, A. G. Ramsay and H. M. Kocher (2013). "Activated pancreatic stellate cells sequester CD8+ T cells to reduce their infiltration of the juxtatumoral compartment of pancreatic ductal adenocarcinoma." Gastroenterology 145(5): 1121-1132.

Erkan, M., C. W. Michalski, S. Rieder, C. Reiser-Erkan, I. Abiatari, A. Kolb, N. A. Giese, I. Esposito, H. Friess and J. Kleeff (2008). "The activated stroma index is a novel and independent prognostic marker in pancreatic ductal adenocarcinoma." Clin Gastroenterol Hepatol 6(10): 1155-1161.

Ferreira, R. M. M., R. Sancho, H. A. Messal, E. Nye, B. Spencer-Dene, R. K. Stone, G. Stamp, I. Rosewell, A. Quaglia and A. Behrens (2017). "Duct- and Acinar-Derived Pancreatic Ductal Adenocarcinomas Show Distinct Tumor Progression and Marker Expression." Cell Rep 21(4): 966-978.

Flowers, B. M., H. Xu, A. S. Mulligan, K. J. Hanson, J. A. Seoane, H. Vogel, C. Curtis, L. D. Wood and L. D. Attardi (2021). "Cell of Origin Influences Pancreatic Cancer Subtype." Cancer Discov 11(3): 660-677.

Gopalan, V., A. Singh, F. Rashidi Mehrabadi, L. Wang, E. Ruppin, H. E. Arda and S. Hannenhalli (2021). "A Transcriptionally Distinct Subpopulation of Healthy Acinar Cells Exhibit Features of Pancreatic Progenitors and PDAC." Cancer Res 81(15): 3958-3970.

Haas, M., D. T. Waldschmidt, M. Stahl, A. Reinacher-Schick, J. Freiberg-Richter, L. Fischer von Weikersthal, F. Kaiser, S. Kanzler, N. Frickhofen, T. Seufferlein, T. Dechow, R. Mahlberg, P. Malfertheiner, G. Illerhaus, S. Kubicka, A. Abdul-Ahad, R. Snijder, S. Kruger, C. B. Westphalen, S. Held, M. von Bergwelt-Baildon, S. Boeck and V. Heinemann (2021). "Afatinib plus gemcitabine versus gemcitabine alone as first-line treatment of metastatic pancreatic cancer: The randomised, open-label phase II ACCEPT study of the Arbeitsgemeinschaft Internistische Onkologie with an integrated analysis of the 'burden of therapy' method." Eur J Cancer 146: 95-106.

Habbe, N., G. Shi, R. A. Meguid, V. Fendrich, F. Esni, H. Chen, G. Feldmann, D. A. Stoffers, S. F. Konieczny, S. D. Leach and A. Maitra (2008). "Spontaneous induction of murine pancreatic intraepithelial neoplasia (mPanIN) by acinar cell targeting of oncogenic Kras in adult mice." Proc Natl Acad Sci U S A 105(48): 18913-18918.

Hingorani, S. R., L. Wang, A. S. Multani, C. Combs, T. B. Deramaudt, R. H. Hruban, A. K. Rustgi, S. Chang and D. A. Tuveson (2005). "Trp53R172H and KrasG12D cooperate to promote

chromosomal instability and widely metastatic pancreatic ductal adenocarcinoma in mice." Cancer Cell 7(5): 469-483.

Hosein, A. N., R. A. Brekken and A. Maitra (2020). "Pancreatic cancer stroma: an update on therapeutic targeting strategies." Nat Rev Gastroenterol Hepatol 17(8): 487-505.

Hruban, R. H., M. Goggins, J. Parsons and S. E. Kern (2000). "Progression model for pancreatic cancer." Clin Cancer Res 6(8): 2969-2972.

Huang, H., Z. Wang, Y. Zhang, R. N. Pradhan, D. Ganguly, R. Chandra, G. Murimwa, S. Wright, X. Gu, R. Maddipati, S. Muller, S. J. Turley and R. A. Brekken (2022). "Mesothelial cell-derived antigen-presenting cancer-associated fibroblasts induce expansion of regulatory T cells in pancreatic cancer." Cancer Cell 40(6): 656-673 e657.

Iacobuzio-Donahue, C. A., B. Ryu, R. H. Hruban and S. E. Kern (2002). "Exploring the host desmoplastic response to pancreatic carcinoma: gene expression of stromal and neoplastic cells at the site of primary invasion." Am J Pathol 160(1): 91-99.

Iwamoto, C., K. Ohuchida, T. Shinkawa, S. Okuda, Y. Otsubo, T. Okumura, A. Sagara, K. Koikawa, Y. Ando, K. Shindo, N. Ikenaga, K. Nakata, T. Moriyama, Y. Miyasaka, T. Ohtsuka, M. Eto, K. Akashi and M. Nakamura (2021). "Bone marrow-derived macrophages converted into cancer-associated fibroblast-like cells promote pancreatic cancer progression." Cancer Lett 512: 15-27.

Jacobetz, M. A., D. S. Chan, A. Neesse, T. E. Bapiro, N. Cook, K. K. Frese, C. Feig, T. Nakagawa, M. E. Caldwell, H. I. Zecchini, M. P. Lolkema, P. Jiang, A. Kultti, C. B. Thompson, D. C. Maneval, D. I. Jodrell, G. I. Frost, H. M. Shepard, J. N. Skepper and D. A. Tuveson (2013). "Hyaluronan impairs vascular function and drug delivery in a mouse model of pancreatic cancer." Gut 62(1): 112-120.

Jiang, Y. and D. P. S. Sohal (2023). "Pancreatic Adenocarcinoma Management." JCO Oncol Pract 19(1): 19-32.

Jones, S., X. Zhang, D. W. Parsons, J. C. Lin, R. J. Leary, P. Angenendt, P. Mankoo, H. Carter, H. Kamiyama, A. Jimeno, S. M. Hong, B. Fu, M. T. Lin, E. S. Calhoun, M. Kamiyama, K. Walter, T. Nikolskaya, Y. Nikolsky, J. Hartigan, D. R. Smith, M. Hidalgo, S. D. Leach, A. P. Klein, E. M. Jaffee, M. Goggins, A. Maitra, C. Iacobuzio-Donahue, J. R. Eshleman, S. E. Kern, R. H. Hruban, R. Karchin, N. Papadopoulos, G. Parmigiani, B. Vogelstein, V. E. Velculescu and K. W. Kinzler (2008). "Core signaling pathways in human pancreatic cancers revealed by global genomic analyses." Science 321(5897): 1801-1806.

Kopp, J. L., C. L. Dubois, D. F. Schaeffer, A. Samani, F. Taghizadeh, R. W. Cowan, A. D. Rhim, B. L. Stiles, M. Valasek and M. Sander (2018). "Loss of Pten and Activation of Kras Synergistically Induce Formation of Intraductal Papillary Mucinous Neoplasia From Pancreatic Ductal Cells in Mice." Gastroenterology 154(5): 1509-1523 e1505.

Kopp, J. L., G. von Figura, E. Mayes, F. F. Liu, C. L. Dubois, J. P. t. Morris, F. C. Pan, H. Akiyama, C. V. Wright, K. Jensen, M. Hebrok and M. Sander (2012). "Identification of Sox9-dependent acinar-to-ductal reprogramming as the principal mechanism for initiation of pancreatic ductal adenocarcinoma." Cancer Cell 22(6): 737-750.

Kundranda, M., A. C. Gracian, S. F. Zafar, E. Meiri, J. Bendell, H. Algul, F. Rivera, E. R. Ahn, D. Watkins, U. Pelzer, V. Charu, A. Zalutskaya, G. Kuesters, J. M. Pipas, S. Santillana, V. Askoxylakis and A. H. Ko (2020). "Randomized, double-blind, placebo-controlled phase II study of istiratumab (MM-141) plus nab-paclitaxel and gemcitabine versus nab-paclitaxel and gemcitabine in front-line metastatic pancreatic cancer (CARRIE)." Ann Oncol 31(1): 79-87.

Lee, A. Y. L., C. L. Dubois, K. Sarai, S. Zarei, D. F. Schaeffer, M. Sander and J. L. Kopp (2019). "Cell of origin affects tumour development and phenotype in pancreatic ductal adenocarcinoma." Gut 68(3): 487-498.

Lee, J. J., V. Bernard, A. Semaan, M. E. Monberg, J. Huang, B. M. Stephens, D. Lin, K. I. Rajapakshe, B. R. Weston, M. S. Bhutani, C. L. Haymaker, C. Bernatchez, C. M. Taniguchi, A. Maitra and P. A. Guerrero (2021). "Elucidation of Tumor-Stromal Heterogeneity and the Ligand-Receptor Interactome by Single-Cell Transcriptomics in Real-world Pancreatic Cancer Biopsies." Clin Cancer Res 27(21): 5912-5921.

Li, D., K. Xie, R. Wolff and J. L. Abbruzzese (2004). "Pancreatic cancer." Lancet 363(9414): 1049-1057.

Liou, G. Y., H. Doppler, B. Necela, M. Krishna, H. C. Crawford, M. Raimondo and P. Storz (2013). "Macrophage-secreted cytokines drive pancreatic acinar-to-ductal metaplasia through NF-kappaB and MMPs." J Cell Biol 202(3): 563-577.

Liu, B., Y. Jia, J. Ma, S. Wu, H. Jiang, Y. Cao, X. Sun, X. Yin, S. Yan, M. Shang and A. Mao (2016). "Tumor-associated macrophage-derived CCL20 enhances the growth and metastasis of pancreatic cancer." Acta Biochim Biophys Sin (Shanghai) 48(12): 1067-1074.

Liu, Q., Y. Li, Z. Niu, Y. Zong, M. Wang, L. Yao, Z. Lu, Q. Liao and Y. Zhao (2016). "Atorvastatin (Lipitor) attenuates the effects of aspirin on pancreatic cancerogenesis and the chemotherapeutic efficacy of gemcitabine on pancreatic cancer by promoting M2 polarized tumor associated macrophages." J Exp Clin Cancer Res 35: 33.

Martinez, F. O., A. Sica, A. Mantovani and M. Locati (2008). "Macrophage activation and polarization." Front Biosci 13: 453-461.

Menjivar, R. E., Z. C. Nwosu, W. Du, K. L. Donahue, H. S. Hong, C. Espinoza, K. Brown, A. Velez-Delgado, W. Yan, F. Lima, A. Bischoff, P. Kadiyala, D. Salas-Escabillas, H. C. Crawford, F. Bednar, E. Carpenter, Y. Zhang, C. J. Halbrook, C. A. Lyssiotis and M. Pasca di Magliano (2023). "Arginase 1 is a key driver of immune suppression in pancreatic cancer." Elife 12.

Miyazaki, Y., T. Oda, Y. Inagaki, H. Kushige, Y. Saito, N. Mori, Y. Takayama, Y. Kumagai, T. Mitsuyama and Y. S. Kida (2021). "Adipose-derived mesenchymal stem cells differentiate into heterogeneous cancer-associated fibroblasts in a stroma-rich xenograft model." Sci Rep 11(1): 4690.

Moffitt, R. A., R. Marayati, E. L. Flate, K. E. Volmar, S. G. Loeza, K. A. Hoadley, N. U. Rashid, L. A. Williams, S. C. Eaton, A. H. Chung, J. K. Smyla, J. M. Anderson, H. J. Kim, D. J. Bentrem, M. S. Talamonti, C. A. Iacobuzio-Donahue, M. A. Hollingsworth and J. J. Yeh (2015). "Virtual microdissection identifies distinct tumor- and stroma-specific subtypes of pancreatic ductal adenocarcinoma." Nat Genet 47(10): 1168-1178.

Neuhofer, P., C. M. Roake, S. J. Kim, R. J. Lu, R. B. West, G. W. Charville and S. E. Artandi (2021). "Acinar cell clonal expansion in pancreas homeostasis and carcinogenesis." Nature 597(7878): 715-719.

Neuzillet, C., A. Tijeras-Raballand, C. Ragulan, J. Cros, Y. Patil, M. Martinet, M. Erkan, J. Kleeff, J. Wilson, M. Apte, M. Tosolini, A. S. Wilson, F. R. Delvecchio, C. Bousquet, V. Paradis, P. Hammel, A. Sadanandam and H. M. Kocher (2019). "Inter- and intra-tumoural heterogeneity in cancer-associated fibroblasts of human pancreatic ductal adenocarcinoma." J Pathol 248(1): 51-65.

Nordh, S., D. Ansari and R. Andersson (2014). "hENT1 expression is predictive of gemcitabine outcome in pancreatic cancer: a systematic review." World J Gastroenterol 20(26): 8482-8490.

O'Kane, G. M., B. T. Grunwald, G. H. Jang, M. Masoomian, S. Picardo, R. C. Grant, R. E. Denroche, A. Zhang, Y. Wang, B. Lam, P. M. Krzyzanowski, I. M. Lungu, J. M. S. Bartlett, M. Peralta, F. Vyas, R. Khokha, J. Biagi, D. Chadwick, S. Ramotar, S. Hutchinson, A. Dodd, J. M. Wilson, F. Notta, G. Zogopoulos, S. Gallinger, J. J. Knox and S. E. Fischer (2020). "GATA6 Expression Distinguishes Classical and Basal-like Subtypes in Advanced Pancreatic Cancer." Clin Cancer Res 26(18): 4901-4910.

Oh, K., Y. J. Yoo, L. A. Torre-Healy, M. Rao, D. Fassler, P. Wang, M. Caponegro, M. Gao, J. Kim, A. Sasson, G. Georgakis, S. Powers and R. A. Moffitt (2023). "Coordinated single-cell tumor microenvironment dynamics reinforce pancreatic cancer subtype." Nat Commun 14(1): 5226.

Ohlund, D., E. Elyada and D. Tuveson (2014). "Fibroblast heterogeneity in the cancer wound." J Exp Med 211(8): 1503-1523.

Ohlund, D., A. Handly-Santana, G. Biffi, E. Elyada, A. S. Almeida, M. Ponz-Sarvise, V. Corbo, T. E. Oni, S. A. Hearn, E. J. Lee, Chio, II, C. I. Hwang, H. Tiriac, L. A. Baker, D. D. Engle, C. Feig, A. Kultti, M. Egeblad, D. T. Fearon, J. M. Crawford, H. Clevers, Y. Park and D. A. Tuveson (2017). "Distinct populations of inflammatory fibroblasts and myofibroblasts in pancreatic cancer." J Exp Med 214(3): 579-596.

Ozdemir, B. C., T. Pentcheva-Hoang, J. L. Carstens, X. Zheng, C. C. Wu, T. R. Simpson, H. Laklai, H. Sugimoto, C. Kahlert, S. V. Novitskiy, A. De Jesus-Acosta, P. Sharma, P. Heidari, U. Mahmood,

L. Chin, H. L. Moses, V. M. Weaver, A. Maitra, J. P. Allison, V. S. LeBleu and R. Kalluri (2014). "Depletion of carcinoma-associated fibroblasts and fibrosis induces immunosuppression and accelerates pancreas cancer with reduced survival." Cancer Cell 25(6): 719-734.

Patzak, M. S., V. Kari, S. Patil, F. H. Hamdan, R. G. Goetze, M. Brunner, J. Gaedcke, J. Kitz, D. I. Jodrell, F. M. Richards, C. Pilarsky, R. Gruetzmann, P. Rummele, T. Knosel, E. Hessmann, V. Ellenrieder, S. A. Johnsen and A. Neesse (2019). "Cytosolic 5'-nucleotidase 1A is overexpressed in pancreatic cancer and mediates gemcitabine resistance by reducing intracellular gemcitabine metabolites." EBioMedicine 40: 394-405.

Philip, P. A., J. Benedetti, C. L. Corless, R. Wong, E. M. O'Reilly, P. J. Flynn, K. M. Rowland, J. N. Atkins, B. C. Mirtsching, S. E. Rivkin, A. A. Khorana, B. Goldman, C. M. Fenoglio-Preiser, J. L. Abbruzzese and C. D. Blanke (2010). "Phase III study comparing gemcitabine plus cetuximab versus gemcitabine in patients with advanced pancreatic adenocarcinoma: Southwest Oncology Group-directed intergroup trial S0205." J Clin Oncol 28(22): 3605-3610.

Pinho, A. V., I. Rooman, M. Reichert, N. De Medts, L. Bouwens, A. K. Rustgi and F. X. Real (2011). "Adult pancreatic acinar cells dedifferentiate to an embryonic progenitor phenotype with concomitant activation of a senescence programme that is present in chronic pancreatitis." Gut 60(7): 958-966.

Poh, A. R. and M. Ernst (2021). "Tumor-Associated Macrophages in Pancreatic Ductal Adenocarcinoma: Therapeutic Opportunities and Clinical Challenges." Cancers (Basel) 13(12).

Principe, D. R., P. W. Underwood, M. Korc, J. G. Trevino, H. G. Munshi and A. Rana (2021). "The Current Treatment Paradigm for Pancreatic Ductal Adenocarcinoma and Barriers to Therapeutic Efficacy." Front Oncol 11: 688377.

Puleo, F., R. Nicolle, Y. Blum, J. Cros, L. Marisa, P. Demetter, E. Quertinmont, M. Svrcek, N. Elarouci, J. Iovanna, D. Franchimont, L. Verset, M. G. Galdon, J. Deviere, A. de Reynies, P. Laurent-Puig, J. L. Van Laethem, J. B. Bachet and R. Marechal (2018). "Stratification of Pancreatic Ductal Adenocarcinomas Based on Tumor and Microenvironment Features." Gastroenterology 155(6): 1999-2013 e1993.

Raber, P., A. C. Ochoa and P. C. Rodriguez (2012). "Metabolism of L-arginine by myeloid-derived suppressor cells in cancer: mechanisms of T cell suppression and therapeutic perspectives." Immunol Invest 41(6-7): 614-634.

Raghavan, S., P. S. Winter, A. W. Navia, H. L. Williams, A. DenAdel, K. E. Lowder, J. Galvez-Reyes, R. L. Kalekar, N. Mulugeta, K. S. Kapner, M. S. Raghavan, A. A. Borah, N. Liu, S. A. Vayrynen, A. D. Costa, R. W. S. Ng, J. Wang, E. K. Hill, D. Y. Ragon, L. K. Brais, A. M. Jaeger, L. F. Spurr, Y. Y. Li, A. D. Cherniack, M. A. Booker, E. F. Cohen, M. Y. Tolstorukov, I. Wakiro, A. Rotem, B. E. Johnson, J. M. McFarland, E. T. Sicinska, T. E. Jacks, R. J. Sullivan, G. I. Shapiro, T. E. Clancy, K. Perez, D. A. Rubinson, K. Ng, J. M. Cleary, L. Crawford, S. R. Manalis, J. A. Nowak, B. M. Wolpin, W. C. Hahn, A. J. Aguirre and A. K. Shalek (2021). "Microenvironment

drives cell state, plasticity, and drug response in pancreatic cancer." Cell 184(25): 6119-6137 e6126.

Rhim, A. D., E. T. Mirek, N. M. Aiello, A. Maitra, J. M. Bailey, F. McAllister, M. Reichert, G. L. Beatty, A. K. Rustgi, R. H. Vonderheide, S. D. Leach and B. Z. Stanger (2012). "EMT and dissemination precede pancreatic tumor formation." Cell 148(1-2): 349-361.

Rhim, A. D., P. E. Oberstein, D. H. Thomas, E. T. Mirek, C. F. Palermo, S. A. Sastra, E. N. Dekleva, T. Saunders, C. P. Becerra, I. W. Tattersall, C. B. Westphalen, J. Kitajewski, M. G. Fernandez-Barrena, M. E. Fernandez-Zapico, C. Iacobuzio-Donahue, K. P. Olive and B. Z. Stanger (2014). "Stromal elements act to restrain, rather than support, pancreatic ductal adenocarcinoma." Cancer Cell 25(6): 735-747.

Rougier, P., H. Riess, R. Manges, P. Karasek, Y. Humblet, C. Barone, A. Santoro, S. Assadourian, L. Hatteville and P. A. Philip (2013). "Randomised, placebo-controlled, double-blind, parallel-group phase III study evaluating aflibercept in patients receiving first-line treatment with gemcitabine for metastatic pancreatic cancer." Eur J Cancer 49(12): 2633-2642.

Schmiechen, Z. C. and I. M. Stromnes (2020). "Mechanisms Governing Immunotherapy Resistance in Pancreatic Ductal Adenocarcinoma." Front Immunol 11: 613815.

Sohal, D. P. S., E. B. Kennedy, P. Cinar, T. Conroy, M. S. Copur, C. H. Crane, I. Garrido-Laguna, M. W. Lau, T. Johnson, S. Krishnamurthi, C. Moravek, E. M. O'Reilly, P. A. Philip, S. Pant, M. A. Shah, V. Sahai, H. E. Uronis, N. Zaidi and D. Laheru (2020). "Metastatic Pancreatic Cancer: ASCO Guideline Update." J Clin Oncol 38(27): 3217-3230.

Sterner, R. C. and R. M. Sterner (2021). "CAR-T cell therapy: current limitations and potential strategies." Blood Cancer J 11(4): 69.

Storz, P. (2017). "Acinar cell plasticity and development of pancreatic ductal adenocarcinoma." Nat Rev Gastroenterol Hepatol 14(5): 296-304.

Strobel, O., Y. Dor, J. Alsina, A. Stirman, G. Lauwers, A. Trainor, C. F. Castillo, A. L. Warshaw and S. P. Thayer (2007). "In vivo lineage tracing defines the role of acinar-to-ductal transdifferentiation in inflammatory ductal metaplasia." Gastroenterology 133(6): 1999-2009.

Stromnes, I. M., J. S. Brockenbrough, K. Izeradjene, M. A. Carlson, C. Cuevas, R. M. Simmons, P. D. Greenberg and S. R. Hingorani (2014). "Targeted depletion of an MDSC subset unmasks pancreatic ductal adenocarcinoma to adaptive immunity." Gut 63(11): 1769-1781.

Swayden, M., J. Iovanna and P. Soubeyran (2018). "Pancreatic cancer chemo-resistance is driven by tumor phenotype rather than tumor genotype." Heliyon 4(12): e01055.

Tape, C. J., S. Ling, M. Dimitriadi, K. M. McMahon, J. D. Worboys, H. S. Leong, I. C. Norrie, C. J. Miller, G. Poulogiannis, D. A. Lauffenburger and C. Jorgensen (2016). "Oncogenic KRAS Regulates Tumor Cell Signaling via Stromal Reciprocation." Cell 165(4): 910-920.

Trovato, R., A. Fiore, S. Sartori, S. Cane, R. Giugno, L. Cascione, S. Paiella, R. Salvia, F. De Sanctis, O. Poffe, C. Anselmi, F. Hofer, S. Sartoris, G. Piro, C. Carbone, V. Corbo, R. Lawlor, S. Solito, L. Pinton, S. Mandruzzato, C. Bassi, A. Scarpa, V. Bronte and S. Ugel (2019). "Immunosuppression by monocytic myeloid-derived suppressor cells in patients with pancreatic ductal carcinoma is orchestrated by STAT3." J Immunother Cancer 7(1): 255.

Vaish, U., T. Jain, A. C. Are and V. Dudeja (2021). "Cancer-Associated Fibroblasts in Pancreatic Ductal Adenocarcinoma: An Update on Heterogeneity and Therapeutic Targeting." Int J Mol Sci 22(24).

Van Cutsem, E., M. A. Tempero, D. Sigal, D. Y. Oh, N. Fazio, T. Macarulla, E. Hitre, P. Hammel, A. E. Hendifar, S. E. Bates, C. P. Li, S. R. Hingorani, C. de la Fouchardiere, A. Kasi, V. Heinemann, A. Maraveyas, N. Bahary, L. Layos, V. Sahai, L. Zheng, J. Lacy, J. O. Park, F. Portales, P. Oberstein, W. Wu, D. Chondros, A. J. Bullock and H. Investigators (2020). "Randomized Phase III Trial of Pegvorhyaluronidase Alfa With Nab-Paclitaxel Plus Gemcitabine for Patients With Hyaluronan-High Metastatic Pancreatic Adenocarcinoma." J Clin Oncol 38(27): 3185-3194.

Vayrynen, S. A., J. Zhang, C. Yuan, J. P. Vayrynen, A. Dias Costa, H. Williams, V. Morales-Oyarvide, M. C. Lau, D. A. Rubinson, R. F. Dunne, M. M. Kozak, W. Wang, D. Agostini-Vulaj, M. G. Drage, L. Brais, E. Reilly, O. Rahma, T. Clancy, J. Wang, D. C. Linehan, A. J. Aguirre, C. S. Fuchs, L. M. Coussens, D. T. Chang, A. C. Koong, A. F. Hezel, S. Ogino, J. A. Nowak and B. M. Wolpin (2021). "Composition, Spatial Characteristics, and Prognostic Significance of Myeloid Cell Infiltration in Pancreatic Cancer." Clin Cancer Res 27(4): 1069-1081.

von Ahrens, D., T. D. Bhagat, D. Nagrath, A. Maitra and A. Verma (2017). "The role of stromal cancer-associated fibroblasts in pancreatic cancer." J Hematol Oncol 10(1): 76.

von Figura, G., A. Fukuda, N. Roy, M. E. Liku, J. P. Morris Iv, G. E. Kim, H. A. Russ, M. A. Firpo, S. J. Mulvihill, D. W. Dawson, J. Ferrer, W. F. Mueller, A. Busch, K. J. Hertel and M. Hebrok (2014). "The chromatin regulator Brg1 suppresses formation of intraductal papillary mucinous neoplasm and pancreatic ductal adenocarcinoma." Nat Cell Biol 16(3): 255-267.

Waddell, N., M. Pajic, A. M. Patch, D. K. Chang, K. S. Kassahn, P. Bailey, A. L. Johns, D. Miller, K. Nones, K. Quek, M. C. Quinn, A. J. Robertson, M. Z. Fadlullah, T. J. Bruxner, A. N. Christ, I. Harliwong, S. Idrisoglu, S. Manning, C. Nourse, E. Nourbakhsh, S. Wani, P. J. Wilson, E. Markham, N. Cloonan, M. J. Anderson, J. L. Fink, O. Holmes, S. H. Kazakoff, C. Leonard, F. Newell, B. Poudel, S. Song, D. Taylor, N. Waddell, S. Wood, Q. Xu, J. Wu, M. Pinese, M. J. Cowley, H. C. Lee, M. D. Jones, A. M. Nagrial, J. Humphris, L. A. Chantrill, V. Chin, A. M. Steinmann, A. Mawson, E. S. Humphrey, E. K. Colvin, A. Chou, C. J. Scarlett, A. V. Pinho, M. Giry-Laterriere, I. Rooman, J. S. Samra, J. G. Kench, J. A. Pettitt, N. D. Merrett, C. Toon, K. Epari, N. Q. Nguyen, A. Barbour, N. Zeps, N. B. Jamieson, J. S. Graham, S. P. Niclou, R. Bjerkvig, R. Grutzmann, D. Aust, R. H. Hruban, A. Maitra, C. A. Iacobuzio-Donahue, C. L. Wolfgang, R. A. Morgan, R. T. Lawlor, V. Corbo, C. Bassi, M. Falconi, G. Zamboni, G. Tortora, M. A. Tempero, I. Australian Pancreatic Cancer Genome, A. J. Gill, J. R. Eshleman, C. Pilarsky, A. Scarpa, E. A.

Musgrove, J. V. Pearson, A. V. Biankin and S. M. Grimmond (2015). "Whole genomes redefine the mutational landscape of pancreatic cancer." Nature 518(7540): 495-501.

Werba, G., D. Weissinger, E. A. Kawaler, E. Zhao, D. Kalfakakou, S. Dhara, L. Wang, H. B. Lim, G. Oh, X. Jing, N. Beri, L. Khanna, T. Gonda, P. Oberstein, C. Hajdu, C. Loomis, A. Heguy, M. H. Sherman, A. W. Lund, T. H. Welling, I. Dolgalev, A. Tsirigos and D. M. Simeone (2023). "Single-cell RNA sequencing reveals the effects of chemotherapy on human pancreatic adenocarcinoma and its tumor microenvironment." Nat Commun 14(1): 797.

Yamamoto, K., A. Venida, J. Yano, D. E. Biancur, M. Kakiuchi, S. Gupta, A. S. W. Sohn, S. Mukhopadhyay, E. Y. Lin, S. J. Parker, R. S. Banh, J. A. Paulo, K. W. Wen, J. Debnath, G. E. Kim, J. D. Mancias, D. T. Fearon, R. M. Perera and A. C. Kimmelman (2020). "Autophagy promotes immune evasion of pancreatic cancer by degrading MHC-I." Nature 581(7806): 100-105.

Yang, S., Q. Liu and Q. Liao (2020). "Tumor-Associated Macrophages in Pancreatic Ductal Adenocarcinoma: Origin, Polarization, Function, and Reprogramming." Front Cell Dev Biol 8: 607209.

Ye, H., Q. Zhou, S. Zheng, G. Li, Q. Lin, L. Wei, Z. Fu, B. Zhang, Y. Liu, Z. Li and R. Chen (2018). "Tumor-associated macrophages promote progression and the Warburg effect via CCL18/NF-kB/VCAM-1 pathway in pancreatic ductal adenocarcinoma." Cell Death Dis 9(5): 453.

Youn, J. I., S. Nagaraj, M. Collazo and D. I. Gabrilovich (2008). "Subsets of myeloid-derived suppressor cells in tumor-bearing mice." J Immunol 181(8): 5791-5802.

Zeisberg, E. M., S. Potenta, L. Xie, M. Zeisberg and R. Kalluri (2007). "Discovery of endothelial to mesenchymal transition as a source for carcinoma-associated fibroblasts." Cancer Res 67(21): 10123-10128.

Zhang, T., Y. Ren, P. Yang, J. Wang and H. Zhou (2022). "Cancer-associated fibroblasts in pancreatic ductal adenocarcinoma." Cell Death Dis 13(10): 897.

Zhang, Y., A. Velez-Delgado, E. Mathew, D. Li, F. M. Mendez, K. Flannagan, A. D. Rhim, D. M. Simeone, G. L. Beatty and M. Pasca di Magliano (2017). "Myeloid cells are required for PD-1/PD-L1 checkpoint activation and the establishment of an immunosuppressive environment in pancreatic cancer." Gut 66(1): 124-136.

Zhou, J., P. Oliveira, X. Li, Z. Chen and G. Bepler (2010). "Modulation of the ribonucleotide reductase-antimetabolite drug interaction in cancer cell lines." J Nucleic Acids 2010: 597098.

Zhu, Y., J. M. Herndon, D. K. Sojka, K. W. Kim, B. L. Knolhoff, C. Zuo, D. R. Cullinan, J. Luo, A. R. Bearden, K. J. Lavine, W. M. Yokoyama, W. G. Hawkins, R. C. Fields, G. J. Randolph and D. G. DeNardo (2017). "Tissue-Resident Macrophages in Pancreatic Ductal Adenocarcinoma Originate from Embryonic Hematopoiesis and Promote Tumor Progression." Immunity 47(3): 597.

Zinzi, L., M. Contino, M. Cantore, E. Capparelli, M. Leopoldo and N. A. Colabufo (2014). "ABC transporters in CSCs membranes as a novel target for treating tumor relapse." Front Pharmacol 5: 163.

Chapter 2 Epigenetic Regulation of the Immunosuppressive Tumor Microenvironment in PDAC Stroma

Introduction

Pancreatic ductal adenocarcinoma (PDAC), characterized by its heightened aggressiveness and resistance to conventional cancer therapies, presents a formidable challenge in the realm of oncology. The promising strides made by immune checkpoint inhibitors in treating challenging cancers such as melanoma, non-small cell lung cancer, urothelial bladder carcinomas, and renal cell carcinoma prompted optimism for their potential application in pancreatic cancer therapy. Regrettably, despite their success in various cancer types, immune checkpoint inhibitors exhibit notably limited efficacy when employed as a standalone therapeutic agent for pancreatic cancer (Royal, Levy et al. 2010). The diminished clinical responses to immune checkpoint inhibitors in pancreatic cancer have been ascribed to factors such as low mutational burdens and a reduced capacity for neo-antigen presentation, characteristics observed in certain cancer types (Snyder, Makarov et al. 2014) (Rizvi, Hellmann et al. 2015) (Voutsadakis 2022). However, the intriguing success of checkpoint inhibitor therapy in renal cell carcinoma, a cancer sharing a comparable mutation load with pancreatic cancer (Jahangir, Yazdani et al. 2022), underscores the existence of additional barriers that hinder the effectiveness of immune checkpoint therapy in pancreatic cancer.

Accumulating evidence underscores the prominent role of an extensive desmoplastic stromal response as a key driver of immune resistance in pancreatic cancer. Constituting up to 90% of the tumor bulk in pancreatic tumors (Xie and Xie 2015), stromal components, including pancreatic stellate cells (PSCs), immune cells, endothelial cells, and the extracellular matrix (ECM), form not only a physical barrier hindering drug delivery into pancreatic cancer (Provenzano, Cuevas et al. 2012) (Sherman, Yu et al. 2017), but also an immunosuppressive tumor

microenvironment (iTME) resistant to single immune checkpoint inhibitors (Falcomata, Barthel et al. 2023). The establishment of this iTME can be attributed to various immunosuppressive cell types (Clark, Hingorani et al. 2007). Aberrantly activated tumor-associated macrophages (TAMs) engage PD-1 and CTLA-4 receptors to inhibit T cell cytotoxic function and promote apoptosis (Kryczek, Zou et al. 2006) (Kuang, Zhao et al. 2009). Myeloid-derived suppressor cells (MDSCs) deplete arginine and cysteine in the TME, inhibiting cytotoxic T cell proliferation and function (Srivastava, Sinha et al. 2010). While regulatory T cells (Tregs) were previously shown to have an inhibitory effect on T helper cells ex vivo (Amedei, Niccolai et al. 2013), recent findings demonstrate their unexpected role in accelerating pancreatic carcinogenesis upon depletion (Zhang, Lazarus et al. 2020). These stromal immunosuppressive cells collectively employ multiple inhibitory strategies, impeding intra-tumoral effector T cells and NK cells. This multi-pronged inhibition results in reduced accumulation, proliferation, and activation of these immune cells (Peng, Zhu et al. 2013) (Bailey, Chang et al. 2016). While immune checkpoint blocking antibodies like αPDL1 can target specific inhibitory pathways, their efficacy is limited when faced with the myriad of immunosuppressive mechanisms at play. As a result, there is a pressing need for novel strategies that globally address immunosuppressive functions across various stromal cell types.

Recently, there has been a growing appreciation for the role of super-enhancers (SEs) in controlling diverse gene expression networks that underlie cellular activation and function (Hnisz, Abraham et al. 2013). SEs typically are an order-of magnitude larger than normal enhancers (~25 kilobase pairs) but represent only a small fraction of total enhancer regions (<3%) across genome. They encompass groups of putative enhancers with high levels of activator binding and/or chromatin modification (Pott and Lieb 2015). Importantly, the cooperative actions of multiple transcription factors within SEs have been proposed to function as coordinated switches to

determine cell fate and cell type-specific gene expression patterns (Heinz, Romanoski et al. 2015). Notably, SEs accumulate H3K27Ac histone marks, which are recognized by the bromodomain (BRD) and extra terminal (BET) family of proteins, particularly BRD2/3/4 (Pott and Lieb 2015). This reading process makes SEs druggable by targeting BRD and BET family of proteins with different kinds of BET and bromodomain inhibitors (BETi), including the widely used tool compound JQ1 and clinical BETi like iBET-762 (hereby referred to as iBET) and OTX-015 (hereby referred to as OTX), etc (Ferri, Petosa et al. 2016). These drugs work by competitively binding with the acetyl-recognizing pockets of BRD2/3/4 and disturb their recognition of H3K27Ac, which accumulates with a higher density at SE regions over typical enhancers, and hence can preferentially block the activity of SEs (Loven, Hoke et al. 2013) (Nakagawa, Adams et al. 2016). These inhibitors have demonstrated efficacy in various cancer types, showcasing their potential as standalone treatments for conditions such as diffuse large B-cell lymphoma (Ceribelli, Kelly et al. 2014), MLL-fusion leukemia (Dawson, Prinjha et al. 2011), neuroblastoma (Puissant, Frumm et al. 2013), NUT midline carcinoma (Stathis, Zucca et al. 2016), prostate cancer (Asangani, Dommeti et al. 2014) and even pancreatic cancer (Xie, Huang et al. 2018). Despite these advancements, the impact of BETi on the PDAC tumor microenvironment (TME) remains insufficiently explored.

In this study, we took an unbiased approach to characterize stromal cell composition in PDAC tumors using single-cell RNA sequencing (scRNA-seq) analysis. We identified diverse clusters of Macrophage/monocyte (referred to as Mye) and Neutrophil (referred to as Neu) populations within PDAC stroma with distinct immunosuppressive potentials. We then revealed that BETi can universally silence immunosuppressive genes in PDAC stromal cells, uncovering an epigenetic regulatory mechanism at the core of the TME immunosuppressive functions.

Moreover, we demonstrated the ability of BETi to sensitize PDAC tumors to immune checkpoint blockade, facilitating increased CD8 T cell recruitment within the tumor. This heightened antitumor response is orchestrated through the IFNγ-CXCL9/10-CXCR3 axis. Our study provides a detailed understanding of the stromal cell composition in PDAC tumors and introduces a novel approach to target their immunosuppressive functions, offering potential avenues for the development of innovative pancreatic cancer treatments.

2.1 BET inhibition reduces tumor burden in a mouse model of PDAC resistant to immune checkpoint inhibitors

The commonly mutated genes, KRAS and TP53, play pivotal roles in human pancreatic cancer. To emulate clinically relevant malignant PDAC tumors, we employed genetic mouse models carrying pancreas-specific (*Pdx1-Cre*) $Kras^{G12D}$ and $Trp53^{R172H}$ mutations (KPC). Establishing a PDAC1245-GFP cell line from a KPC mouse tumor allowed us to create an orthotopic mouse model, where aggressive PDAC tumors formed within 4 weeks of injecting tumor cells into the mouse pancreas. As anticipated, treatment with αPDL1 in this model failed to impede tumor progression (Figure 2.1A) and did not induce CD8+ T cell accumulation as observed in other cancer types (Figure 2.1B). Survival studies further revealed no prolonged benefit with extended αPDL1 treatment (Figure 2.2), mirroring the immunotherapy-resistant phenotype seen in human PDAC patients. Remarkably, BET inhibition using JQ1, OTX, or iBET significantly reduced tumor burden (Figure 2.3). These results provide a solid foundation for further investigating the epigenetic regulation of immunotherapy resistance in PDAC mouse models.

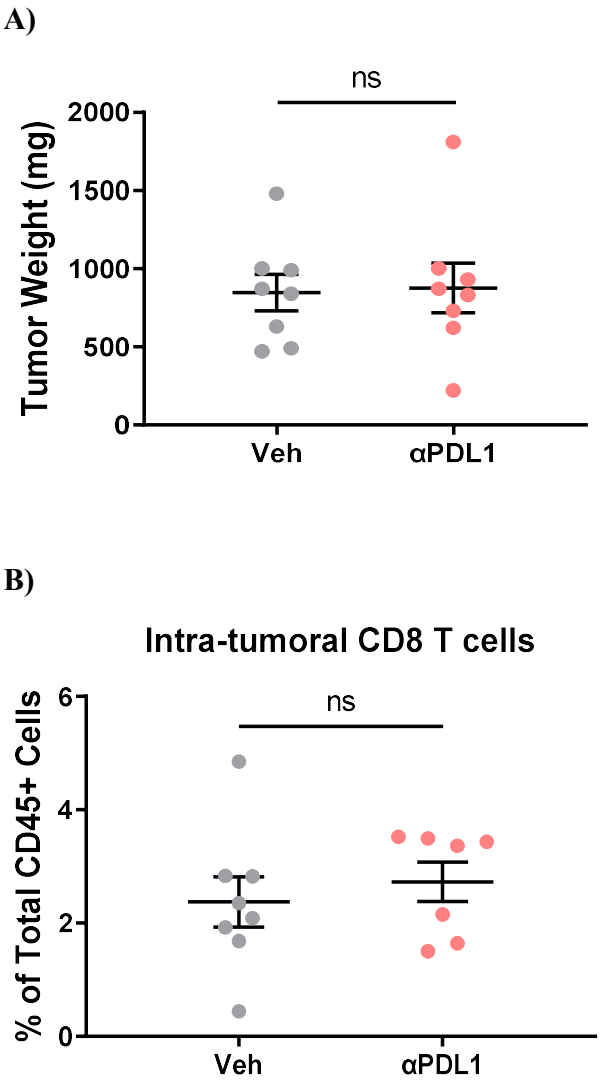

Figure 2.1 Orthotopic PDAC tumor is resistant to immune checkpoint inhibitors.

A) Tumor weight measurement in orthotopic mouse model of PDAC. Mice were treated once every three days with Veh or 10mg/kg αPDL1 (i.p.) for two weeks.
B) Intra-tumoral CD8+ T cell accumulation was measured by flow cytometry.
Data are presented as dot plots, with each dot representing an individual tumor, horizontal lines indicating means and error bars indicating SEMs. Data significance was analyzed by Two-tailed Unpaired t-test in Prism.

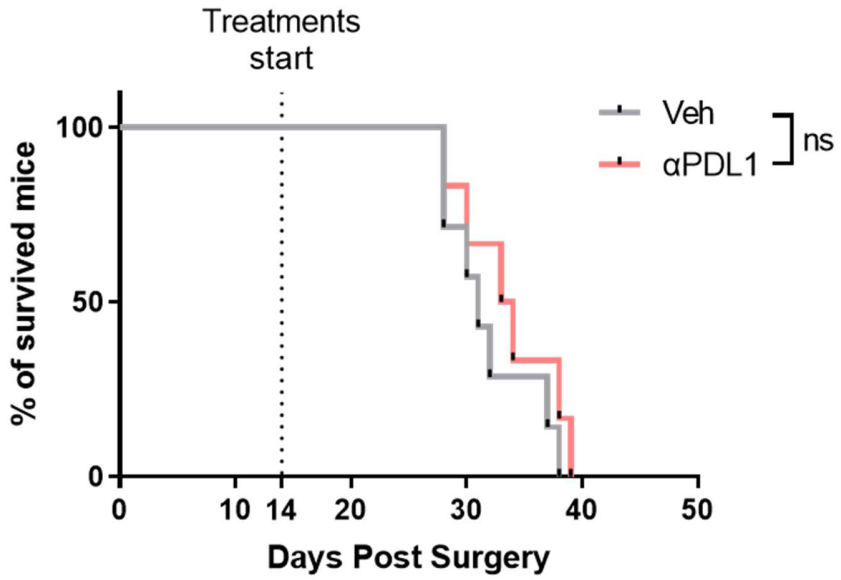

Figure 2.2 Immune checkpoint inhibitors fail to extend life span of PDAC-bearing mouse.

Survival study of mice bearing orthotopically transplanted PDAC1245-GFP tumor. Mice were treated once every three days with Veh or 10mg/kg αPDL1 (i.p.). Data significance was analyzed by Log-rank test in Prism.

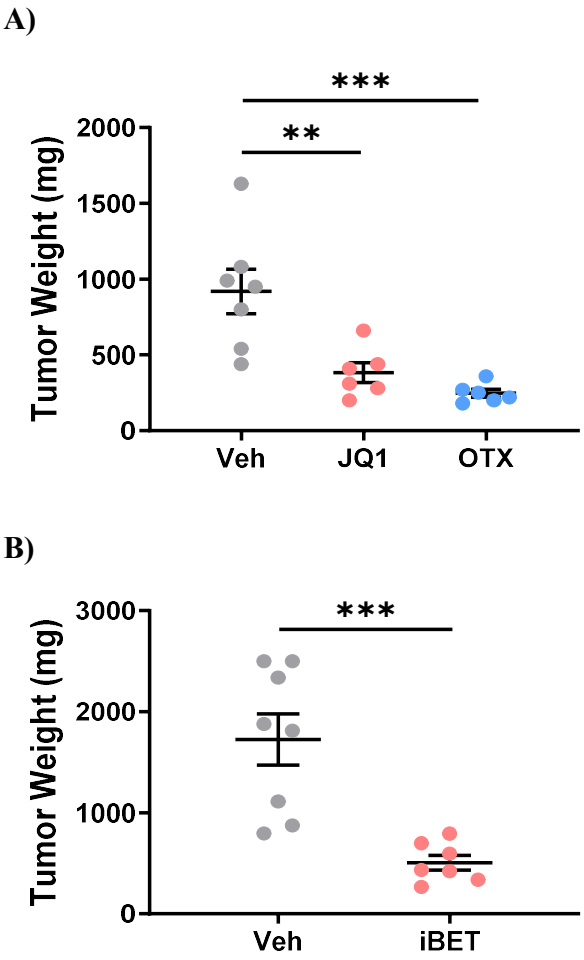

Figure 2.3 BETi blocks PDAC tumor growth as single agents.

A) Tumor weight measurement in orthotopic mouse model of PDAC. Mice were treated daily with Veh, 50mg/kg JQ1 (o.g.) or 75mg/kg OTX (o.g.) for two weeks. Data are presented as dot plots, with each dot representing an individual tumor, horizontal lines indicating means and error bars indicating SEMs. Data significance was analyzed by Ordinary one-way ANOVA in Prism. **P<0.01, ***P<0.001.

B) Tumor weight measurement in orthotopic mouse model of PDAC. Mice were treated daily with Veh or 75mg/kg iBET-762 (o.g.) for two weeks. Data are presented as dot plots, with each dot representing an individual tumor, horizontal lines indicating means and error bars indicating SEMs. Data significance was analyzed by Two-tailed Unpaired t-test in Prism. ***P<0.001.

2.2 The immunosuppressive functions in stromal cells can be universally blocked with BET inhibition

To delineate the characteristics of stromal cells in PDAC and understand the impact of BET inhibition on immunosuppressive features, we enriched stromal immune cells (defined as CD45+) using Fluorescence-activated Cell Sorting (FACS) and conducted single-cell RNA sequencing (scRNA-seq) analysis on PDAC tumor samples treated with vehicle (Veh) or OTX for 2 weeks. Unsupervised, graph-based clustering and Uniform Manifold Approximation and Projection (UMAP) visualization revealed twenty-seven distinct cell clusters/subclusters (Figure 2.4). These clusters were annotated based on canonical markers and gene expression profiles (Figure 2.5). Two major clusters were identified, harboring neutrophil and macrophage/monocyte cell features, along with lower frequency populations of NK cells, T cells, B cells, and dendritic cells (DCs). This composition of stromal cells suggests a subdued anti-tumor immune response within PDAC tumors. Interestingly, both Neutrophil and Macrophage/monocyte clusters exhibited further subdivision into multiple subclusters with distinct gene expression profiles (Figure 2.5), highlighting heterogeneity within these clusters.

In the Macrophage/monocyte cluster, feature genes included CX3CR1 marking tissue resident monocytes and macrophages, CCR2 for bone-marrow derived monocytes and macrophages, Arg1 for alternatively polarized macrophages (M2), and Isg15 indicating pro-tumorigenic potentials. Comparative analysis of immunosuppressive signature gene expression across six distinct Macrophage/monocyte subclusters demonstrated significant heterogeneity in immunosuppressive potentials (Figure 2.6). For instance, Mye3 appeared more immunosuppressive than other subclusters due to high expression of Arg1, Nos2, Il6, and Thbs1, while Mye1, characterized by MHCII expression, might have immune stimulatory potential. Similar observations were made in the Neutrophil cluster, where Neu5 seemed

immunosuppressive due to high CD274 (PDL1) expression, while Neu6 displayed lower expression of suppressive genes in general (Figure 2.6). Notably, in the context of BETi treatment, OTX appeared to universally block immunosuppressive gene expression among all these subclusters (Figure 2.7) without having as obvious effect on altering subcluster composition in Macrophage/monocyte and Neutrophil clusters (Figure 2.8).

To validate the impact of BET inhibition on stromal cell's immunosuppressive function, we sorted intra-tumoral myeloid cells based on CD11b and MHCII surface markers and examined their suppressive function on naïve CD4/CD8 T cell proliferation. Surprisingly, MHCII+ myeloid cells exhibited higher immunosuppressive function on both naïve CD8 and naïve CD4 T cell proliferation compared to MHCII- myeloid cells (Figure 2.9). This finding contradicted our scRNA-seq analysis where MHCII- Mye3 was suggested to have strong immunosuppressive functions. Several factors may contribute to this inconsistency. Mye3 population might have lost its suppressive features due to its high plasticity or low viability *in vitro*. It is also possible that its function cannot be fully investigated in naïve T cells. Despite the need for optimization in sorting myeloid subclusters individually and refining proliferation assays to better reflect *in vivo* conditions, it is evident that some immunosuppressive functions of the myeloid cluster can be confirmed with naïve T cell proliferation assays, and *in vivo* treatment with OTX can inhibit these functions. Overall, these findings underscore the potential of epigenetic targeting with BETi to counteract the iTME in PDAC tumors.

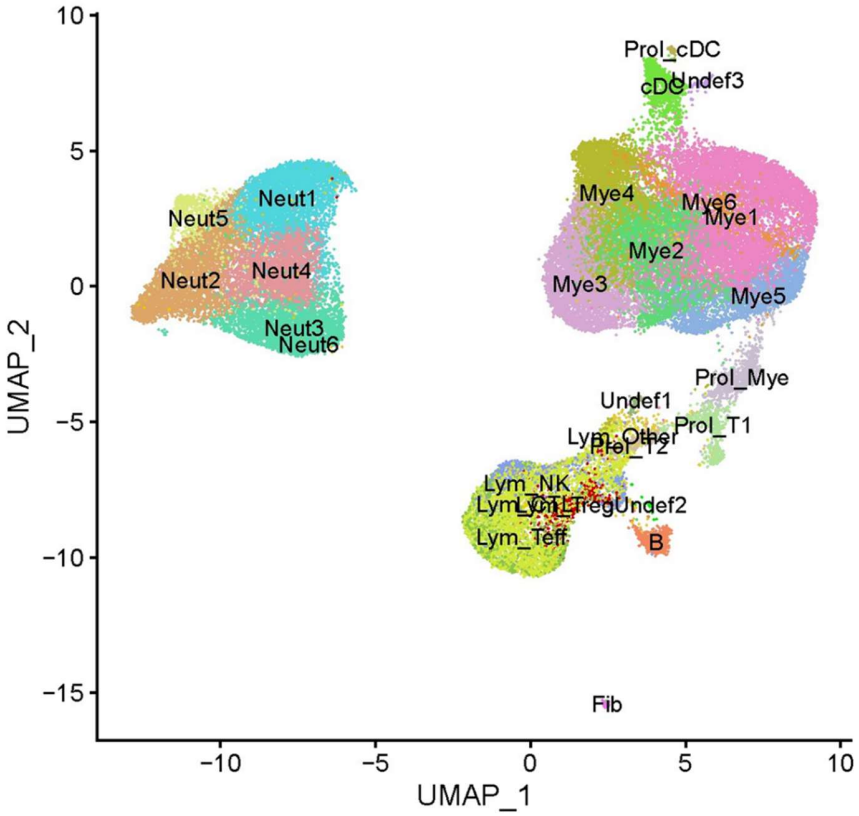

Figure 2.4 CD45+ Stromal cell clusters and subclusters identified in PDAC tumors.

UMAP plot of scRNA-seq analysis highlighting all clusters identified. Data represent an integration of Veh and OTX arms.

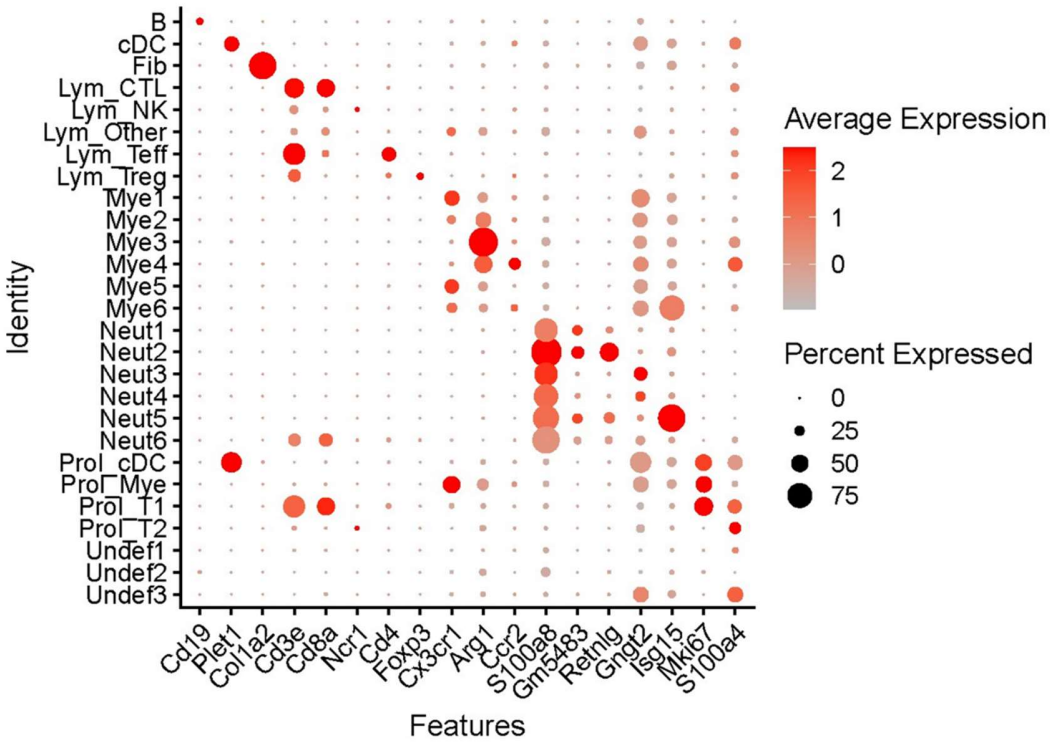

Figure 2.5 Signature genes used to distinguish different CD45+ stromal cell clusters.

Dot map highlighting signature gene expression representative in each cluster identified. Data represent an integration analysis of Veh and OTX arms.

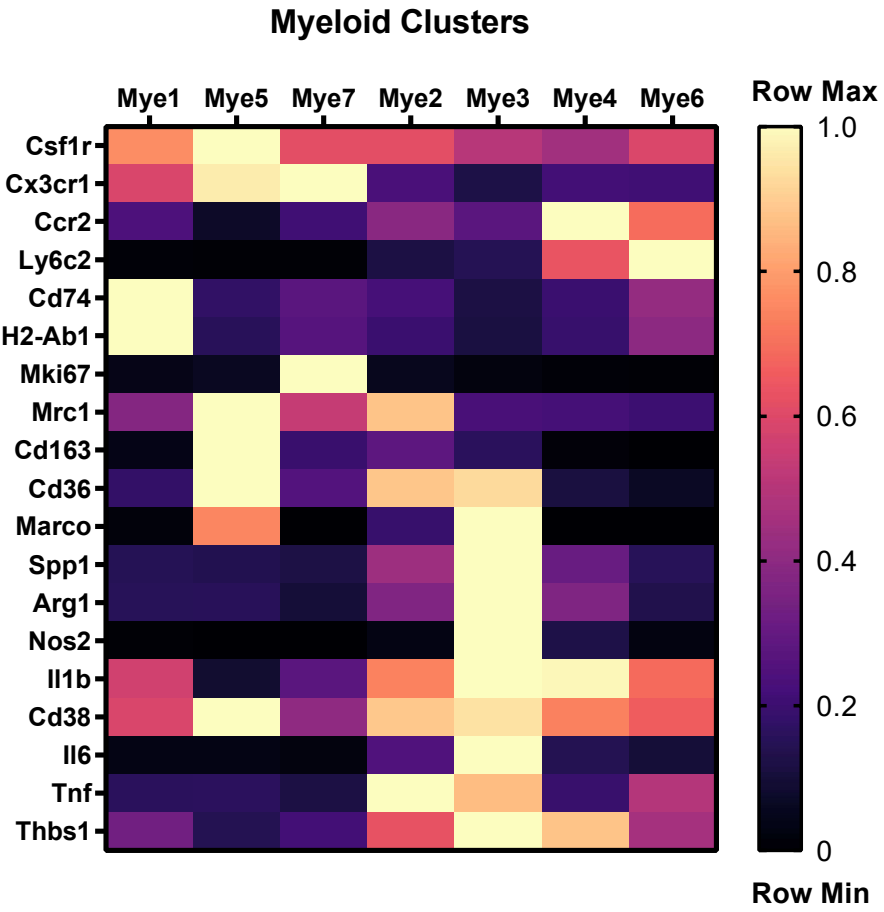

Figure 2.6 Immunosuppressive gene signatures in Macrophage/monocyte (Mye) subclusters.

Heatmap comparing immunosuppressive gene signature across different Macrophage/monocyte subclusters.

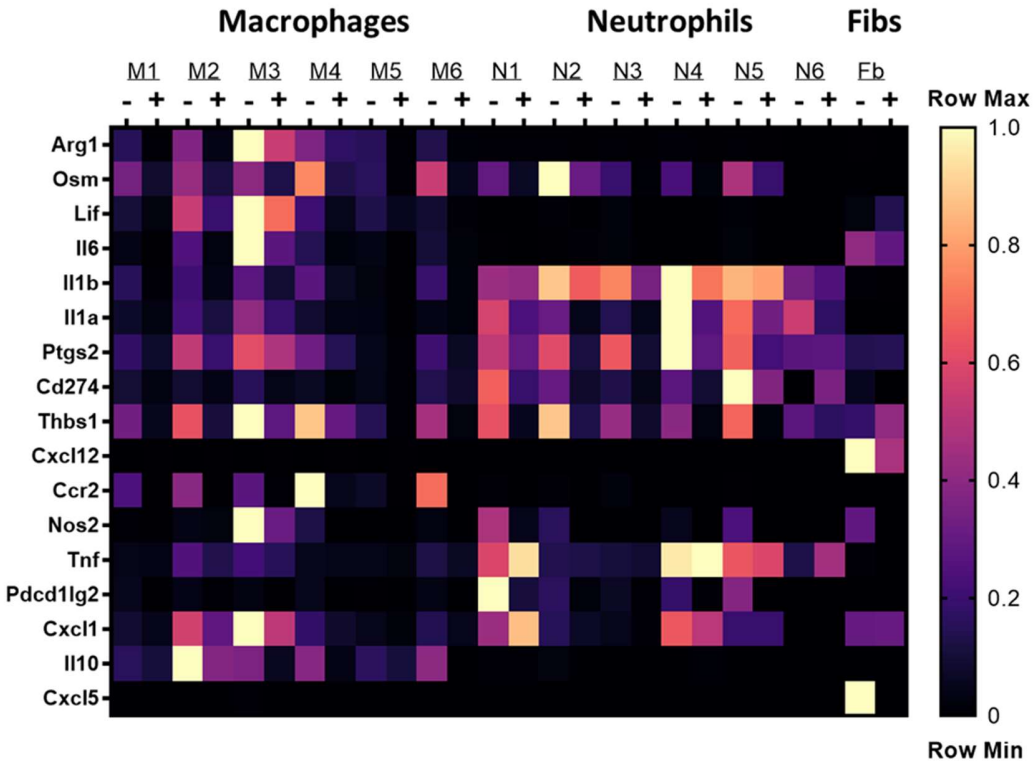

Figure 2.7 Impact of OTX on immunosuppressive gene expression in stromal subclusters.

Heatmap comparing immunosuppressive signature gene expression between Veh and OTX arms across different Macrophage/monocyte and Neutrophil subclusters.

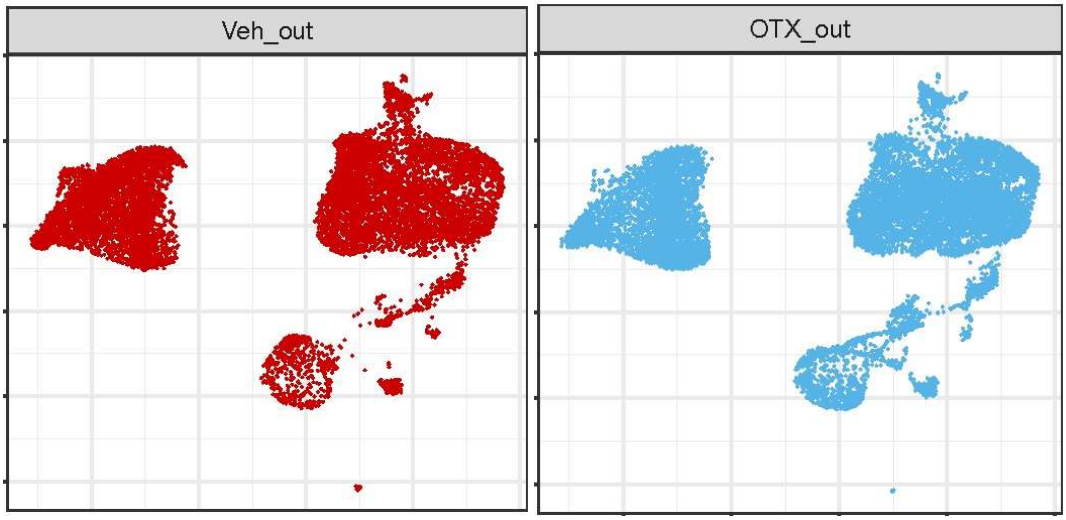

Figure 2.8 Composition change of CD45+ stromal cell clusters upon OTX treatment. UMAP plot of scRNA-seq analysis separating apart Veh (left) and OTX (right) arms.

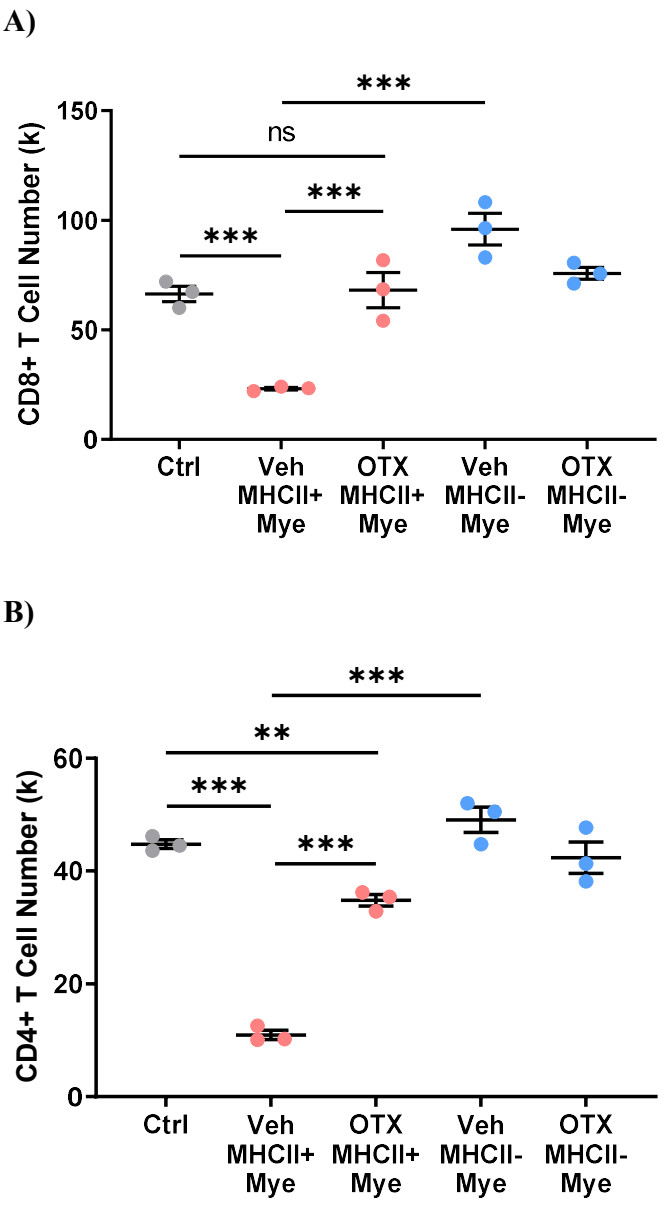

Figure 2.9 Intra-tumoral myeloid cells block naïve T cell proliferation ex vivo.

A) Impact of sorted intra-tumoral myeloid cells in naïve CD8 T cell proliferation assay. Data were measured by counting beads-based flow cytometry assay.
B) Impact of sorted intra-tumoral myeloid cells in naïve CD4 T cell proliferation assay. Data were measured by counting beads-based flow cytometry assay.
Data are presented as dot plots, with each dot representing an individual value, horizontal lines indicating means and error bars indicating SEMs. Data significance was analyzed by Ordinary one-way ANOVA in Prism. **P<0.01, ***P<0.001.

2.3 BET inhibition sensitizes PDAC tumor to immune checkpoint blockade

Given our previous observation that OTX can counteract the iTME established by stromal cells, we next sought to investigate the potential of combining OTX with αPDL1 to sensitize PDAC tumors to enhanced immune responses. Remarkably, while OTX treatment alone significantly reduced tumor burden, the introduction of αPDL1 in combination with OTX prominently augmented the blockade of tumor progression (Figure 2.10A). More strikingly, flow cytometry analysis of tumor-infiltrating immune cells unveiled that the synergistic combination of OTX and αPDL1 treatment was necessary to induce a robust accumulation of CD8+ T cells within the TME, which was not elicited by OTX or αPDL1 as individual agents (Figure 2.10B). To ascertain that the augmented intra-tumoral CD8 T cell accumulation was more than just a change in ratio, we conducted CD8α immunohistochemistry staining and found a substantial increase in the absolute count of CD8α+ cells within the tumor following the O+P treatment regimen (Figure 2.11). Furthermore, in-depth investigation into the state and functionality of intra-tumoral CD8 T cells was conducted through a comprehensive flow cytometry analysis encompassing various cytotoxic T cell markers. Our findings indicated that these CD8+ T cells isolated from PDAC tumors displayed heightened activation (PD1+ CD69+) (Figure 2.12A and 2.12B) and, although not significant, a trend of reduced exhaustion (Tim3+) (Figure 2.12C). They also exhibited a distinctive shift away from the central memory phenotype (CD62L+ CD44+) towards an effector memory phenotype (CD62L- CD44+) (Figure 2.12D), implying functional differences. Notably, these intra-tumoral CD8+ T cells demonstrated enhanced proliferation (KI67+) and an improved potential for cytotoxicity (Gzmb+) (Figure 2.12E and 2.12F). Collectively, these findings underscore the promising potential of synergizing BETi with immune checkpoint inhibitors to

effectively trigger a potent anti-tumor CD8 T cell response within the challenging PDAC tumor microenvironment.

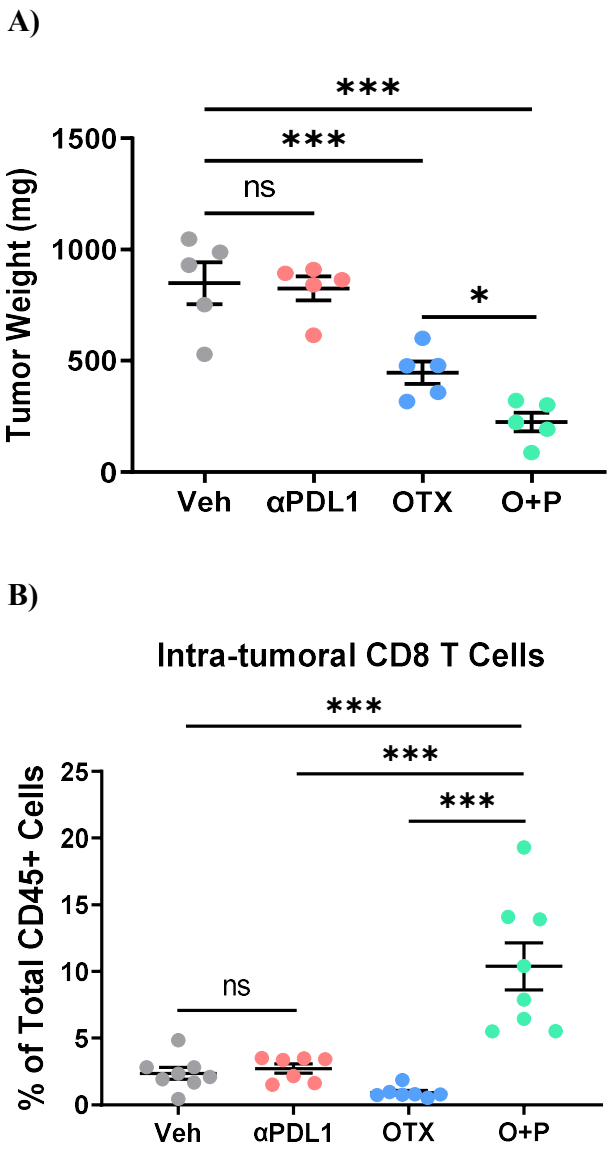

Figure 2.10 OTX and αPDL1 synergistically promote anti-tumor CD8 T cell response in PDAC tumor.

A) Tumor weight measurement in orthotopic mouse model of PDAC. Mice were treated with Veh, 10mg/kg αPDL1 (once every 3 days, i.p.) and/or 75mg/kg OTX (daily, o.g.) for two weeks.
B) Intra-tumoral CD8 T cell accumulation was measured by flow cytometry after two weeks of treatment.
Data are presented as dot plots, with each dot representing an individual tumor, horizontal lines indicating means and error bars indicating SEMs. Data significance was analyzed by Ordinary one-way ANOVA in Prism. *P<0.05, ***P<0.001.

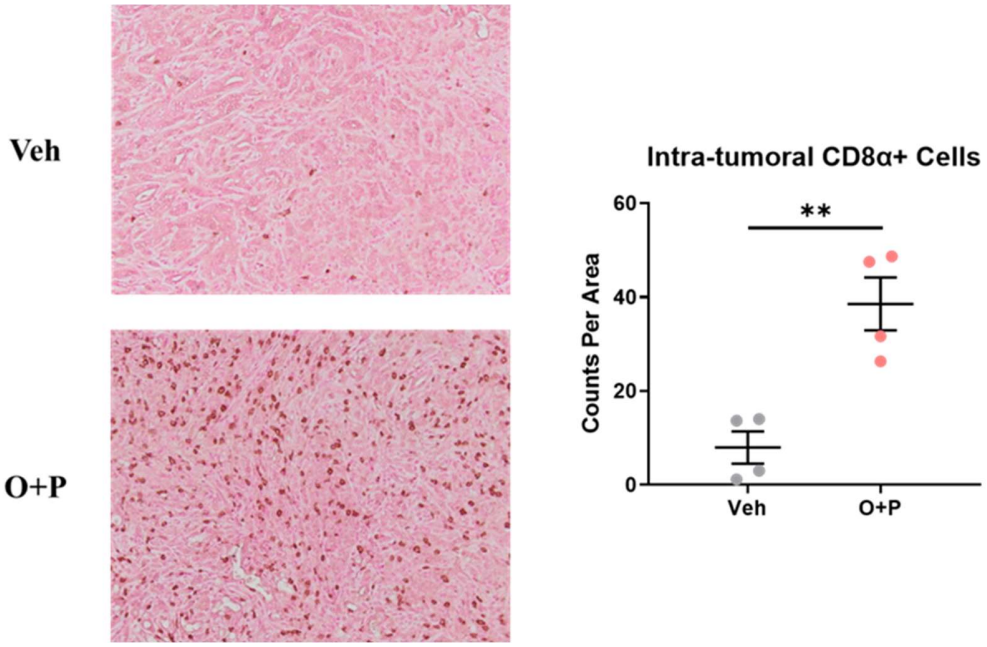

Figure 2.11 OTX+αPDL1 induces CD8 T cell accumulation in tumors.

Immunohistochemistry staining of the CD8 marker in orthotopic mouse model of PDAC. Mice were treated with Veh or a combination of 10mg/kg αPDL1 (once every 3 days, i.p.) and 75mg/kg OTX (daily, o.g.) for two weeks. Representative pictures of stained sample slides are shown on the left. Statistics of CD8α+ cell counts are shown on the right. Data are presented as dot plots, with each dot representing the average counts of 5 distinct area randomly picked from an individual tumor slice sample. Horizontal lines indicate means and error bars indicate SEMs. Data significance was analyzed by Two-tailed Unpaired t-test in Prism. **P<0.01.

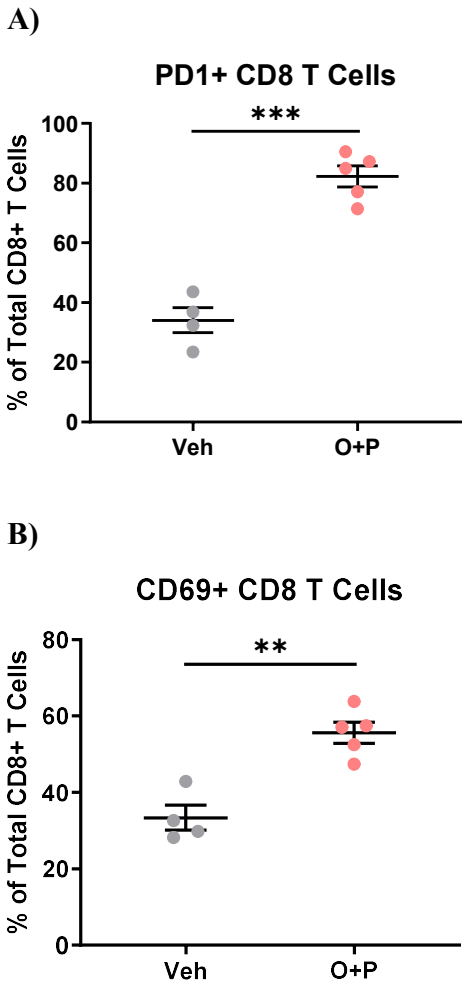

Figure 2.12 OTX+αPDL1 improves CD8 T cell performance in PDAC tumors.

A) Flow cytometry analysis of the PD1 marker in intra-tumoral CD8 T cells. PD1+ marks activated T cells sensitive to checkpoint regulation.
B) Flow cytometry analysis of the CD69 marker in intra-tumoral CD8 T cells. CD69+ marks activated T cells.
Data are presented as dot plots, with each dot representing an individual tumor, horizontal lines indicating means and error bars indicating SEMs. Data significance was analyzed by Two-tailed Unpaired t-test in Prism. **P<0.01, ***P<0.001.

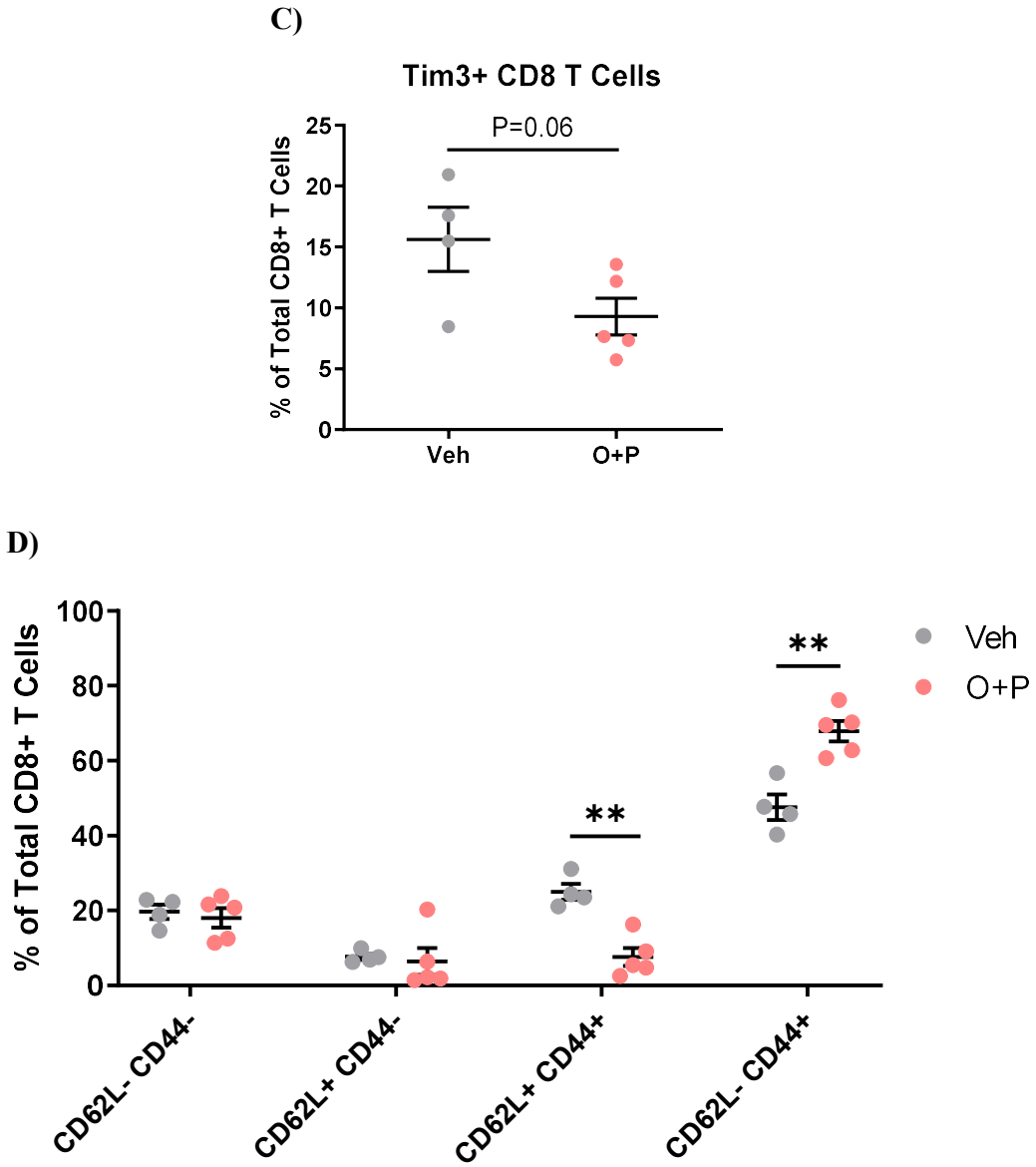

Figure 2.12 (continued) OTX+αPDL1 improves CD8 T cell performance in PDAC tumors.

C) Flow cytometry analysis of the Tim3 marker in intra-tumoral CD8 T cells. Tim3+ marks exhausted T cells.
D) Flow cytometry analysis of the CD62L and CD44 markers in intra-tumoral CD8 T cells. CD62L+ CD44- marks naïve CD8 T cells, CD62L+ CD44+ marks central memory CD8 T cells, and CD62L- CD44+ marks effector memory T cells.
Data are presented as dot plots, with each dot representing an individual tumor, horizontal lines indicating means and error bars indicating SEMs. Data significance was analyzed by Two-tailed Unpaired t-test in Prism. **P<0.01.

E)

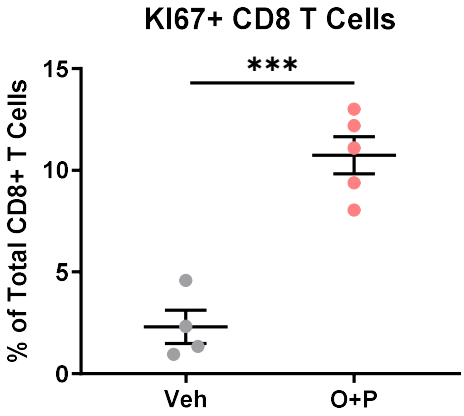

F)

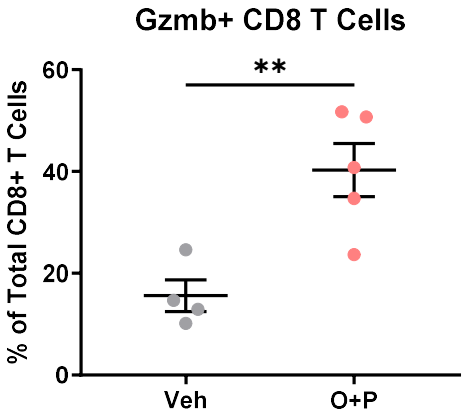

Figure 2.12 (continued) OTX+αPDL1 improves CD8 T cell performance in PDAC tumor.

E) Flow cytometry analysis of the KI67 marker in intra-tumoral CD8 T cells. KI67+ marks Proliferating T cells.
F) Flow cytometry analysis of the Gzmb marker in intra-tumoral CD8 T cells. Gzmb+ marks T cells with cytotoxic function.
Data are presented as dot plots, with each dot representing an individual tumor, horizontal lines indicating means and error bars indicating SEMs. Data significance was analyzed by Two-tailed Unpaired t-test in Prism. **P<0.01, ***P<0.001.

2.4 T cell infiltration induced with O+P combination treatment is mediated through IFNγ-CXCL9/10 axis

The CD8 T cell accumulation in the PDAC tumor can be attributed to either increased proliferation within the tumor, enhanced recruitment from circulation into the tumor, or a combination of both. Our previous results have already indicated that increased proliferation could contribute to the observed CD8 T cell accumulation within PDAC tumors following the O+P treatment (Figure 2.12E).

We next sought to determine whether CD8 T cell recruitment into the tumor could also be influenced by the combination therapy. To address this, we first took an unbiased approach to compare the expression of all detectable chemokine receptors across major CD45+ stromal cell clusters in our scRNA-seq dataset. Ccr8, Cxcr3, and Cxcr6 were the three major chemokine receptors significantly expressed in CD8 T cell cluster (T1) and CD4 T cell cluster (T2). This indicates that intra-tumoral T cell recruitment is likely mainly mediated through these three receptors (Figure 2.13). Importantly, we noticed that while the expression of other chemokine receptors was dramatically reduced in non-T cell clusters upon O+P treatment, the expression of Ccr8, Cxcr3, and Cxcr6 was relatively unaffected by O+P treatment (Figure 2.13).

To identify stromal cell clusters responsible for producing ligands for these three receptors within the tumor, we investigated the gene expression of chemokine ligands that bind to CCR8 (CCL1 and CCL8), CXCR3 (CXCL9 and CXCL10), and CXCR6 (CXCL16) across stromal cell clusters in the scRNA-seq dataset. Results showed that all these five chemokine genes were highly expressed by certain stromal clusters in PDAC tumors. But importantly, CXCL9 and CXCL10 were the only two chemokines that were consistently upregulated by O+P treatment, particularly in Macrophage/monocyte subclusters and to some extent in some Neutrophil subclusters, the dendritic cell (DCs) cluster, and the fibroblast cluster (Figure 2.14). These findings suggest that

the CXCL9/10-CXCR3 axis likely accounts for the intra-tumoral CD8 T cell infiltration induced with O+P treatment. In line with our findings, CXCL9 and CXCL10 have been shown previously in macrophages and dendritic cells to be able to guide CD8 T cells' migration to sites of infection and inflammation through interaction with CXCR3 (Tokunaga, Zhang et al. 2018).

To investigate whether CXCL9 and CXCL10 protein levels go up in PDAC tumors upon O+P treatment as implied from scRNA-seq analysis, we quantified the levels of these chemokines within PDAC tumors using ELISA. Results showed that only the combination treatment of O+P significantly elevated CXCL9 and CXCL10 levels—an effect not observed with OTX or anti-PDL1 alone (Figure 2.15). Notably, when we experimentally blocked CXCL9/10-CXCR3 signaling *in vivo* using a CXCR3 blocking antibody, the CD8 T cell accumulation phenotype was completely abrogated (Figure 2.16). These results underscore the indispensable role of augmented CXCL9/10-CXCR3 signaling in facilitating CD8 T cell recruitment to tumors during O+P treatment.

To determine the altered signaling pathways that could lead to Cxcl9 and Cxcl10 upregulation in stromal cells, we ran a gene ontology analysis on gene sets identified in PDAC stromal samples that are induced with O+P treatment. Interestingly, we found that the IFNγ response pathway was the most prominently upregulated pathway following O+P treatment (Figure 2.17). As a potent inflammatory cytokine produced primarily by T cells and NK cells, IFNγ has been previously reported to regulate Cxcl9 and Cxcl10 expression in macrophages (House, Savas et al. 2020) and fibroblasts (Ohta, Shigeishi et al. 2008). In line with this, our scRNA-seq analysis showed that IFNγ expression was enhanced in the T helper cell cluster receiving O+P treatment (data not shown). *In vitro* treatment of primary pancreatic stellate cells with IFNγ was able to confirm Cxcl9 and Cxcl10 upregulation (Figure 2.18). These findings

suggest that IFNγ could be the key drivers of O+P induced intra-tumoral CXCL9/10 production and thereby key drivers of CD8 T cell recruitment into PDAC tumors. To test this hypothesis, we compared the efficacy of O+P treatment in PDAC tumor-bearing mice with or without a functional IFNγ receptor. Impressively, the CD8 T cell accumulation phenotype was attenuated when IFNγ signaling was disrupted in stromal cells (Figure 2.19). Collectively, these findings shed light on the pivotal role of the IFNγ-CXCL9/10-CXCR3 axis in orchestrating CD8 T cell recruitment triggered by O+P combination therapy within the PDAC TME.

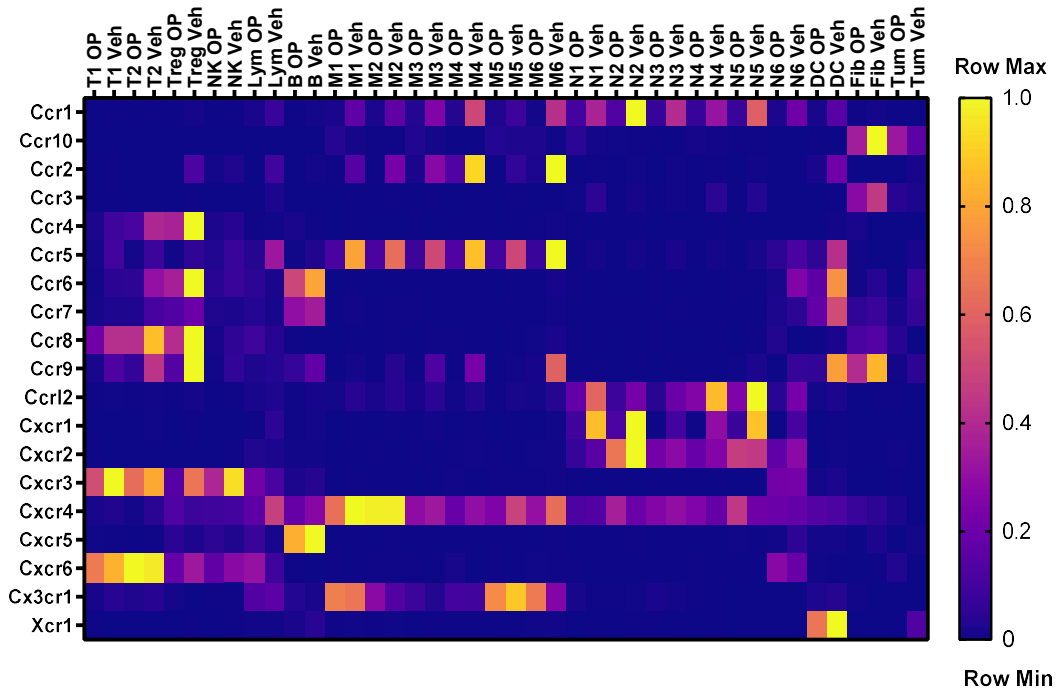

Figure 2.13 Impact of O+P on chemokine receptor expression across stromal cell clusters.

Heatmap comparing chemokine receptor gene expression across multiple stromal cell clusters. Four columns from left indicate CD8 T cell cluster (T1) and CD4 T cell cluster (T2). M1-6: Macrophage/monocyte subcluster 1-6, N1-6: Neutrophil subcluster 1-6.

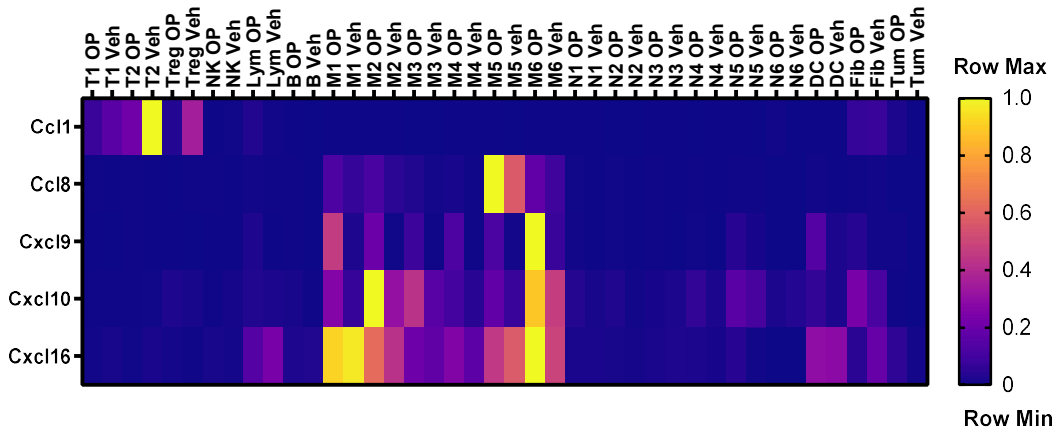

Figure 2.14 Impact of O+P on chemokine expression across stromal cell clusters.

Heatmap comparing chemokine gene expression across multiple stromal cell clusters. M1-6: Macrophage/monocyte subcluster 1-6, N1-6: Neutrophil subcluster 1-6.

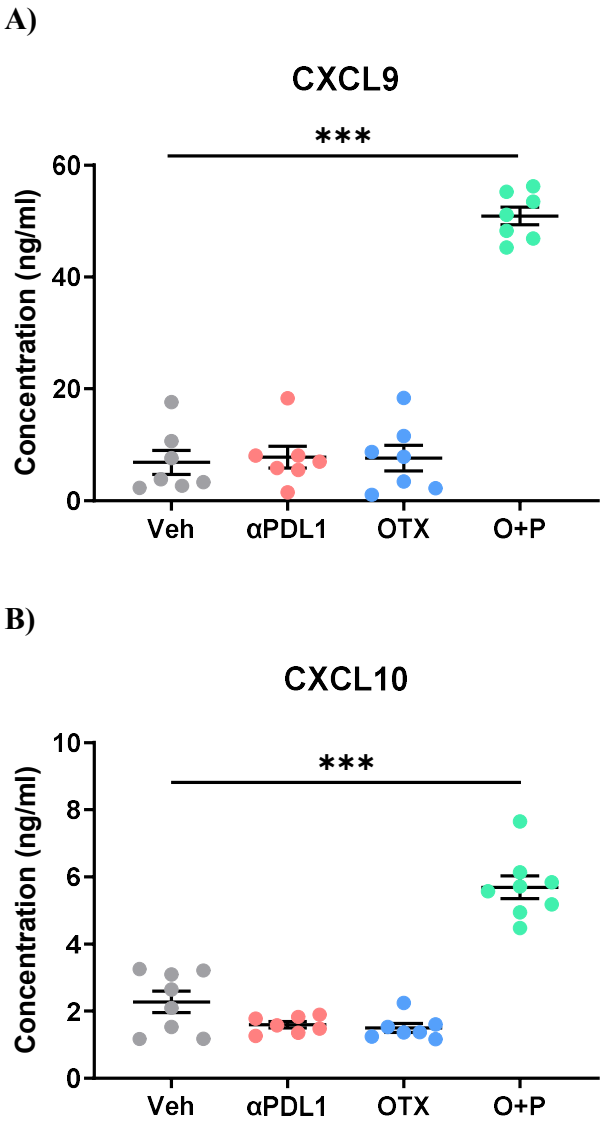

Figure 2.15 OTX and αPDL1 synergistically induces CXCL9 and CXCL10 level in PDAC tumors.

A) ELISA analysis of CXCL9 level in PDAC tumors. Mice were treated with Veh, 10mg/kg αPDL1 (once every 3 days, i.p.) and/or 75mg/kg OTX (daily, o.g.) for two weeks.
B) ELISA analysis of CXCL10 level in PDAC tumors.
Data are presented as dot plots, with each dot representing an individual tumor, horizontal lines indicating means and error bars indicating SEMs. Data significance was analyzed by Ordinary one-way ANOVA in Prism. ***P<0.001.

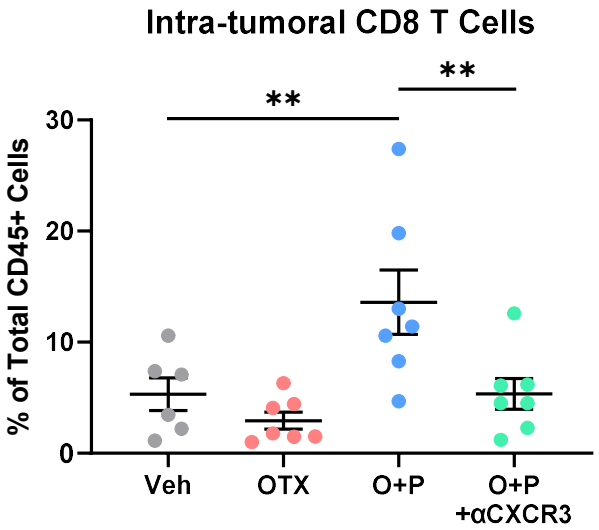

Figure 2.16 Blockade of CXCL9/10-CXCR3 signaling abolishes intra-tumoral CD8 T cell accumulation induced with O+P.

Flow cytometry analysis of intra-tumoral CD8 T cells in an orthotopic mouse model of PDAC. Mice were treated with Veh or different combinations of 10mg/kg αPDL1 (once every 3 days, i.p.), 10mg/kg αCXCR3 (once every 3 days, i.p.) and/or 75mg/kg OTX (daily, o.g.) for two weeks. Data are presented as dot plots, with each dot representing an individual tumor, horizontal lines indicating means and error bars indicating SEMs. Data significance was analyzed by Ordinary one-way ANOVA in Prism. **P<0.01.

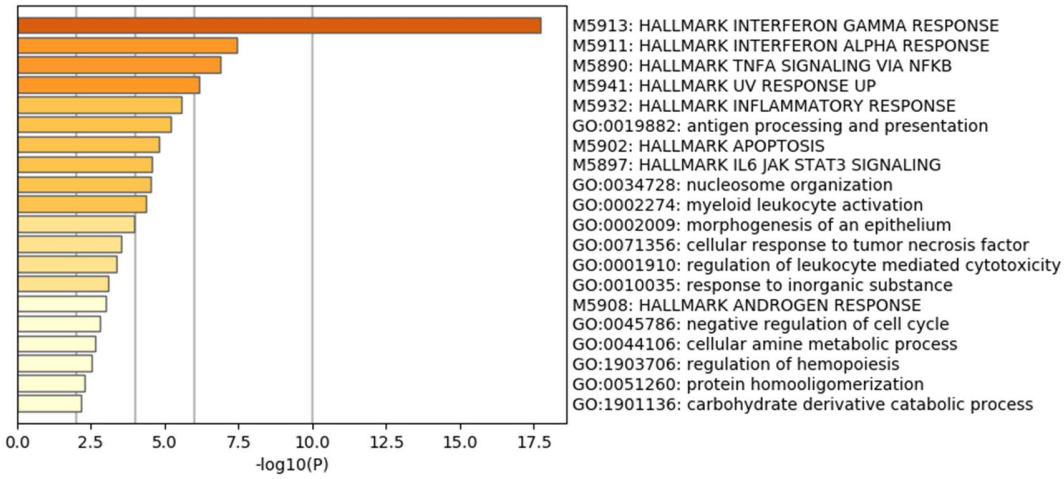

Figure 2.17 Pathways induced with O+P treatment in PDAC stromal cells.

Gene Ontology (Pathway Enrichment) analysis of gene sets in PDAC stromal cells that were significantly induced upon O+P treatment. Analysis was performed by Metascape, where gene lists referred to are “HALLMARK” and “GO”.

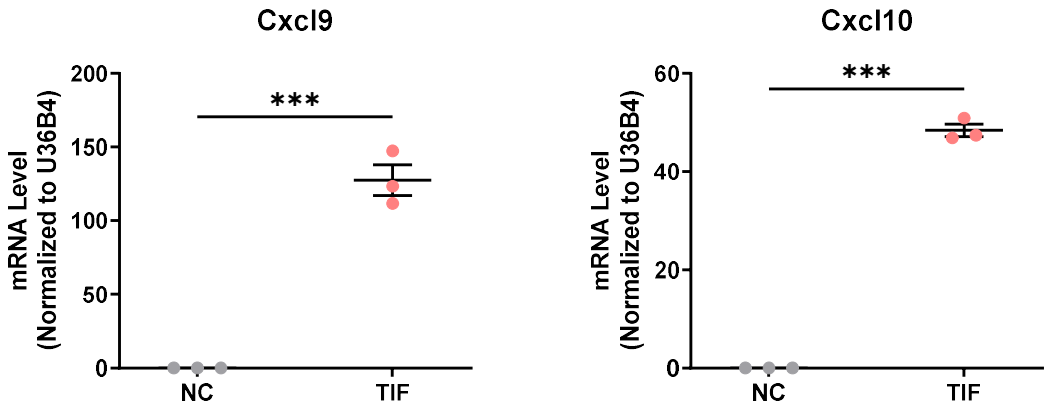

Figure 2.18 IFNγ induces Cxcl9 and Cxcl10 expression in cultured PSCs.

qPCR analysis of Cxcl9 (left) and Cxcl10 (right) expression in primary pancreatic stellate cells receiving 10ng/ml IFNγ treatment. Data are presented as dot plots, with each dot representing an individual value, horizontal lines indicating means and error bars indicating SEMs. Data significance was analyzed by Two-tailed Unpaired t-test in Prism. ***P<0.001.

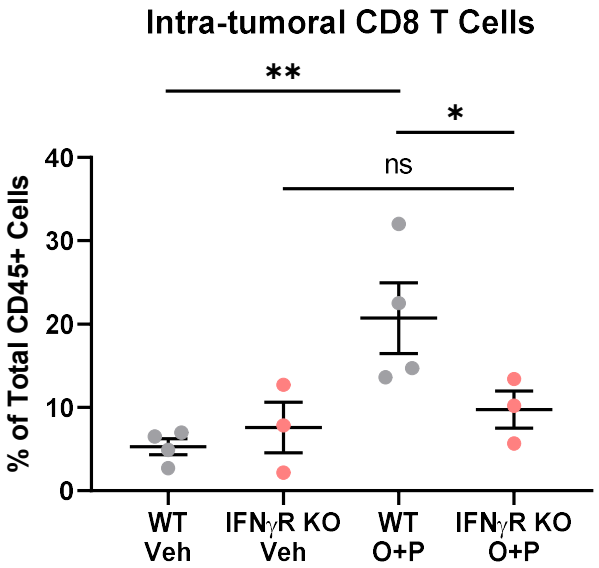

Figure 2.19 Knockout of IFNγR in stromal cells abolishes intra-tumoral CD8 T cell accumulation induced with O+P.

Flow cytometry analysis of intra-tumoral CD8 T cells in orthotopic mouse model of PDAC. WT mice or whole-body IFNγR KO mice were transplanted with PDAC1245-GFP (harboring WT IFNγR) and were treated with Veh or a combination of 10mg/kg αPDL1 (once every 3 days, i.p.) and 75mg/kg OTX (daily, o.g.) for two weeks. Data are presented as dot plots, with each dot representing an individual tumor, horizontal lines indicating means and error bars indicating SEMs. Data significance was analyzed by Ordinary one-way ANOVA in Prism. *P<0.05, **P<0.01.

Discussion

Despite the promising success of immune checkpoint inhibitors in various cancers, their efficacy in PDAC remains limited, which can be attributed to challenges such as drug delivery issues and the immunosuppressive TME. In this study, we established an orthotopic mouse model of PDAC mirroring the resistance observed in human patients to immune checkpoint inhibitors like αPDL1. Our comprehensive characterization, utilizing scRNA-seq analysis, revealed functional heterogeneity among stromal myeloid cells in this model. These distinct cell populations harbored unique immunosuppressive gene signatures, suggesting an underlying epigenetic regulatory profile. BETi emerged as promising candidates capable of blocking these immunosuppressive gene features. While BET inhibition alone did not completely restore the anti-tumor T cell response, its combination with immune checkpoint inhibitors exhibited a synergistic effect. This combined treatment not only significantly reduced tumor burden but also fostered the accumulation of active and functional CD8 T cells within the tumor. The observed increase in CD8 T cell accumulation was attributed not only to enhanced proliferation but also to improved recruitment from circulation. Further investigations unveiled a regulatory mechanism governing T cell recruitment into the PDAC tumor, mediated through the IFNγ (T cells)-CXCL9/10 (macrophage/monocyte cells and fibroblasts)-CXCR3 (T cells) axis. These findings deepen our understanding of the intricately controlled immunosuppressive stromal response in PDAC. The identification of BETi as potential regulators and their synergistic effects with immune checkpoint inhibitors offer novel therapeutic strategies for PDAC treatment. This study provides valuable insights into the complexity of PDAC's immunosuppressive TME, laying the groundwork for future developments in combined BETi and immune checkpoint inhibitor therapies.

The malignancy of PDAC is believed to stem from the intricate interactions between tumor cells and the surrounding stroma, involving various "tumor signaling-hijacked" somatic cells. The advent of single-cell techniques, such as scRNA-seq, has revolutionized our ability to analyze gene expression, genomics, and molecular features at the individual cell level in the pancreas (Barthel, Falcomata et al. 2023) (Cephas, Hwang et al. 2023). Leveraging scRNA-seq in this study, we uncovered distinct clusters of cells with neutrophil or macrophage gene signatures exhibiting immunosuppressive potentials at a high resolution (Figure 2.7). These findings align with numerous other single-cell analyses reported in both human PDAC (Yousuf, Qiu et al. 2023) (Werba, Weissinger et al. 2023) (Lin, Noel et al. 2020) (Raghavan, Winter et al. 2021) (Peng, Sun et al. 2019) and mouse PDAC (Carstens, Yang et al. 2021) (Schlesinger, Yosefov-Levi et al. 2020) (Elyada, Bolisetty et al. 2019) (Hosein, Huang et al. 2019).

While our primary focus in this work centers on the universal inhibition of immunosuppressive functions in stromal cells through epigenetic-targeting inhibitions, an outstanding question remains: does a specific immunosuppressive subcluster exhibit a notable capacity to block the anti-tumor T cell response and thus can get preferentially targeted over other subclusters? For instance, the Mye3 cluster displays significantly higher expression of Arg1, which encodes arginase 1 known to impede T cell function through metabolic consumption of arginine in pancreatic cancer (Menjivar, Nwosu et al. 2023). However, assessing the function of Arg1 *in vitro* using standard culture media with sufficient arginine supply cannot fully reflect its immunosuppressive potential, as observed in our naïve T cell proliferation assay where MHCII- myeloid cells did not exhibit immune suppression (Figure 2.9). Intriguingly, Mye3 also expresses high levels of LIF, a IL6 family of cytokine previously reported in pancreatic stellate cells (PSCs) to play a crucial role in crosstalk with tumor cells, driving their differentiation, epithelial-

mesenchymal transition (EMT) status, and resistance to chemotherapy (Shi, Gao et al. 2019). However, due to the limited fibroblast cluster identified in our scRNA-seq analysis, which resulted from the enrichment of stromal immune cells using the CD45 marker, a comprehensive comparison with Mye subclusters for LIF production may be challenging.

Conversely, the Neu5 cluster stands out with its remarkable expression of PDL1. While myeloid cells in PDAC tumors have been reported to induce PDL1 expression in tumor cells in an EGFR-AMPK-dependent manner (Zhang, Velez-Delgado et al. 2017), the immunosuppressive role of neutrophils, also known as granulocytic myeloid-derived suppressor cells (gMDSCs) expressing PDL1 in PDAC tumors, warrants further examination (Lu, Redd et al. 2016). Unfortunately, neutrophils, being generally short-lived, may quickly lose their suppressive features after sorting and exposure to standard *in vitro* conditions (data not shown). Lastly, it is crucial to highlight the fibroblast cluster identified in our scRNA-seq analysis, characterized by strong expression of Cxcl12. Consistent with this, other studies have demonstrated that CAFs in PDAC tumors express high levels of CXCL12, a pro-tumorigenic factor implicated in promoting tumor progression and inhibiting anti-tumor immune responses through interactions with various stromal cell types (Malik, Westcott et al. 2021).

Taken together, the identification of these immunosuppressive cell types in PDAC tumors motivates future research to delve deeper into validating and comparing their immunosuppressive roles *in vitro*. This endeavor requires optimized surface marker staining to allow FACS separation of each unique subcluster, conditioned *in vitro* assays to evaluate diverse immunosuppressive features of sorted cells, and consideration of potential immunostimulatory effects in certain subclusters, which have not been explored in this study, but could counteract their suppressive efficacy.

Targeting distinct immunosuppressive gene features in multiple cell types simultaneously poses a considerable challenge, but recent breakthroughs in understanding enhancers and super-enhancers offer a promising solution. Enhancers and super-enhancers, which epigenetically regulate gene expression in a cell type and function-dependent manner, have opened avenues for precisely modulating gene expression (Hnisz, Abraham et al. 2013) (Whyte, Orlando et al. 2013) (Heinz, Romanoski et al. 2015). The disruption of reading H3K27Ac marks, preferentially enriched in these genomic regions by BET and BRD family proteins, emerges as a viable strategy. Supporting this concept, our study demonstrates that BETi can universally block immunosuppressive gene expression across different stromal cell clusters (Figure 2.7). However, the precise mechanism through which BET inhibition achieves this effect remains unclear. It could operate through direct interference with regulatory regions physically associated with immunosuppressive genes or through an indirect mechanism, where it influences the expression of specific transcription factors that, in turn, act on immunosuppressive genes, or a combination of both. To unravel this mystery, it is imperative to characterize the enhancer and super-enhancer profiles of stromal cells using advanced techniques such as scATAC-seq (Semenkovich, Planer et al. 2016) (Philip, Fairchild et al. 2017), scGRO-seq (Mahat, Tippens et al. 2023), or the H3K27Ac CUT&Tag technique at the single-cell level (Bartosovic, Kabbe et al. 2021). An additional question that arises in this context is how to functionally demonstrate the essential role of an identified enhancer or super-enhancer region in mediating immunosuppressive functions in specific cell types. This query can be effectively addressed by generating enhancer/super-enhancer knockout cell lines or mouse lines using CRISPR-mediated genome editing, as outlined in recent studies (Antal, Oh et al. 2023). Disrupting specific enhancer/super-enhancer elements allows for a targeted investigation into how their disruption impacts immune suppression phenotypes.

While our study demonstrates that BET inhibition effectively blocks immunosuppressive cell functions within PDAC tumors, it falls short of independently triggering CD8 T cell accumulation (Figure 2.10B). This limitation could be attributed to the role played by BET and BRD family proteins in mediating gene expression related to the cell cycle (Yang, He et al. 2008) (Sinha, Faller et al. 2005). Despite reports indicating that BETi can impede PDAC tumor cell proliferation (Xie, Huang et al. 2018), they also exhibit the capacity to inhibit T cell proliferation *in vitro* (Georgiev, Wang et al. 2019). This dual functionality of BETi raises concerns about their suppressive impact on T cells residing within secondary lymphoid tissues, such as the spleen and lymph nodes. Although, in combination with immune checkpoint inhibitors, the adverse effects of BETi can be counteracted within PDAC tumors through significantly improved T cell recruitment and activation, there remains room for further enhancing the efficacy of BETi. The exploration of tumor-specific drug delivery and drug release techniques holds promise for advancing the application of BETi in PDAC treatment in the future (Veselov, Nosyrev et al. 2022). This concept will be expanded upon in the following chapter, where we will delve into nanoparticle-assisted BETi delivery methods.

In conclusion, here by characterizing intra-tumoral stromal cells with scRNA-seq analysis, we uncovered novel macrophage/monocyte and neutrophil populations that have immunosuppressive potentials. We found that BETi can block immunosuppressive gene expression in PDAC stromal cells, leading to the discovery of sensitizing PDAC tumor to immune checkpoint inhibitors with BET inhibition. Our scRNA-seq data, in combination with single-cell epigenetic profiling of tumor stromal cells proposed above, could provide unprecedented insight into the epigenetic programs governing intra-tumoral immune cell function and determine the therapeutic potential of targeting these pathways to promote tumor immunity. This work also has

immediate and important clinical relevance as BETi are currently the focus of several clinical trials in pancreatic cancer. It could also broadly inform the treatment of other cancer types that fail to respond to immune checkpoint therapy.

Acknowledgements

Chapter 2, in full, is currently being prepared for submission for publication of the material. Work in this chapter was done in collaboration with Morgan Truitt, who helped with experiments, and Tae Gyu Oh, who helped with bioinformatic analysis of scRNA-seq data. Senada Bashi, Hanna Dhiyebi, Mariel Burquez and Yang Dai provided technical support. The dissertation author was the primary researcher and author of this material. This chapter was written under the guidance of Morgan Truitt, Michael Downes, Annette Atkins, Ruth Yu and Ronald Evans.

References

Amedei, A., E. Niccolai, M. Benagiano, C. Della Bella, F. Cianchi, P. Bechi, A. Taddei, L. Bencini, M. Farsi, P. Cappello, D. Prisco, F. Novelli and M. M. D'Elios (2013). "Ex vivo analysis of pancreatic cancer-infiltrating T lymphocytes reveals that ENO-specific Tregs accumulate in tumor tissue and inhibit Th1/Th17 effector cell functions." Cancer Immunol Immunother 62(7): 1249-1260.

Antal, C. E., T. G. Oh, S. Aigner, E. C. Luo, B. A. Yee, T. Campos, H. Tiriac, K. L. Rothamel, Z. Cheng, H. Jiao, A. Wang, N. Hah, E. Lenkiewicz, J. C. Lumibao, M. L. Truitt, G. Estepa, E. Banayo, S. Bashi, E. Esparza, R. M. Munoz, J. K. Diedrich, N. M. Sodir, J. R. Mueller, C. R. Fraser, E. Borazanci, D. Propper, D. D. Von Hoff, C. Liddle, R. T. Yu, A. R. Atkins, H. Han, A. M. Lowy, M. T. Barrett, D. D. Engle, G. I. Evan, G. W. Yeo, M. Downes and R. M. Evans (2023). "A super-enhancer-regulated RNA-binding protein cascade drives pancreatic cancer." Nat Commun 14(1): 5195.

Asangani, I. A., V. L. Dommeti, X. Wang, R. Malik, M. Cieslik, R. Yang, J. Escara-Wilke, K. Wilder-Romans, S. Dhanireddy, C. Engelke, M. K. Iyer, X. Jing, Y. M. Wu, X. Cao, Z. S. Qin, S. Wang, F. Y. Feng and A. M. Chinnaiyan (2014). "Therapeutic targeting of BET bromodomain proteins in castration-resistant prostate cancer." Nature 510(7504): 278-282.

Bailey, P., D. K. Chang, M. A. Forget, F. A. Lucas, H. A. Alvarez, C. Haymaker, C. Chattopadhyay, S. H. Kim, S. Ekmekcioglu, E. A. Grimm, A. V. Biankin, P. Hwu, A. Maitra and J. Roszik (2016). "Exploiting the neoantigen landscape for immunotherapy of pancreatic ductal adenocarcinoma." Sci Rep 6: 35848.

Barthel, S., C. Falcomata, R. Rad, F. J. Theis and D. Saur (2023). "Single-cell profiling to explore pancreatic cancer heterogeneity, plasticity and response to therapy." Nat Cancer 4(4): 454-467.

Bartosovic, M., M. Kabbe and G. Castelo-Branco (2021). "Single-cell CUT&Tag profiles histone modifications and transcription factors in complex tissues." Nat Biotechnol 39(7): 825-835.

Carstens, J. L., S. Yang, P. Correa de Sampaio, X. Zheng, S. Barua, K. M. McAndrews, A. Rao, J. K. Burks, A. D. Rhim and R. Kalluri (2021). "Stabilized epithelial phenotype of cancer cells in primary tumors leads to increased colonization of liver metastasis in pancreatic cancer." Cell Rep 35(2): 108990.

Cephas, A. T., W. L. Hwang, A. Maitra, O. Parnas and K. E. DelGiorno (2023). "It is better to light a candle than to curse the darkness: single-cell transcriptomics sheds new light on pancreas biology and disease." Gut 72(6): 1211-1219.

Ceribelli, M., P. N. Kelly, A. L. Shaffer, G. W. Wright, W. Xiao, Y. Yang, L. A. Mathews Griner, R. Guha, P. Shinn, J. M. Keller, D. Liu, P. R. Patel, M. Ferrer, S. Joshi, S. Nerle, P. Sandy, E. Normant, C. J. Thomas and L. M. Staudt (2014). "Blockade of oncogenic IkappaB kinase activity in diffuse large B-cell lymphoma by bromodomain and extraterminal domain protein inhibitors." Proc Natl Acad Sci U S A 111(31): 11365-11370.

Clark, C. E., S. R. Hingorani, R. Mick, C. Combs, D. A. Tuveson and R. H. Vonderheide (2007). "Dynamics of the immune reaction to pancreatic cancer from inception to invasion." Cancer Res 67(19): 9518-9527.

Dawson, M. A., R. K. Prinjha, A. Dittmann, G. Giotopoulos, M. Bantscheff, W. I. Chan, S. C. Robson, C. W. Chung, C. Hopf, M. M. Savitski, C. Huthmacher, E. Gudgin, D. Lugo, S. Beinke, T. D. Chapman, E. J. Roberts, P. E. Soden, K. R. Auger, O. Mirguet, K. Doehner, R. Delwel, A. K. Burnett, P. Jeffrey, G. Drewes, K. Lee, B. J. Huntly and T. Kouzarides (2011). "Inhibition of BET recruitment to chromatin as an effective treatment for MLL-fusion leukaemia." Nature 478(7370): 529-533.

Elyada, E., M. Bolisetty, P. Laise, W. F. Flynn, E. T. Courtois, R. A. Burkhart, J. A. Teinor, P. Belleau, G. Biffi, M. S. Lucito, S. Sivajothi, T. D. Armstrong, D. D. Engle, K. H. Yu, Y. Hao, C. L. Wolfgang, Y. Park, J. Preall, E. M. Jaffee, A. Califano, P. Robson and D. A. Tuveson (2019). "Cross-Species Single-Cell Analysis of Pancreatic Ductal Adenocarcinoma Reveals Antigen-Presenting Cancer-Associated Fibroblasts." Cancer Discov 9(8): 1102-1123.

Falcomata, C., S. Barthel, G. Schneider, R. Rad, M. Schmidt-Supprian and D. Saur (2023). "Context-Specific Determinants of the Immunosuppressive Tumor Microenvironment in Pancreatic Cancer." Cancer Discov 13(2): 278-297.

Ferri, E., C. Petosa and C. E. McKenna (2016). "Bromodomains: Structure, function and pharmacology of inhibition." Biochem Pharmacol 106: 1-18.

Georgiev, P., Y. Wang, E. S. Muise, M. L. Bandi, W. Blumenschein, M. Sathe, E. M. Pinheiro and S. D. Shumway (2019). "BET Bromodomain Inhibition Suppresses Human T Cell Function." Immunohorizons 3(7): 294-305.

Heinz, S., C. E. Romanoski, C. Benner and C. K. Glass (2015). "The selection and function of cell type-specific enhancers." Nat Rev Mol Cell Biol 16(3): 144-154.

Hnisz, D., B. J. Abraham, T. I. Lee, A. Lau, V. Saint-Andre, A. A. Sigova, H. A. Hoke and R. A. Young (2013). "Super-enhancers in the control of cell identity and disease." Cell 155(4): 934-947.

Hosein, A. N., H. Huang, Z. Wang, K. Parmar, W. Du, J. Huang, A. Maitra, E. Olson, U. Verma and R. A. Brekken (2019). "Cellular heterogeneity during mouse pancreatic ductal adenocarcinoma progression at single-cell resolution." JCI Insight 5(16).

House, I. G., P. Savas, J. Lai, A. X. Y. Chen, A. J. Oliver, Z. L. Teo, K. L. Todd, M. A. Henderson, L. Giuffrida, E. V. Petley, K. Sek, S. Mardiana, T. N. Gide, C. Quek, R. A. Scolyer, G. V. Long, J. S. Wilmott, S. Loi, P. K. Darcy and P. A. Beavis (2020). "Macrophage-Derived CXCL9 and CXCL10 Are Required for Antitumor Immune Responses Following Immune Checkpoint Blockade." Clin Cancer Res 26(2): 487-504.

Jahangir, M., O. Yazdani, M. S. Kahrizi, S. Soltanzadeh, H. Javididashtbayaz, A. Mivefroshan, S. Ilkhani and R. Esbati (2022). "Clinical potential of PD-1/PD-L1 blockade therapy for renal cell carcinoma (RCC): a rapidly evolving strategy." Cancer Cell Int 22(1): 401.

Kryczek, I., L. Zou, P. Rodriguez, G. Zhu, S. Wei, P. Mottram, M. Brumlik, P. Cheng, T. Curiel, L. Myers, A. Lackner, X. Alvarez, A. Ochoa, L. Chen and W. Zou (2006). "B7-H4 expression identifies a novel suppressive macrophage population in human ovarian carcinoma." J Exp Med 203(4): 871-881.

Kuang, D. M., Q. Zhao, C. Peng, J. Xu, J. P. Zhang, C. Wu and L. Zheng (2009). "Activated monocytes in peritumoral stroma of hepatocellular carcinoma foster immune privilege and disease progression through PD-L1." J Exp Med 206(6): 1327-1337.

Lin, W., P. Noel, E. H. Borazanci, J. Lee, A. Amini, I. W. Han, J. S. Heo, G. S. Jameson, C. Fraser, M. Steinbach, Y. Woo, Y. Fong, D. Cridebring, D. D. Von Hoff, J. O. Park and H. Han (2020). "Single-cell transcriptome analysis of tumor and stromal compartments of pancreatic ductal adenocarcinoma primary tumors and metastatic lesions." Genome Med 12(1): 80.

Loven, J., H. A. Hoke, C. Y. Lin, A. Lau, D. A. Orlando, C. R. Vakoc, J. E. Bradner, T. I. Lee and R. A. Young (2013). "Selective inhibition of tumor oncogenes by disruption of super-enhancers." Cell 153(2): 320-334.

Lu, C., P. S. Redd, J. R. Lee, N. Savage and K. Liu (2016). "The expression profiles and regulation of PD-L1 in tumor-induced myeloid-derived suppressor cells." Oncoimmunology 5(12): e1247135.

Mahat, D. B., N. D. Tippens, J. D. Martin-Rufino, S. K. Waterton, J. Fu, S. E. Blatt and P. A. Sharp (2023). "Single-cell nascent RNA sequencing using click-chemistry unveils coordinated transcription." bioRxiv.

Malik, S., J. M. Westcott, R. A. Brekken and F. J. Burrows (2021). "CXCL12 in Pancreatic Cancer: Its Function and Potential as a Therapeutic Drug Target." Cancers (Basel) 14(1).

Menjivar, R. E., Z. C. Nwosu, W. Du, K. L. Donahue, H. S. Hong, C. Espinoza, K. Brown, A. Velez-Delgado, W. Yan, F. Lima, A. Bischoff, P. Kadiyala, D. Salas-Escabillas, H. C. Crawford, F. Bednar, E. Carpenter, Y. Zhang, C. J. Halbrook, C. A. Lyssiotis and M. Pasca di Magliano (2023). "Arginase 1 is a key driver of immune suppression in pancreatic cancer." Elife 12.

Nakagawa, A., C. E. Adams, Y. Huang, S. R. Hamarneh, W. Liu, K. N. Von Alt, M. Mino-Kenudson, R. A. Hodin, K. D. Lillemoe, C. Fernandez-Del Castillo, A. L. Warshaw and A. S. Liss (2016). "Selective and reversible suppression of intestinal stem cell differentiation by pharmacological inhibition of BET bromodomains." Sci Rep 6: 20390.

Ohta, K., H. Shigeishi, M. Taki, H. Nishi, K. Higashikawa, M. Takechi and N. Kamata (2008). "Regulation of CXCL9/10/11 in oral keratinocytes and fibroblasts." J Dent Res 87(12): 1160-1165.

Peng, J., B. F. Sun, C. Y. Chen, J. Y. Zhou, Y. S. Chen, H. Chen, L. Liu, D. Huang, J. Jiang, G. S. Cui, Y. Yang, W. Wang, D. Guo, M. Dai, J. Guo, T. Zhang, Q. Liao, Y. Liu, Y. L. Zhao, D. L. Han, Y. Zhao, Y. G. Yang and W. Wu (2019). "Single-cell RNA-seq highlights intra-tumoral heterogeneity and malignant progression in pancreatic ductal adenocarcinoma." Cell Res 29(9): 725-738.

Peng, Y. P., Y. Zhu, J. J. Zhang, Z. K. Xu, Z. Y. Qian, C. C. Dai, K. R. Jiang, J. L. Wu, W. T. Gao, Q. Li, Q. Du and Y. Miao (2013). "Comprehensive analysis of the percentage of surface receptors and cytotoxic granules positive natural killer cells in patients with pancreatic cancer, gastric cancer, and colorectal cancer." J Transl Med 11: 262.

Philip, M., L. Fairchild, L. Sun, E. L. Horste, S. Camara, M. Shakiba, A. C. Scott, A. Viale, P. Lauer, T. Merghoub, M. D. Hellmann, J. D. Wolchok, C. S. Leslie and A. Schietinger (2017). "Chromatin states define tumour-specific T cell dysfunction and reprogramming." Nature 545(7655): 452-456.

Pott, S. and J. D. Lieb (2015). "What are super-enhancers?" Nat Genet 47(1): 8-12.

Provenzano, P. P., C. Cuevas, A. E. Chang, V. K. Goel, D. D. Von Hoff and S. R. Hingorani (2012). "Enzymatic targeting of the stroma ablates physical barriers to treatment of pancreatic ductal adenocarcinoma." Cancer Cell 21(3): 418-429.

Puissant, A., S. M. Frumm, G. Alexe, C. F. Bassil, J. Qi, Y. H. Chanthery, E. A. Nekritz, R. Zeid, W. C. Gustafson, P. Greninger, M. J. Garnett, U. McDermott, C. H. Benes, A. L. Kung, W. A. Weiss, J. E. Bradner and K. Stegmaier (2013). "Targeting MYCN in neuroblastoma by BET bromodomain inhibition." Cancer Discov 3(3): 308-323.

Raghavan, S., P. S. Winter, A. W. Navia, H. L. Williams, A. DenAdel, K. E. Lowder, J. Galvez-Reyes, R. L. Kalekar, N. Mulugeta, K. S. Kapner, M. S. Raghavan, A. A. Borah, N. Liu, S. A. Vayrynen, A. D. Costa, R. W. S. Ng, J. Wang, E. K. Hill, D. Y. Ragon, L. K. Brais, A. M. Jaeger, L. F. Spurr, Y. Y. Li, A. D. Cherniack, M. A. Booker, E. F. Cohen, M. Y. Tolstorukov, I. Wakiro, A. Rotem, B. E. Johnson, J. M. McFarland, E. T. Sicinska, T. E. Jacks, R. J. Sullivan, G. I. Shapiro, T. E. Clancy, K. Perez, D. A. Rubinson, K. Ng, J. M. Cleary, L. Crawford, S. R. Manalis, J. A. Nowak, B. M. Wolpin, W. C. Hahn, A. J. Aguirre and A. K. Shalek (2021). "Microenvironment drives cell state, plasticity, and drug response in pancreatic cancer." Cell 184(25): 6119-6137 e6126.

Rizvi, N. A., M. D. Hellmann, A. Snyder, P. Kvistborg, V. Makarov, J. J. Havel, W. Lee, J. Yuan, P. Wong, T. S. Ho, M. L. Miller, N. Rekhtman, A. L. Moreira, F. Ibrahim, C. Bruggeman, B. Gasmi, R. Zappasodi, Y. Maeda, C. Sander, E. B. Garon, T. Merghoub, J. D. Wolchok, T. N. Schumacher and T. A. Chan (2015). "Cancer immunology. Mutational landscape determines sensitivity to PD-1 blockade in non-small cell lung cancer." Science 348(6230): 124-128.

Royal, R. E., C. Levy, K. Turner, A. Mathur, M. Hughes, U. S. Kammula, R. M. Sherry, S. L. Topalian, J. C. Yang, I. Lowy and S. A. Rosenberg (2010). "Phase 2 trial of single agent

Ipilimumab (anti-CTLA-4) for locally advanced or metastatic pancreatic adenocarcinoma." J Immunother 33(8): 828-833.

Schlesinger, Y., O. Yosefov-Levi, D. Kolodkin-Gal, R. Z. Granit, L. Peters, R. Kalifa, L. Xia, A. Nasereddin, I. Shiff, O. Amran, Y. Nevo, S. Elgavish, K. Atlan, G. Zamir and O. Parnas (2020). "Single-cell transcriptomes of pancreatic preinvasive lesions and cancer reveal acinar metaplastic cells' heterogeneity." Nat Commun 11(1): 4516.

Semenkovich, N. P., J. D. Planer, P. P. Ahern, N. W. Griffin, C. Y. Lin and J. I. Gordon (2016). "Impact of the gut microbiota on enhancer accessibility in gut intraepithelial lymphocytes." Proc Natl Acad Sci U S A 113(51): 14805-14810.

Sherman, M. H., R. T. Yu, T. W. Tseng, C. M. Sousa, S. Liu, M. L. Truitt, N. He, N. Ding, C. Liddle, A. R. Atkins, M. Leblanc, E. A. Collisson, J. M. Asara, A. C. Kimmelman, M. Downes and R. M. Evans (2017). "Stromal cues regulate the pancreatic cancer epigenome and metabolome." Proc Natl Acad Sci U S A 114(5): 1129-1134.

Shi, Y., W. Gao, N. K. Lytle, P. Huang, X. Yuan, A. M. Dann, M. Ridinger-Saison, K. E. DelGiorno, C. E. Antal, G. Liang, A. R. Atkins, G. Erikson, H. Sun, J. Meisenhelder, E. Terenziani, G. Woo, L. Fang, T. P. Santisakultarm, U. Manor, R. Xu, C. R. Becerra, E. Borazanci, D. D. Von Hoff, P. M. Grandgenett, M. A. Hollingsworth, M. Leblanc, S. E. Umetsu, E. A. Collisson, M. Scadeng, A. M. Lowy, T. R. Donahue, T. Reya, M. Downes, R. M. Evans, G. M. Wahl, T. Pawson, R. Tian and T. Hunter (2019). "Targeting LIF-mediated paracrine interaction for pancreatic cancer therapy and monitoring." Nature 569(7754): 131-135.

Sinha, A., D. V. Faller and G. V. Denis (2005). "Bromodomain analysis of Brd2-dependent transcriptional activation of cyclin A." Biochem J 387(Pt 1): 257-269.

Snyder, A., V. Makarov, T. Merghoub, J. Yuan, J. M. Zaretsky, A. Desrichard, L. A. Walsh, M. A. Postow, P. Wong, T. S. Ho, T. J. Hollmann, C. Bruggeman, K. Kannan, Y. Li, C. Elipenahli, C. Liu, C. T. Harbison, L. Wang, A. Ribas, J. D. Wolchok and T. A. Chan (2014). "Genetic basis for clinical response to CTLA-4 blockade in melanoma." N Engl J Med 371(23): 2189-2199.

Srivastava, M. K., P. Sinha, V. K. Clements, P. Rodriguez and S. Ostrand-Rosenberg (2010). "Myeloid-derived suppressor cells inhibit T-cell activation by depleting cystine and cysteine." Cancer Res 70(1): 68-77.

Stathis, A., E. Zucca, M. Bekradda, C. Gomez-Roca, J. P. Delord, T. de La Motte Rouge, E. Uro-Coste, F. de Braud, G. Pelosi and C. A. French (2016). "Clinical Response of Carcinomas Harboring the BRD4-NUT Oncoprotein to the Targeted Bromodomain Inhibitor OTX015/MK-8628." Cancer Discov 6(5): 492-500.

Tokunaga, R., W. Zhang, M. Naseem, A. Puccini, M. D. Berger, S. Soni, M. McSkane, H. Baba and H. J. Lenz (2018). "CXCL9, CXCL10, CXCL11/CXCR3 axis for immune activation - A target for novel cancer therapy." Cancer Treat Rev 63: 40-47.

Veselov, V. V., A. E. Nosyrev, L. Jicsinszky, R. N. Alyautdin and G. Cravotto (2022). "Targeted Delivery Methods for Anticancer Drugs." Cancers (Basel) 14(3).

Voutsadakis, I. A. (2022). "Urothelial Bladder Carcinomas with High Tumor Mutation Burden Have a Better Prognosis and Targetable Molecular Defects beyond Immunotherapies." Curr Oncol 29(3): 1390-1407.

Werba, G., D. Weissinger, E. A. Kawaler, E. Zhao, D. Kalfakakou, S. Dhara, L. Wang, H. B. Lim, G. Oh, X. Jing, N. Beri, L. Khanna, T. Gonda, P. Oberstein, C. Hajdu, C. Loomis, A. Heguy, M. H. Sherman, A. W. Lund, T. H. Welling, I. Dolgalev, A. Tsirigos and D. M. Simeone (2023). "Single-cell RNA sequencing reveals the effects of chemotherapy on human pancreatic adenocarcinoma and its tumor microenvironment." Nat Commun 14(1): 797.

Whyte, W. A., D. A. Orlando, D. Hnisz, B. J. Abraham, C. Y. Lin, M. H. Kagey, P. B. Rahl, T. I. Lee and R. A. Young (2013). "Master transcription factors and mediator establish super-enhancers at key cell identity genes." Cell 153(2): 307-319.

Xie, D. and K. Xie (2015). "Pancreatic cancer stromal biology and therapy." Genes Dis 2(2): 133-143.

Xie, F., M. Huang, X. Lin, C. Liu, Z. Liu, F. Meng, C. Wang and Q. Huang (2018). "The BET inhibitor I-BET762 inhibits pancreatic ductal adenocarcinoma cell proliferation and enhances the therapeutic effect of gemcitabine." Sci Rep 8(1): 8102.

Yang, Z., N. He and Q. Zhou (2008). "Brd4 recruits P-TEFb to chromosomes at late mitosis to promote G1 gene expression and cell cycle progression." Mol Cell Biol 28(3): 967-976.

Yousuf, S., M. Qiu, L. Voith von Voithenberg, J. Hulkkonen, I. Macinkovic, A. R. Schulz, D. Hartmann, F. Mueller, M. Mijatovic, D. Ibberson, K. T. AlHalabi, J. Hetzer, S. Anders, B. Brune, H. E. Mei, C. D. Imbusch, B. Brors, M. Heikenwalder, M. M. Gaida, M. W. Buchler, A. Weigert, T. Hackert and S. Roth (2023). "Spatially Resolved Multi-Omics Single-Cell Analyses Inform Mechanisms of Immune Dysfunction in Pancreatic Cancer." Gastroenterology 165(4): 891-908 e814.

Zhang, Y., J. Lazarus, N. G. Steele, W. Yan, H. J. Lee, Z. C. Nwosu, C. J. Halbrook, R. E. Menjivar, S. B. Kemp, V. R. Sirihorachai, A. Velez-Delgado, K. Donahue, E. S. Carpenter, K. L. Brown, V. Irizarry-Negron, A. C. Nevison, A. Vinta, M. A. Anderson, H. C. Crawford, C. A. Lyssiotis, T. L. Frankel, F. Bednar and M. Pasca di Magliano (2020). "Regulatory T-cell Depletion Alters the Tumor Microenvironment and Accelerates Pancreatic Carcinogenesis." Cancer Discov 10(3): 422-439.

Zhang, Y., A. Velez-Delgado, E. Mathew, D. Li, F. M. Mendez, K. Flannagan, A. D. Rhim, D. M. Simeone, G. L. Beatty and M. Pasca di Magliano (2017). "Myeloid cells are required for PD-1/PD-L1 checkpoint activation and the establishment of an immunosuppressive environment in pancreatic cancer." Gut 66(1): 124-136.

Chapter 3 Harnessing BET Inhibitors for PDAC Immunotherapy: Bridging Insights to Applications

Introduction

In the preceding chapter, we explored the impact of BET inhibitors (BETi) in disrupting the iTME in PDAC. Our investigation revealed that while BETi alone can impede tumor progression, it does not fully restore the anti-tumor T cell response. However, the combination of BETi and αPDL1 exhibited a remarkable enhancement in CD8 T cell accumulation within PDAC tumors, resulting in a further substantial reduction of tumor burden. This aligns with the rationale behind exploring the therapeutic benefits of combining targeted therapy (such as BETi) and immunotherapy (such as αPDL1) in PDAC treatment as previously described.

However, several limitations exist in testing the survival benefit of BETi+αPDL1 in mouse models of PDAC. Firstly, given that the current standard of care for PDAC involves chemotherapy (Jiang and Sohal 2023), it is imperative to explore how chemotherapy could impact the efficacy of BETi+αPDL1. Secondly, BETi has been reported to have toxicity concerns, necessitating careful consideration of dosing applications to ensure suitability for long-term treatments. Moreover, the potential impact of BETi on cell proliferation raises concerns about its systemic delivery impairing T cell development in secondary lymphoid organs, which could limit its ability to promote T cell responses in combination with αPDL1 when administered as a free drug. To address these limitations, this chapter adopts three separate strategies to: 1. Investigate the impact of gemcitabine in conjunction with OTX+αPDL1 treatment. 2. Test different dosing strategies to minimize OTX toxicity for long-term applications. 3. Explore the efficacy of nanoparticles in facilitating tumor-specific OTX delivery while reducing systemic toxicity.

The rationale for combining chemotherapy with BETi+αPDL1 stems from chemotherapy's potential to induce tumor cell death, leading to the release of tumor antigens that facilitate T cell priming. Concurrently, tumor cell death promotes an inflammatory response by releasing damage-associated molecular patterns (DAMPs) and inflammatory mediators within the tumor (Zhang, Zhou et al. 2022), thereby facilitating immune cell recruitment. Moreover, chemotherapy has demonstrated the ability in various cancer types to reduce the number of myeloid-derived suppressor cells (MDSC) that can impair anti-tumor T cell response (Koinis, Vetsika et al. 2016) (Eriksson, Wenthe et al. 2016). These effects suggest the potential to enhance the efficacy of BETi+αPDL1 with chemotherapy.

Despite the promising potential of BETi, their clinical utility is hindered by notable toxicity, including common hematological adverse events such as thrombocytopenia, anemia, and neutropenia. Non-hematological syndromes, including diarrhea, nausea, fatigue, dysgeusia, myocardial infarction and arrhythmias have also been reported (Sun, Han et al. 2020) (Piquereau, Boet et al. 2019). Such toxicity can be minimized through lower dosages, less frequent dosing strategies, or periodic dosing that allows recipients to recover from cumulative toxicity during a drug-free window. However, considering the relatively short half-life of clinical BETi compounds like OTX-015 (3-7 hours) and iBET-762 (3-7 hours), less than daily applications of BETi would likely reduce their effectiveness. Striking a careful balance between BETi toxicity and efficacy is imperative, especially in the context of combination therapies where the toxicity of other drugs, such as gemcitabine or αPDL1, must also be considered.

In addition to systemic toxicity, another major hurdle for PDAC drug development is the challenge of intra-tumoral drug delivery. The hypovascularized and hyper-pressured PDAC stroma has been reported to hinder the administration of small molecule drugs such as gemcitabine

(Jacobetz, Chan et al. 2013). However, the emergence of nanoparticle drug carriers presents a promising avenue in solid tumor therapeutics, offering a strategic approach to enhance drug delivery into the tumor while mitigating systemic toxicity. Various types of nanomaterial-based carriers, including polymeric, lipidic, inorganic, and vesicular nanoparticles (Liu, Kshirsagar et al. 2022), can be designed to meet diverse drug delivery needs. These carriers work through the conjugation or encapsulation of therapeutic payloads, providing advantages such as prolonged circulation, site-specific delivery, controllable release, reduced side effects, and even co-delivery of multiple agents (Hou, Yang et al. 2022). Notably, nanoparticle-aided drug delivery holds significant promise for PDAC therapy, as nanoparticles, with proper size control, can penetrate the dense PDAC stroma where molecular drugs face challenges (Meng and Nel 2018). FDA-approved nano-formulated chemotherapy drugs, such as albumin-bound paclitaxel (nab-paclitaxel) (Yardley 2013) and liposomal irinotecan+5-fluorouracil (Frampton 2020), have demonstrated improved distribution, lower toxicity, and superior therapeutic outcomes compared to their free drug counterparts. Numerous other nanoparticle drugs are currently undergoing clinical trials to enhance PDAC immunotherapy (Hou, Yang et al. 2022). Here, we investigate the role of nanoparticle conjugation in concentrating BETi within PDAC tumors while mitigating systemic toxicity.

3.1 Chemotherapy does not potentiate synergistic effect of OTX and αPDL1 combination treatment

It has been previously reported in pancreatic cancer that BETi can serve as effective monotherapy due to their suppressive impact on both tumor cells and pancreatic stellate cells (PSCs) (Jauset, Masso-Valles et al. 2018) (Kumar, DeCant et al. 2017) (Garcia, Miller et al. 2016). To investigate whether chemotherapy could synergize with BETi in the absence of immune checkpoint inhibitors, we conducted *in vitro* co-treatment experiments with OTX and gemcitabine on PDAC1245-GFP cells, revealing a significant synergy between the two (Figure 3.1). Notably, similar synergies were also observed between OTX and other chemotherapy drugs, including Paclitaxel, SN38, Mitomycin C and Cisplatin (data not shown).

However, when tested in an orthotopic mouse model of PDAC, where gemcitabine and OTX each separately slowed down tumor growth, combining the two did not result in a further reduction of tumor burden (Figure 3.2). This outcome aligns with prior research demonstrating that JQ1, another BETi, and gemcitabine did not synergize in a KPC mouse model of PDAC (Mazur, Herner et al. 2015). In contrast, patient-derived xenograft PDAC models showed synergistic responses between JQ1, iBET-762, and gemcitabine (Miller, Garcia et al. 2021) (Xie, Huang et al. 2018). This discrepancy may be attributed to differences between mouse and human cells or the absence of a T cell response in xenograft PDAC models. Importantly, the lack of synergy in mouse PDAC tumors may be due to *in vivo* complexity, where factors such as absorption, distribution, metabolism, excretion, and toxicity (ADMET) can influence drug pharmacokinetics and pharmacodynamics. The differential ADMET of BETi and gemcitabine could lead to a suboptimal drug ratio, falling outside the synergy range observed *in vitro*.

As previously discussed, chemotherapy has the potential to synergize with BETi+αPDL1 to induce anti-tumor T cell responses. To explore this, we initially examined the combination of

gemcitabine and αPDL1 on orthotopic PDAC tumors, but no synergy was observed between these two agents (Figure 3.3). Given our previous data indicating the insufficiency of αPDL1 in inducing an anti-tumor T cell response on its own, we next investigated whether gemcitabine could enhance the efficacy of BETi+αPDL1 combination treatment. Surprisingly, co-treatment with gemcitabine inhibited, rather than promoted, CD8 T cell accumulation induced by BETi+αPDL1 treatment in PDAC tumors (Figure 3.4). This unexpected result may be attributed to the possibility that the function of chemotherapy in blocking rapidly proliferating cells not only affects tumor cells but also naïve and mature T cells, as supported by existing literature (Das, O'Connor et al. 2020) (Das, Vernau et al. 2019).

In light of these findings, we have chosen to optimize BETi+αPDL1 therapy independently of chemotherapy for PDAC treatment. However, it is crucial to note that the immune stimulatory potential of chemotherapy may be better realized with optimized dosage and application windows (Truong, Gargett et al. 2021).

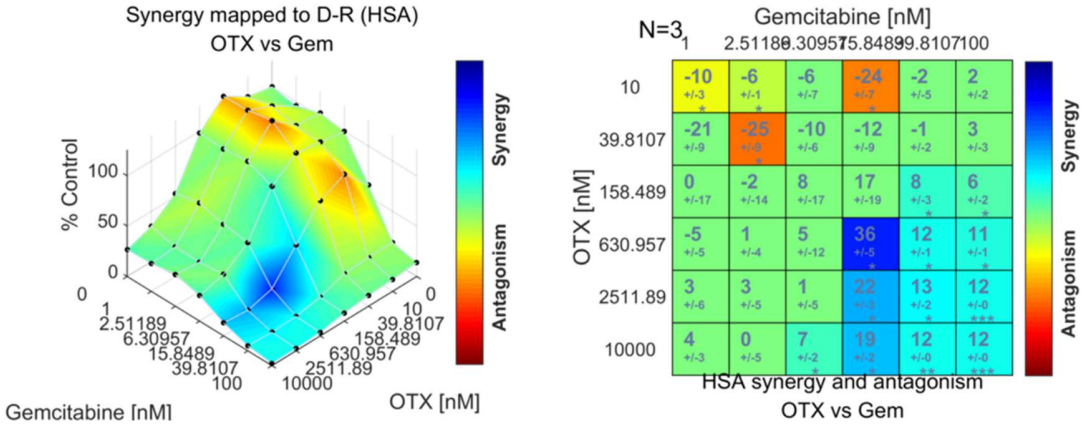

Figure 3.1 Synergy analysis of OTX and gemcitabine on PDAC1245-GFP tumor cells *in vitro*.

Each data point represents the average of triplicates. Synergy analysis was performed with Combenefit software. Both graphical heatmap plot (left) and synergy score table (right) are presented.

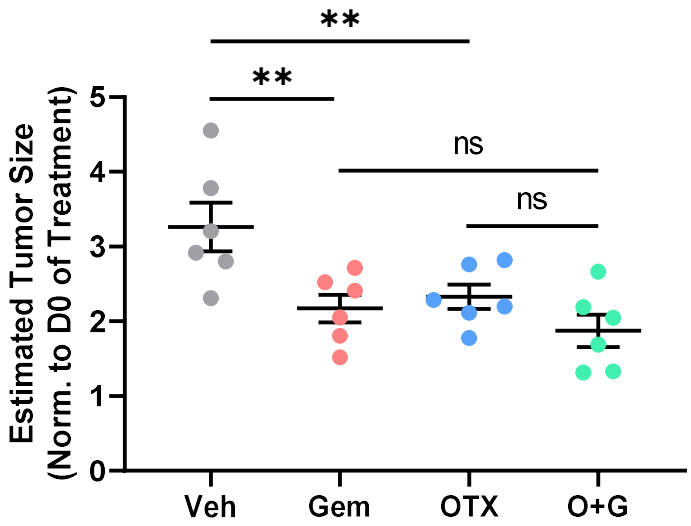

Figure 3.2 Impact on orthotopic tumor growth by OTX and gemcitabine *in vivo*.

PDAC1245-GFP bearing mice were treated with 10mg/kg gemcitabine (once every three days, i.p.) and/or 75mg/kg OTX (daily, o.g.) for two weeks. Tumor volume was measured by ultrasound imaging. Data are presented as dot plots, with each dot representing an individual tumor, horizontal lines indicating means and error bars indicating SEMs. Data significance was analyzed by Ordinary one-way ANOVA in Prism. **P<0.01.

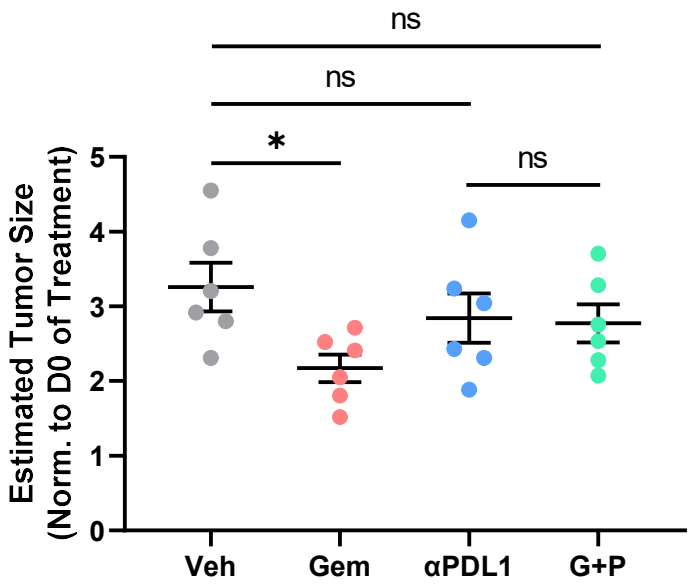

Figure 3.3 Impact on orthotopic tumor growth by αPDL1 and gemcitabine *in vivo*.

PDAC1245-GFP bearing mice were treated with 10mg/kg gemcitabine (once every three days, i.p.) and/or 10mg/kg αPDL1 (once every three days, i.p.) for two weeks. Tumor volume was measured by ultrasound imaging. Data are presented as dot plots, with each dot representing an individual tumor, horizontal lines indicating means and error bars indicating SEMs. Data significance was analyzed by Ordinary one-way ANOVA in Prism. *P<0.05.

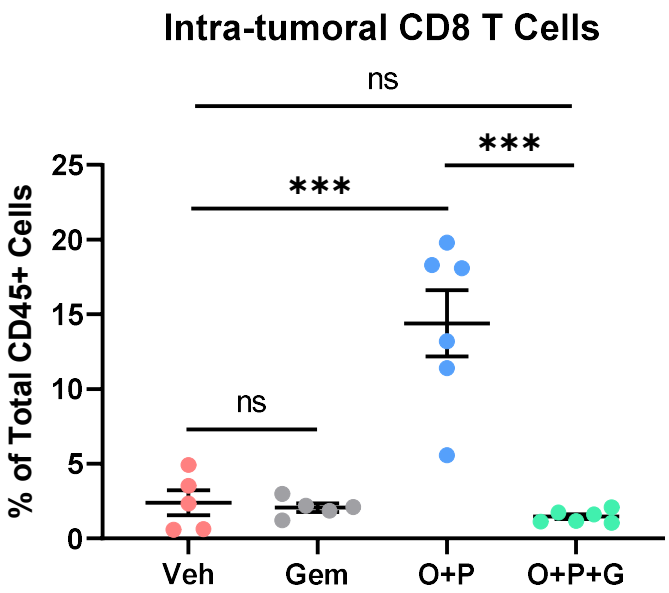

Figure 3.4 Impact on intra-tumoral CD8 T cell accumulation by O+P and gemcitabine *in vivo*.

PDAC1245-GFP bearing mice were treated with 10mg/kg gemcitabine (once every three days, i.p.), and/or 75mg/kg OTX (daily, o.g.)+10mg/kg αPDL1 (once every three days, i.p.) for two weeks. Intra-tumoral CD8 T cell accumulation was measured by flow cytometry. Data are presented as dot plots, with each dot representing an individual tumor, horizontal lines indicating means and error bars indicating SEMs. Data significance was analyzed by Ordinary one-way ANOVA in Prism. ***P<0.001.

3.2 Toxicity effect of OTX can be partially reduced with alternative dosing strategies

With previous findings of OTX+αPDL1 on synergistically reducing tumor burden, we next assessed whether this effect translated into a survival benefit in mice bearing PDAC. Unfortunately, daily treatment with 75mg/kg OTX daily in combination with αPDL1 did not result in a significant extension of lifespan (Figure 3.5). Upon closer examination of mice in each group, it became evident that mice treated with OTX or OTX+αPDL1 often succumbed with smaller and less advanced PDAC tumors compared to those treated with vehicle or αPDL1. However, these mice exhibited symptoms of body weight loss, pale liver, and bloody ascites at a higher frequency (data not shown), raising concerns about the toxicity associated with the current OTX dosing strategy (75mg/kg daily) in the long term. Indeed, the dose-limiting toxicities of BETi have been previously documented (Cochran, Conery et al. 2019).

We next investigated whether BETi toxicity could be mitigated with alternative OTX dosing strategies. This included lowering the dose of OTX from 75mg/kg daily (high dose) to 50mg/kg daily (medium dose) or providing mice with a one-week break after two weeks of OTX (75mg/kg daily) treatment. Results indicated that medium dose of OTX could still induce intra-tumoral CD8 T cell accumulation in combination with αPDL1 after three weeks of treatment. However, when mice were given a one-week break from OTX treatment, the enhanced T cell phenotype could no longer be observed in the tumor (Figure 3.6). These results suggest that the modulatory effect of BETi on the iTME cannot be maintained when BETi treatment is discontinued.

To further explore the impact of alternative BETi dosing strategies on the synergistic efficacy with αPDL1, we then treated PDAC-bearing mice with either 37.5mg/kg OTX daily (low dose) or 75mg/kg OTX once every two days (low frequency). The results indicated that neither of

these dosing strategies could maintain the CD8 T cell accumulation phenotype observed with high daily doses of OTX treatment after 2.5 weeks (Figure 3.7). Notably, as the treatment duration increased, both strategies resulted in a significant improvement in survival in PDAC-bearing mice, suggesting reduced toxicity with lower OTX dosages (Figure 3.8 and 3.9). However, the synergistic effect between OTX and αPDL1 was not significant in both survival assays.

In summary, our findings indicate that the synergistic phenotype of BETi and αPDL1 in promoting anti-tumor T cell responses requires sustained treatment with BETi at high dosages. However, the current dosing strategy for OTX in its free drug form is suboptimal for therapeutic purposes, given concerns regarding both toxicity and efficacy. Therefore, optimization beyond dosing strategy is imperative to ensure adequate concentration of BETi within the tumor while minimizing systemic impact on healthy organs.

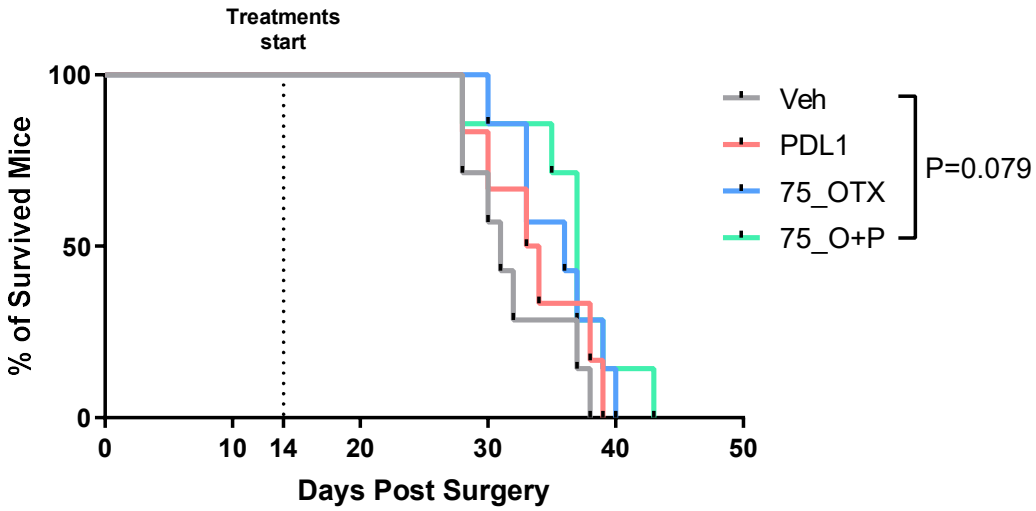

Figure 3.5 Survival impact on orthotopic PDAC mouse model with O+P treatment.

Survival study of mice bearing orthotopically transplanted PDAC1245-GFP tumor. Mice were treated with 75mg/kg OTX (daily, o.g.) and/or 10mg/kg αPDL1 (once every three days, i.p.). Data significance was analyzed by Log-rank test in Prism. P value is indicated in the figure.

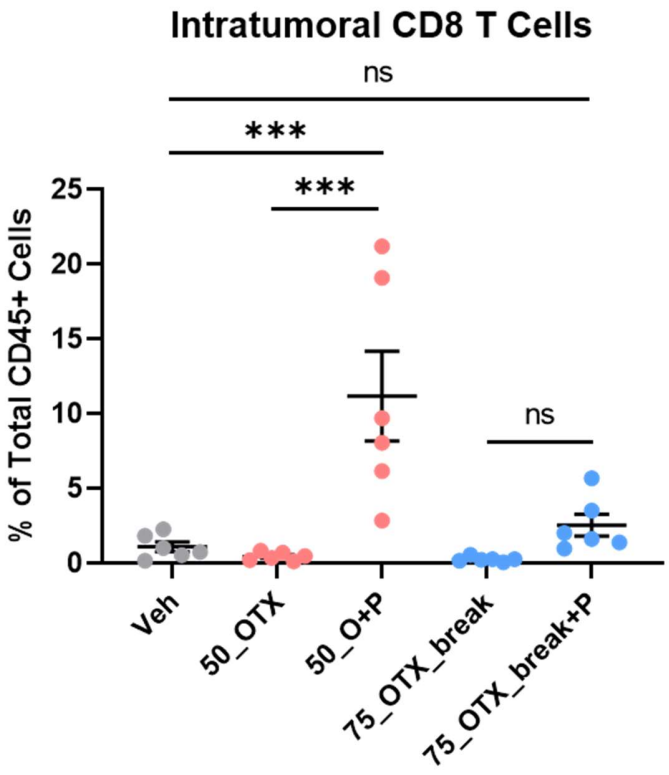

Figure 3.6 Impact on intra-tumoral CD8 T cell accumulation with alternative O+P dosing strategies *in vivo*.

PDAC1245-GFP bearing mice were treated with 10mg/kg αPDL1 (once every three days, i.p.) for three weeks in combination with 50mg/kg OTX (daily for three weeks, o.g.) or 75 mg/kg OTX (daily for two weeks followed by one week break, o.g.). Intra-tumoral CD8 T cell accumulation was measured by flow cytometry. Data are presented as dot plots, with each dot representing an individual tumor, horizontal lines indicating means and error bars indicating SEMs. Data significance was analyzed by Ordinary one-way ANOVA in Prism. ***P<0.001.

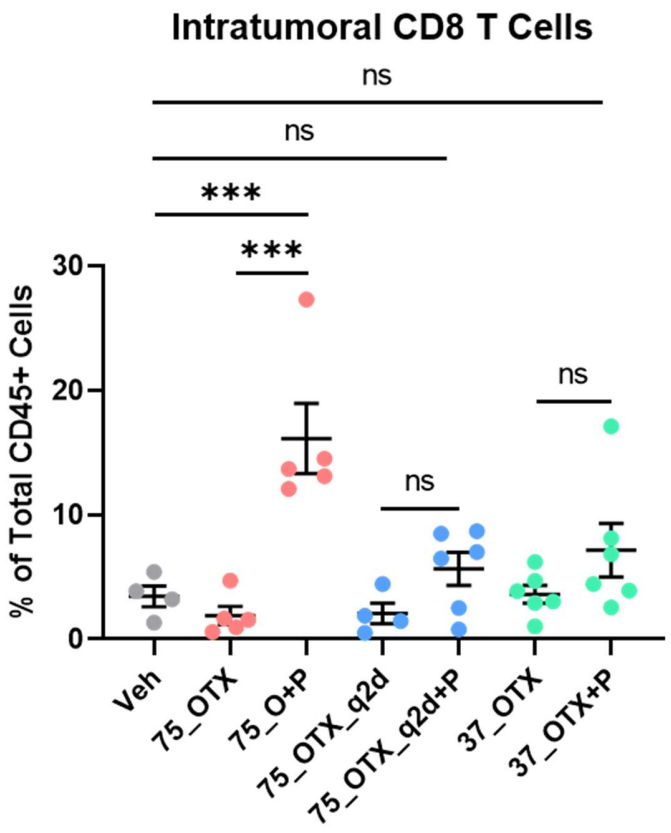

Figure 3.7 Impact on intra-tumoral CD8 T cell accumulation with alternative O+P dosing strategies *in vivo*.

PDAC1245-GFP bearing mice were treated with 10mg/kg αPDL1 (once every three days, i.p.) for two and half weeks in combination with 75mg/kg OTX (daily, o.g.) or 75 mg/kg OTX (q2d, once every 2 days, o.g.) or 37.5mg/kg OTX (daily, o.g.). Intra-tumoral CD8 T cell accumulation was measured by flow cytometry. Data are presented as dot plots, with each dot representing an individual tumor, horizontal lines indicating means and error bars indicating SEMs. Data significance was analyzed by Ordinary one-way ANOVA in Prism. ***P<0.001.

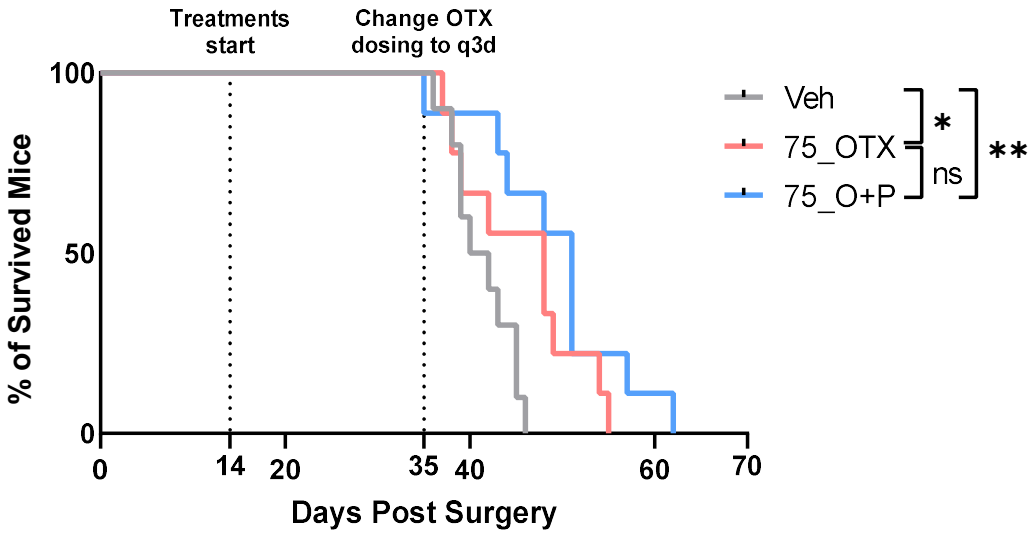

Figure 3.8 Survival impact on orthotopic PDAC mouse model with alternative O+P dosing strategies.

Survival study of mice bearing orthotopically transplanted PDAC1245-GFP tumor. Mice were treated with 10mg/kg αPDL1 (once every three days, i.p.) in combination with 75mg/kg OTX (daily, o.g.) for three weeks, after which dosing strategy for OTX was switched to 75mg/kg once every 3 days o.g.. Data significance was analyzed by Log-rank test in Prism. *P<0.05, **P<0.01.

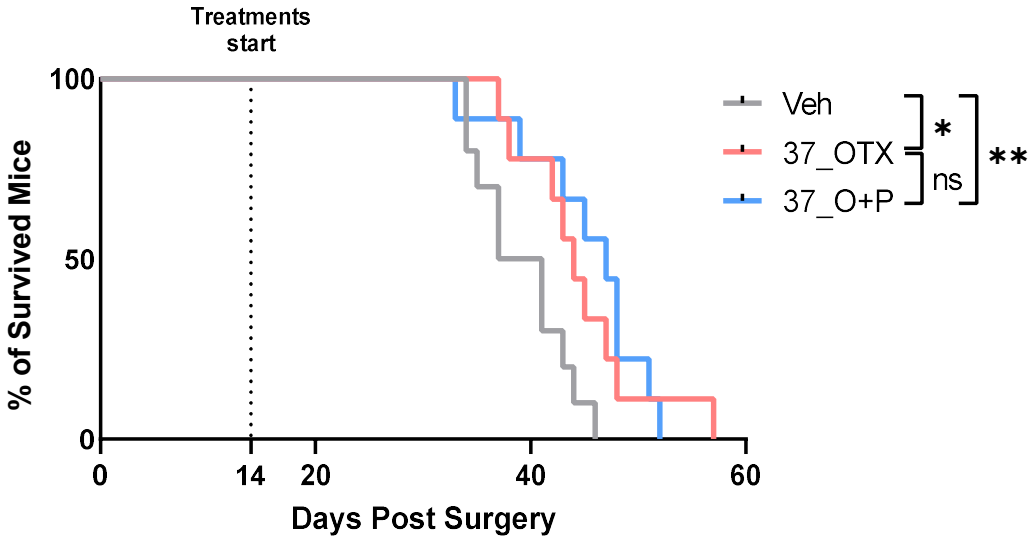

Figure 3.9 Survival impact on orthotopic PDAC mouse model with alternative O+P dosing strategies.

Survival study of mice bearing orthotopically transplanted PDAC1245-GFP tumor. Mice were treated with 10mg/kg αPDL1 (once every three days, i.p.) in combination with 37.5mg/kg OTX (daily, o.g.). Data significance was analyzed by Log-rank test in Prism. *P<0.05, **P<0.01.

3.3 BPD nanoparticles enable PDAC tumor-specific drug delivery and reduce toxicity

Given the challenge posed by the paradoxical nature of BETi's toxicity and efficacy, alternative dosing strategies alone may not effectively address this issue. Therefore, we turned to nanoparticle technologies to enhance tumor delivery and reduce systemic toxicity.

Previous research conducted in Jeremiah Johnson's group has demonstrated the effectiveness of the Bottlebrush Polymer Prodrug (BPD) platform, a nanoparticle-aided drug delivery system (Johnson, Lu et al. 2010). This system involves conjugating target drugs and polyethylene-glycol (PEG)-based polymers with switchable linkers, allowing for preferential drug accumulation in specific organs/tissues by adjusting the size of nanoparticles determined by the degree of PEG polymerization. Moreover, it enables condition-specific drug release using different linkers, such as ester-based linkers for targeted drug release in tumor tissue with high esterase activity. In their recent work, Jeremiah Johnson's team demonstrated the efficacy of BPD-OTX in treating a mouse model of triple-negative breast cancer, showing improved drug accumulation and OTX release within tumor tissue compared to free OTX. Importantly, BPD-OTX inhibited tumor growth more effectively than an equivalent dose of free OTX without inducing toxicity-related body weight loss (Vohidov, Andersen et al. 2021). While their study focused on a different tumor type, it underscores the feasibility of enhancing BETi efficacy and reducing its toxicity using BPD nanoparticles.

To assess the applicability of this technique in PDAC tumors, we collaborated with Jeremiah Johnson’s Lab and obtained BPD-OTX nanoparticles (Figure 3.10). To evaluate their tumor-accumulation effect, Cyanine 5.5-labeled nanoparticles (BPD-Cy5.5) were utilized in mice bearing orthotopic PDAC tumors. The results demonstrated a preferential accumulation of Cy5.5 fluorescence in PDAC tumors compared to other organs (Figure 3.11). Subsequently, to assess the

on-target efficacy of nanoparticle-aided BETi delivery in PDAC tumors, BPD-OTX and free-OTX were administered to mice with orthotopic PDAC tumors, evaluating their impact on blocking immunosuppressive gene expression in intra-tumoral stromal cells, as introduced in the previous chapter. The results showed comparable efficacy between BPD-OTX q3d and free-OTX q1d in blocking the immunosuppressive potential of tumor-associated macrophages (TAMs) in PDAC tumors (Figure 3.12). Furthermore, when tested in combination with immune checkpoint inhibitors, BPD-OTX q3d exhibited superior synergy with αPDL1 in enhancing intra-tumoral CD8 T cell accumulation compared to free-OTX q1d (Figures 3.13 and 3.14).

Taken together, these findings validate the functionality of BPD nanoparticles in promoting BETi accumulation in PDAC tumors and reducing its toxicity impact on other organs. This encourages further evaluation of BPD-OTX+αPDL1 on the survival of PDAC-bearing mice in future studies. Notably, the observation that BPD-OTX, enriched in the tumor, still synergizes with αPDL1 indicates that mechanistically, BETi's direct impact on tumor tissue, rather than secondary lymphoid organs, should account for its synergy with immune checkpoint inhibitors.

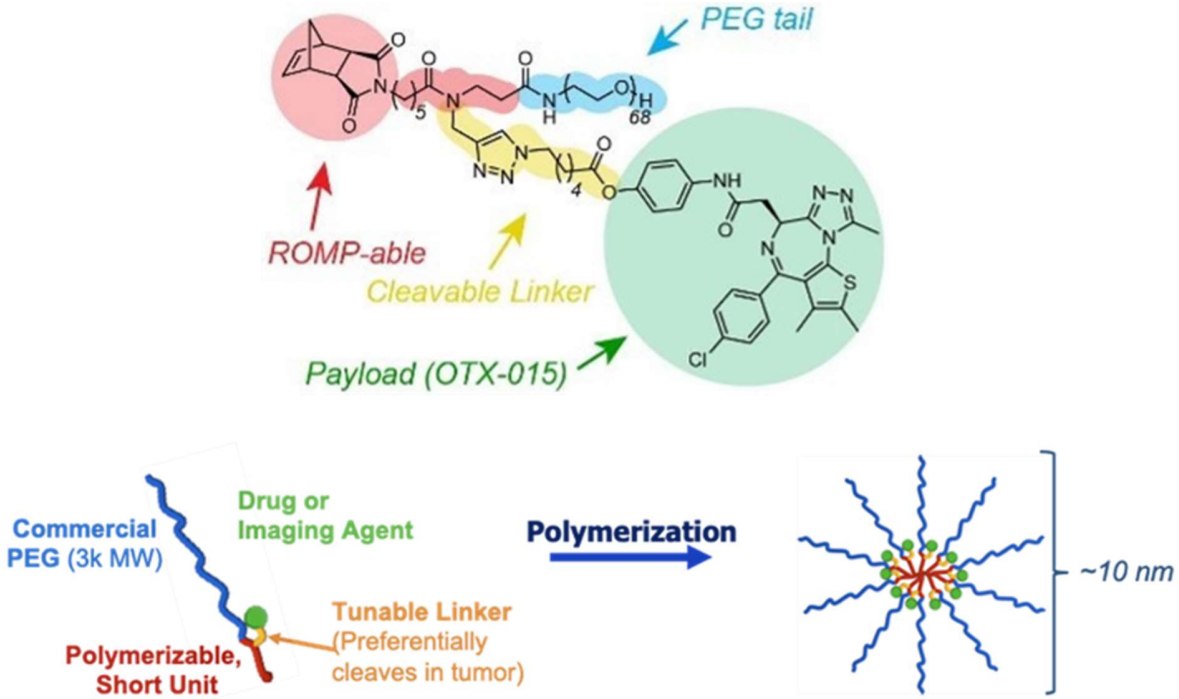

Figure 3.10 Diagram demonstrating the design of BPD-OTX.

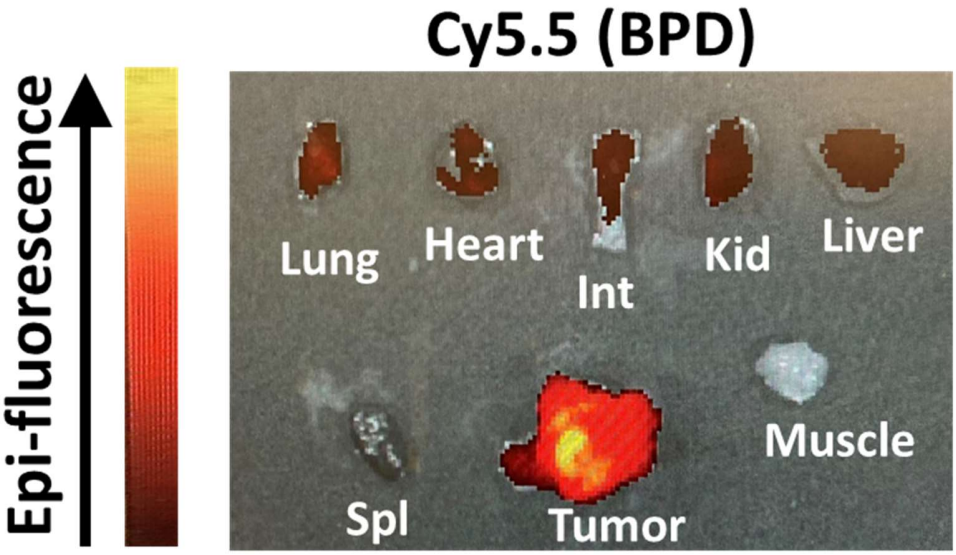

Figure 3.11 Analysis of BPD distribution across mouse tissues after injection.

Mice bearing orthotopically transplanted PDAC1245 tumor were treated with 5mg/mouse BPD-Cy5.5 (i.p.), after 1 day fluorescence of tumor and different organs were measured on the IVIS platform.

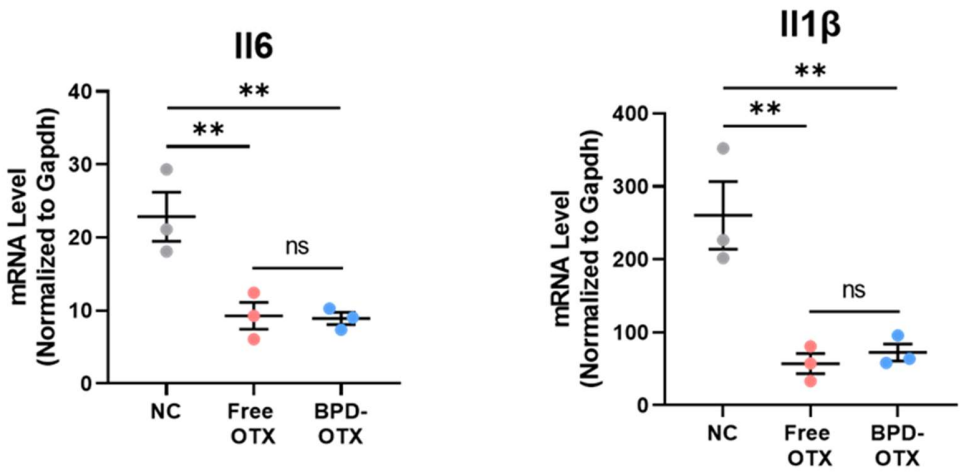

Figure 3.12 BPD-OTX treatment blocks immunosuppressive gene expression in TAMs as efficient as free-OTX.

PDAC1245-GFP bearing mice were treated with 75mg/kg free-OTX (daily, o.g.) or 75mg/kg BPD-OTX (once every three days, i.p.) for two weeks, after which intra-tumoral macrophages (CD45+, CD11b+, F4/80+) were sorted out by FACS. mRNA levels of Il6 and Il1β in sorted macrophages were measured by qPCR. Data are presented as dot plots, with each dot representing an individual tumor, horizontal lines indicating means and error bars indicating SEMs. Data significance was analyzed by Ordinary one-way ANOVA in Prism. **P<0.01.

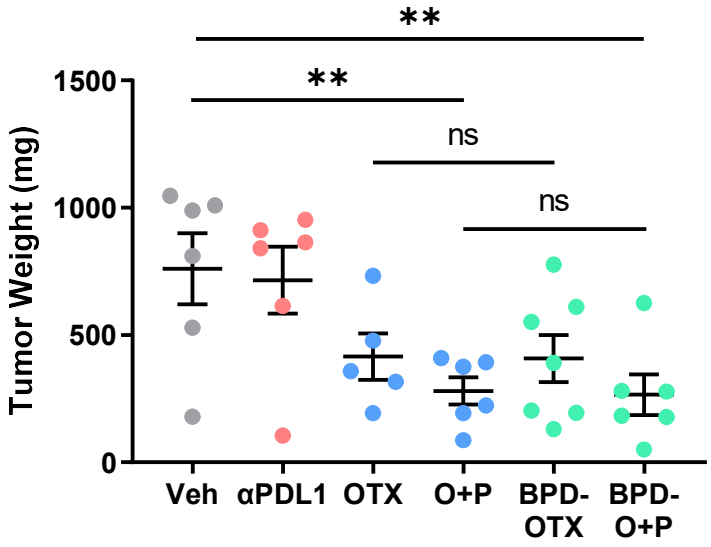

Figure 3.13 BPD-OTX has comparable effect as free-OTX on reducing tumor burden.

PDAC1245-GFP bearing mice were treated with 10mg/kg αPDL1 (once every three days, i.p.) in combination with 75mg/kg free-OTX (daily, o.g.) or 75mg/kg BPD-OTX (once every three days, i.p.) for two weeks. Data are presented as dot plots, with each dot representing an individual tumor, horizontal lines indicating means and error bars indicating SEMs. Data significance was analyzed by Ordinary one-way ANOVA in Prism. **P<0.01.

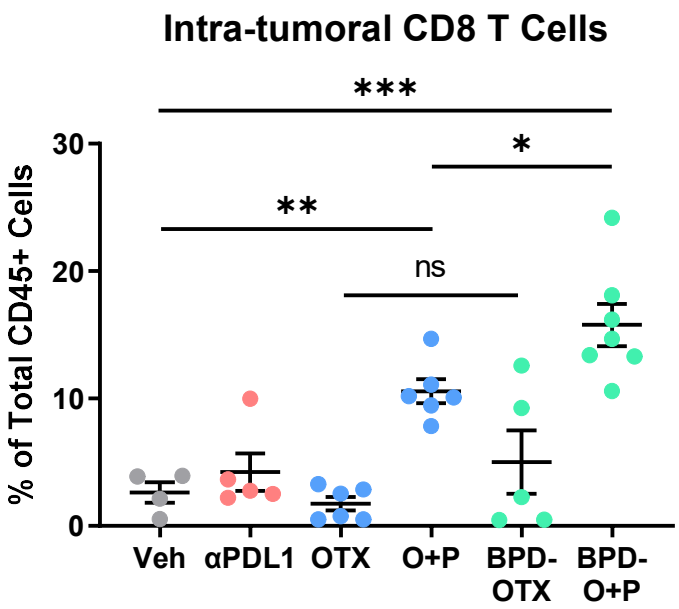

Figure 3.14 BPD-OTX shows superior effect over free-OTX on inducing CD8 T cell accumulation in combination with αPDL1.

PDAC1245-GFP bearing mice were treated with 10mg/kg αPDL1 (once every three days, i.p.) in combination with 75mg/kg free-OTX (daily, o.g.) or 75mg/kg BPD-OTX (once every three days, i.p.) for two weeks. Intra-tumoral CD8 T cell accumulation was measured by flow cytometry. Data are presented as dot plots, with each dot representing an individual tumor, horizontal lines indicating means and error bars indicating SEMs. Data significance was analyzed by Ordinary one-way ANOVA in Prism. *P<0.05, **P<0.01, ***P<0.001.

Discussion

PDAC is notorious for its resistance to immune checkpoint inhibitors. In the preceding chapter, we introduced a novel approach to sensitize PDAC to immunotherapy through the application of BETi. In this study, we aimed to enhance the therapeutic efficacy of the BETi+αPDL1 combination treatment. We found that co-application of chemotherapy inhibited rather than promoted T cell responses induced by BETi+αPDL1. We also found that while alternative dosing strategies could mitigate BETi toxicity, they compromised the synergistic effect with immune checkpoint inhibitors. To address this dosage-efficacy dilemma, we employed BPD nanoparticle-aided drug delivery technology and demonstrated that BPD-OTX achieved superior efficacy in sensitizing PDAC tumors to αPDL1 compared to free OTX. These findings highlight the potential of combining BPD-conjugated BETi with immune checkpoint inhibitors to develop novel therapeutic strategies for PDAC.

Translating *in vitro* findings into *in vivo* outcomes presents significant challenges due to differences in ADMET properties, leading to suboptimal biodistribution and tissue accumulation. In contrast to our *in vitro* results, our *in vivo* findings suggest that the addition of chemotherapy, such as gemcitabine, antagonizes the effect of OTX+αPDL1 in promoting anti-tumor CD8 T cell responses (Figure 3.4). This observation is supported by evidence indicating that chemotherapy can reduce the risk of immune-related pneumonitis in solid tumor-bearing patients receiving αPD1 treatment (Long, Sun et al. 2022). Furthermore, *in vitro* chemotherapy treatment has been shown to impair the proliferation and activation of CAR-T cells (Das, O'Connor et al. 2020). These findings underscore the antagonistic role of chemotherapy in anti-tumor immune responses.

However, chemotherapy's inhibitory effect on T cells has been shown to be temporary and dose-dependent. While high-dose chemotherapy can initially induce a transient decrease in CD8

T cell numbers, these cells can gradually recover after chemotherapy discontinuation (Scurr, Pembroke et al. 2017) (Fagnoni, Lozza et al. 2002) (Mackall, Fleisher et al. 1997). Importantly, after the recovery period, CD8 T cells demonstrate strengthened cytotoxic activity and effector memory phenotypes (Turtle, Swanson et al. 2009) (Coleman, Clayton et al. 2005). Furthermore, the impact of chemotherapy on CD8 T cells varies with dosage. For example, high-dose platinum-based chemotherapy may induce lymphopenia in colon cancer-bearing mice, whereas low-dose platinum-based chemotherapy results in increased T cell numbers and enhanced T cell responses (Fu, Wu et al. 2020). These findings underscore the potential of chemotherapy to facilitate anti-tumor T cell responses if administered at the proper dose and given sufficient time for recovery before immunotherapy (Truong, Gargett et al. 2021). In the context of PDAC treatment, it remains to be investigated whether pre-application of low-dose gemcitabine, followed by a break and subsequent BETi+αPDL1 combination treatment, could further enhance the anti-tumor T cell response. While challenging to examine in the current orthotopic mouse model due to its limited treatment window post-transplantation, such a strategy should be explored in the KPC mouse model with a longer dosing window in future studies. Additionally, different chemotherapy drugs or even combinations of chemotherapy should be tested alongside BETi and αPDL1, considering their distinct mechanisms of action.

The development of BPD nanoparticles opens up a promising avenue for achieving organ/tissue-specific drug accumulation while mitigating off-target side effects. Our findings highlight the enhanced efficacy of BPD-conjugated OTX in blocking the iTME compared to its free counterpart. Importantly, this design significantly reduces OTX's toxicity to secondary lymphoid tissues and other organs. Despite these advances, there is still room for further

refinement in current BPD-BETi+αPDL1 therapeutic strategies by leveraging other advantageous features of BPD nanoparticles.

One notable feature is the capability for co-delivering multiple drugs to the desired site. The ring-opening metathesis polymerization (ROMP) chemistry used in BPD formation allows for the quantitative incorporation of macromonomer stoichiometry into the resulting nanoparticle. This enables the incorporation of various macromonomers containing distinct linkers and small-molecule drugs into the same nanoparticle, facilitating co-delivery with desired kinetics and drug ratios (Hu, Sun et al. 2016) (Mignani, Bryszewska et al. 2015). Successful delivery of three different chemotherapy drugs at the desired ratio for ovarian cancer treatment has been reported using this feature of BPD nanoparticles (Liao, Liu et al. 2014). To further enhance the efficacy of BETi+αPDL1, co-delivery of other drugs with BPD nanoparticles for PDAC tumor treatment could be explored. For example, FAK inhibition has shown promise in reducing immunosuppressive MDSCs, TAMs, and Tregs in PDAC tumors and promoting CD8 T cell accumulation (Jiang, Hegde et al. 2016). The combination of FAK inhibitors and αPD1 has been demonstrated to boost the anti-tumor immune response in PDAC (Blair, Wang et al. 2022), suggesting the potential for further enhancement of BETi+αPDL1 efficacy. Another promising candidate for combination treatment is a recently developed KRAS inhibitor (Kim, Herdeis et al. 2023), given the pro-tumorigenic features of PDAC stroma and tumor cells induced and maintained with activated KRAS signaling (Zhang, Zhang et al. 2023). Co-delivery of these drugs in combination with BETi by BPD nanoparticles has the potential to further sensitize PDAC tumors further to immunotherapies.

Another advantageous feature of BPD nanoparticles that may improve the current treatment strategy is cell-type-specific drug delivery through conjugation with molecules such as

peptides, aptamers, oligonucleotides, and monoclonal antibodies (mAbs) that recognize cell surface epitopes (Zhao, Ukidve et al. 2020). Antibody-aided drug delivery with nanoparticles has already proven effective in treating various cancer types (Wathoni, Puluhulawa et al. 2022) (Juan, Cimas et al. 2020). In the context of PDAC, nanoparticles conjugated with anti-Ly6C demonstrated specific targeting of macrophages and endothelial cells (Yokoi, Godin et al. 2013). While the side effects on T cells in secondary lymphoid tissues can be avoided with intra-tumoral drug enrichment in the current BPD-BETi design, T cells within PDAC tumors might still be affected by BETi. To address this, the conjugation of cell-type-specific antibodies with BPD nanoparticles could enable specific targeting of myeloid cells and tumor cells without affecting T cells in PDAC tumors. This approach could maximize BETi efficacy by promoting its inhibition of immunosuppressive cells while reducing effects on T cell proliferation. Similarly, a tumor cell-targeting chemotherapy design could maximize inhibition of tumor cell proliferation without affecting T cell proliferation. Collectively, a combination of tumor cell-targeting BPD-gemcitabine, myeloid cell-targeting BPD-BETi and αPDL1 may represent a promising strategy for PDAC treatment.

In the development of BPD nanoparticle-conjugated BETi, we have effectively alleviated its toxicity on T cells outside the PDAC tumor, particularly in secondary lymphoid tissues, while simultaneously enhancing its concentration within the tumor. This not only facilitates the effective reprogramming of the iTME by BETi but also enables sustained synergy with immune checkpoint inhibitors, fostering a long-lasting anti-tumor T cell response without systemic toxicity concerns. The potential of this strategy extends beyond PDAC therapy, offering valuable insights for addressing drug toxicity and off-target effects in the treatment of various cancer types.

Acknowledgements

Chapter 3, in full, is currently being prepared for submission for publication of the material. Work in this chapter was done in collaboration with Morgan Truitt, who helped with experiments, and Hung VanThanh Nguyen, who helped with BPD-OTX production. Senada Bashi, Hanna Dhiyebi and Mariel Burquez provided technical support. The dissertation author was the primary researcher and author of this material. This chapter was written under the guidance of Morgan Truitt, Michael Downes, Annette Atkins, Ruth Yu and Ronald Evans.

References

Blair, A. B., J. Wang, J. Davelaar, A. Baker, K. Li, N. Niu, J. Wang, Y. Shao, V. Funes, P. Li, J. A. Pachter, D. C. Maneval, F. Dezem, J. Plummer, K. S. Chan, J. Gong, A. E. Hendifar, S. J. Pandol, R. Burkhart, Y. Zhang, L. Zheng and A. Osipov (2022). "Dual Stromal Targeting Sensitizes Pancreatic Adenocarcinoma for Anti-Programmed Cell Death Protein 1 Therapy." Gastroenterology 163(5): 1267-1280 e1267.

Cochran, A. G., A. R. Conery and R. J. Sims, 3rd (2019). "Bromodomains: a new target class for drug development." Nat Rev Drug Discov 18(8): 609-628.

Coleman, S., A. Clayton, M. D. Mason, B. Jasani, M. Adams and Z. Tabi (2005). "Recovery of CD8+ T-cell function during systemic chemotherapy in advanced ovarian cancer." Cancer Res 65(15): 7000-7006.

Das, R. K., R. S. O'Connor, S. A. Grupp and D. M. Barrett (2020). "Lingering effects of chemotherapy on mature T cells impair proliferation." Blood Adv 4(19): 4653-4664.

Das, R. K., L. Vernau, S. A. Grupp and D. M. Barrett (2019). "Naive T-cell Deficits at Diagnosis and after Chemotherapy Impair Cell Therapy Potential in Pediatric Cancers." Cancer Discov 9(4): 492-499.

Eriksson, E., J. Wenthe, S. Irenaeus, A. Loskog and G. Ullenhag (2016). "Gemcitabine reduces MDSCs, tregs and TGFbeta-1 while restoring the teff/treg ratio in patients with pancreatic cancer." J Transl Med 14(1): 282.

Fagnoni, F. F., L. Lozza, C. Zibera, A. Zambelli, L. Ponchio, N. Gibelli, B. Oliviero, L. Pavesi, R. Gennari, R. Vescovini, P. Sansoni, G. Da Prada and G. Robustelli Della Cuna (2002). "T-cell dynamics after high-dose chemotherapy in adults: elucidation of the elusive CD8+ subset reveals multiple homeostatic T-cell compartments with distinct implications for immune competence." Immunology 106(1): 27-37.

Frampton, J. E. (2020). "Liposomal Irinotecan: A Review in Metastatic Pancreatic Adenocarcinoma." Drugs 80(10): 1007-1018.

Fu, D., J. Wu, J. Lai, Y. Liu, L. Zhou, L. Chen and Q. Zhang (2020). "T cell recruitment triggered by optimal dose platinum compounds contributes to the therapeutic efficacy of sequential PD-1 blockade in a mouse model of colon cancer." Am J Cancer Res 10(2): 473-490.

Garcia, P. L., A. L. Miller, K. M. Kreitzburg, L. N. Council, T. L. Gamblin, J. D. Christein, M. J. Heslin, J. P. Arnoletti, J. H. Richardson, D. Chen, C. A. Hanna, S. L. Cramer, E. S. Yang, J. Qi, J. E. Bradner and K. J. Yoon (2016). "The BET bromodomain inhibitor JQ1 suppresses growth of pancreatic ductal adenocarcinoma in patient-derived xenograft models." Oncogene 35(7): 833-845.

Hou, W., B. Yang and H. Zhu (2022). "Nanoparticle-Based Therapeutic Strategies for Enhanced Pancreatic Ductal Adenocarcinoma Immunotherapy." Pharmaceutics 14(10):2033.

Hu, Q., W. Sun, C. Wang and Z. Gu (2016). "Recent advances of cocktail chemotherapy by combination drug delivery systems." Adv Drug Deliv Rev 98: 19-34.

Jacobetz, M. A., D. S. Chan, A. Neesse, T. E. Bapiro, N. Cook, K. K. Frese, C. Feig, T. Nakagawa, M. E. Caldwell, H. I. Zecchini, M. P. Lolkema, P. Jiang, A. Kultti, C. B. Thompson, D. C. Maneval, D. I. Jodrell, G. I. Frost, H. M. Shepard, J. N. Skepper and D. A. Tuveson (2013). "Hyaluronan impairs vascular function and drug delivery in a mouse model of pancreatic cancer." Gut 62(1): 112-120.

Jauset, T., D. Masso-Valles, S. Martinez-Martin, M. E. Beaulieu, L. Foradada, F. P. Fiorentino, J. Yokota, B. Haendler, S. Siegel, J. R. Whitfield and L. Soucek (2018). "BET inhibition is an effective approach against KRAS-driven PDAC and NSCLC." Oncotarget 9(27): 18734-18746.

Jiang, H., S. Hegde, B. L. Knolhoff, Y. Zhu, J. M. Herndon, M. A. Meyer, T. M. Nywening, W. G. Hawkins, I. M. Shapiro, D. T. Weaver, J. A. Pachter, A. Wang-Gillam and D. G. DeNardo (2016). "Targeting focal adhesion kinase renders pancreatic cancers responsive to checkpoint immunotherapy." Nat Med 22(8): 851-860.

Jiang, Y. and D. P. S. Sohal (2023). "Pancreatic Adenocarcinoma Management." JCO Oncol Pract 19(1): 19-32.

Johnson, J. A., Y. Y. Lu, A. O. Burts, Y. Xia, A. C. Durrell, D. A. Tirrell and R. H. Grubbs (2010). "Drug-loaded, bivalent-bottle-brush polymers by graft-through ROMP." Macromolecules 43(24): 10326-10335.

Juan, A., F. J. Cimas, I. Bravo, A. Pandiella, A. Ocana and C. Alonso-Moreno (2020). "Antibody Conjugation of Nanoparticles as Therapeutics for Breast Cancer Treatment." Int J Mol Sci 21(17).

Kim, D., L. Herdeis, D. Rudolph, Y. Zhao, J. Bottcher, A. Vides, C. I. Ayala-Santos, Y. Pourfarjam, A. Cuevas-Navarro, J. Y. Xue, A. Mantoulidis, J. Broker, T. Wunberg, O. Schaaf, J. Popow, B. Wolkerstorfer, K. G. Kropatsch, R. Qu, E. de Stanchina, B. Sang, C. Li, D. B. McConnell, N. Kraut and P. Lito (2023). "Pan-KRAS inhibitor disables oncogenic signalling and tumour growth." Nature.

Koinis, F., E. K. Vetsika, D. Aggouraki, E. Skalidaki, A. Koutoulaki, M. Gkioulmpasani, V. Georgoulias and A. Kotsakis (2016). "Effect of First-Line Treatment on Myeloid-Derived Suppressor Cells' Subpopulations in the Peripheral Blood of Patients with Non-Small Cell Lung Cancer." J Thorac Oncol 11(8): 1263-1272.

Kumar, K., B. T. DeCant, P. J. Grippo, R. F. Hwang, D. J. Bentrem, K. Ebine and H. G. Munshi (2017). "BET inhibitors block pancreatic stellate cell collagen I production and attenuate fibrosis in vivo." JCI Insight 2(3): e88032.

Liao, L., J. Liu, E. C. Dreaden, S. W. Morton, K. E. Shopsowitz, P. T. Hammond and J. A. Johnson (2014). "A convergent synthetic platform for single-nanoparticle combination cancer therapy:

ratiometric loading and controlled release of cisplatin, doxorubicin, and camptothecin." J Am Chem Soc 136(16): 5896-5899.

Liu, L., P. G. Kshirsagar, S. K. Gautam, M. Gulati, E. I. Wafa, J. C. Christiansen, B. M. White, S. K. Mallapragada, M. J. Wannemuehler, S. Kumar, J. C. Solheim, S. K. Batra, A. K. Salem, B. Narasimhan and M. Jain (2022). "Nanocarriers for pancreatic cancer imaging, treatments, and immunotherapies." Theranostics 12(3): 1030-1060.

Long, Y. X., Y. Sun, R. Z. Liu, M. Y. Zhang, J. Zhao, Y. Q. Wang, Y. W. Zhou, K. Cheng, Y. Chen, C. R. Zhu and J. Y. Liu (2022). "Immune-Related Pneumonitis Was Decreased by Addition of Chemotherapy with PD-1/L1 Inhibitors: Systematic Review and Network Meta-Analysis of Randomized Controlled Trials (RCTs)." Curr Oncol 29(1): 267-282.

Mackall, C. L., T. A. Fleisher, M. R. Brown, M. P. Andrich, C. C. Chen, I. M. Feuerstein, I. T. Magrath, L. H. Wexler, D. S. Dimitrov and R. E. Gress (1997). "Distinctions between CD8+ and CD4+ T-cell regenerative pathways result in prolonged T-cell subset imbalance after intensive chemotherapy." Blood 89(10): 3700-3707.

Mazur, P. K., A. Herner, S. S. Mello, M. Wirth, S. Hausmann, F. J. Sanchez-Rivera, S. M. Lofgren, T. Kuschma, S. A. Hahn, D. Vangala, M. Trajkovic-Arsic, A. Gupta, I. Heid, P. B. Noel, R. Braren, M. Erkan, J. Kleeff, B. Sipos, L. C. Sayles, M. Heikenwalder, E. Hessmann, V. Ellenrieder, I. Esposito, T. Jacks, J. E. Bradner, P. Khatri, E. A. Sweet-Cordero, L. D. Attardi, R. M. Schmid, G. Schneider, J. Sage and J. T. Siveke (2015). "Combined inhibition of BET family proteins and histone deacetylases as a potential epigenetics-based therapy for pancreatic ductal adenocarcinoma." Nat Med 21(10): 1163-1171.

Meng, H. and A. E. Nel (2018). "Use of nano engineered approaches to overcome the stromal barrier in pancreatic cancer." Adv Drug Deliv Rev 130: 50-57.

Mignani, S., M. Bryszewska, B. Klajnert-Maculewicz, M. Zablocka and J. P. Majoral (2015). "Advances in combination therapies based on nanoparticles for efficacious cancer treatment: an analytical report." Biomacromolecules 16(1): 1-27.

Miller, A. L., P. L. Garcia, S. C. Fehling, T. L. Gamblin, R. B. Vance, L. N. Council, D. Chen, E. S. Yang, R. van Waardenburg and K. J. Yoon (2021). "The BET Inhibitor JQ1 Augments the Antitumor Efficacy of Gemcitabine in Preclinical Models of Pancreatic Cancer." Cancers (Basel) 13(14).

Piquereau, J., A. Boet, C. Pechoux, F. Antigny, M. Lambert, M. Gressette, B. Ranchoux, N. Gambaryan, V. Domergue, S. Mumby, D. Montani, I. M. Adcock, M. Humbert, A. Garnier, C. Rucker-Martin and F. Perros (2019). "The BET Bromodomain Inhibitor I-BET-151 Induces Structural and Functional Alterations of the Heart Mitochondria in Healthy Male Mice and Rats." Int J Mol Sci 20(7).

Scurr, M., T. Pembroke, A. Bloom, D. Roberts, A. Thomson, K. Smart, H. Bridgeman, R. Adams, A. Brewster, R. Jones, S. Gwynne, D. Blount, R. Harrop, R. Hills, A. Gallimore and A. Godkin

(2017). "Low-Dose Cyclophosphamide Induces Antitumor T-Cell Responses, which Associate with Survival in Metastatic Colorectal Cancer." Clin Cancer Res 23(22): 6771-6780.

Sun, Y., J. Han, Z. Wang, X. Li, Y. Sun and Z. Hu (2020). "Safety and Efficacy of Bromodomain and Extra-Terminal Inhibitors for the Treatment of Hematological Malignancies and Solid Tumors: A Systematic Study of Clinical Trials." Front Pharmacol 11: 621093.

Truong, N. T. H., T. Gargett, M. P. Brown and L. M. Ebert (2021). "Effects of Chemotherapy Agents on Circulating Leukocyte Populations: Potential Implications for the Success of CAR-T Cell Therapies." Cancers (Basel) 13(9).

Turtle, C. J., H. M. Swanson, N. Fujii, E. H. Estey and S. R. Riddell (2009). "A distinct subset of self-renewing human memory CD8+ T cells survives cytotoxic chemotherapy." Immunity 31(5): 834-844.

Vohidov, F., J. N. Andersen, K. D. Economides, M. V. Shipitsin, O. Burenkova, J. C. Ackley, B. Vangamudi, H. V. Nguyen, N. M. Gallagher, P. Shieh, M. R. Golder, J. Liu, W. K. Dahlberg, D. J. C. Ehrlich, J. Kim, S. L. Kristufek, S. J. Huh, A. M. Neenan, J. Baddour, S. Paramasivan, E. de Stanchina, G. Kc, D. J. Turnquist, J. K. Saucier-Sawyer, P. W. Kopesky, S. W. Brady, M. J. Jessel, L. A. Reiter, D. E. Chickering, J. A. Johnson and P. Blume-Jensen (2021). "Design of BET Inhibitor Bottlebrush Prodrugs with Superior Efficacy and Devoid of Systemic Toxicities." J Am Chem Soc 143(12): 4714-4724.

Wathoni, N., L. E. Puluhulawa, I. M. Joni, M. Muchtaridi, A. F. A. Mohammed, K. M. Elamin, T. Milanda and D. Gozali (2022). "Monoclonal antibody as a targeting mediator for nanoparticle targeted delivery system for lung cancer." Drug Deliv 29(1): 2959-2970.

Xie, F., M. Huang, X. Lin, C. Liu, Z. Liu, F. Meng, C. Wang and Q. Huang (2018). "The BET inhibitor I-BET762 inhibits pancreatic ductal adenocarcinoma cell proliferation and enhances the therapeutic effect of gemcitabine." Sci Rep 8(1): 8102.

Yardley, D. A. (2013). "nab-Paclitaxel mechanisms of action and delivery." J Control Release 170(3): 365-372.

Yokoi, K., B. Godin, C. J. Oborn, J. F. Alexander, X. Liu, I. J. Fidler and M. Ferrari (2013). "Porous silicon nanocarriers for dual targeting tumor associated endothelial cells and macrophages in stroma of orthotopic human pancreatic cancers." Cancer Lett 334(2): 319-327.

Zhang, L., C. Zhou, S. Zhang, X. Chen, J. Liu, F. Xu and W. Liang (2022). "Chemotherapy reinforces anti-tumor immune response and enhances clinical efficacy of immune checkpoint inhibitors." Front Oncol 12: 939249.

Zhang, Z., H. Zhang, X. Liao and H. I. Tsai (2023). "KRAS mutation: The booster of pancreatic ductal adenocarcinoma transformation and progression." Front Cell Dev Biol 11: 1147676.

Zhao, Z., A. Ukidve, J. Kim and S. Mitragotri (2020). "Targeting Strategies for Tissue-Specific Drug Delivery." Cell 181(1): 151-167.

Chapter 4 Stromal Education of Tumor Cells Promotes PDAC Immune Evasion

Introduction

PDAC stands out as a formidable disease, notorious for its resistance to conventional chemotherapy and radiation therapy. Moreover, various immunotherapy strategies have proven ineffective against this malignancy, primarily due to the intricate mechanisms of immune evasion orchestrated within both tumor cells and the tumor stroma.

The challenge in achieving successful immunotherapy for PDAC partially lies in the complex interplay of immune evasion mechanisms within tumor stroma. Stromal cell components, including tumor-associated macrophages (TAMs), myeloid-derived suppressor cells (MDSCs), regulatory T cells (Tregs), and cancer-associated fibroblasts (CAFs), collectively contribute to the creation of an immunosuppressive niche that impedes the function of immune effector cells. Notably, CCR2+ TNFα-producing TAMs have been identified as mediators of dendritic cell and cytotoxic T cell activity in an IL33-dependent manner (Dixit, Sarver et al. 2022). Meanwhile, the accumulation of CXCR2+ MDSCs in PDAC tumors not only fosters tumor metastasis but also inhibits T cell infiltration (Steele, Karim et al. 2016). CAFs are the major producers of CXCL12 in PDAC tumor which, through formation of CXCL12-keratin-19 coating on tumor cell surface, can suppress T cell-mediated killing (Wang, Moresco et al. 2022) (Malik, Westcott et al. 2021).

Simultaneously, tumor cell-inherent resistance mechanisms further impede antitumor immunity. The oncogenic KRAS mutation, known for its pro-tumorigenic roles in regulating tumor cell proliferation, migration, invasion, apoptosis inhibition, and metabolic adaptation (Waters and Der 2018), has been found to mediate immune resistance. Mutant KRAS induces granulocyte-macrophage colony-stimulating factor (GM-CSF) production through classical Raf/MAPK and PI3K signaling pathways, recruiting Gr1+CD11b+ myeloid cells to block anti-

tumor immune responses (Pylayeva-Gupta, Lee et al. 2012). More recent studies have identified BRAF and MYC as key mediators of KRAS-induced immune evasion (Ischenko, D'Amico et al. 2021). Furthermore, KRAS activation can promote reactive oxygen species (ROS) generation, leading to PDL1 upregulation in PDAC tumor cells in an FGFR1-dependent manner (Glorieux, Xia et al. 2021). Another layer of immune evasion involves the downregulation of major histocompatibility complex class I (MHC I) proteins in PDAC tumor cells (Hiraoka, Ino et al. 2020). Studies indicate that enhanced autophagy mediates MHC I degradation in tumor cells. This results in reduced presentation of tumor antigens to CD8 T cells, thereby disrupts T cells' recognition and killing (Yamamoto, Venida et al. 2020).

While stromal cells and tumor cells employ distinct strategies to thwart anti-tumor immune responses, it is crucial to recognize their interactions. The tumor-stroma crosstalk, facilitated through either direct cell-cell contact or the exchange of secreted factors within the TME, likely plays a significant role in orchestrating these immune-evading functions. For instance, PDAC tumor cells can produce transforming growth factor-β (TGF-β) and platelet-derived growth factor (PDGF) to reprogram quiescent resident fibroblasts and pancreatic stellate cells (PSCs) into CAFs (Vaish, Jain et al. 2021) (Li, Guo et al. 2021) (Lohr, Schmidt et al. 2001). These CAFs can produce growth factors such as insulin-like growth factor 1 (IGF1), growth arrest-specific gene 6 (GAS6) and leukemia inhibitory factor (LIF) which in turn trigger PI3K/Akt or JAK/STAT3 signaling within tumor cells to mediate their growth and metastasis (Ireland, Luckett et al. 2020) (Mutgan, Besikcioglu et al. 2018) (Shi, Gao et al. 2019). These CAFs can also foster reciprocal signaling cascades, amplifying autonomous KRAS signaling in tumor cells (Tape, Ling et al. 2016). Moreover, PDAC tumor cells, through the production of IL-1β, attract immune cells with tolerogenic functions into the TME. This includes TAMs, MDSCs, Th17 cells and regulatory B

cells (Das, Shapiro et al. 2020). While the mechanisms by which PDAC tumor cells recruit various stromal cells to form an iTME are becoming clearer, the understanding of how this TME educates tumor cells and triggers their intrinsic immune evasive mechanisms remains limited.

The conventional immune response against cancer typically relies on the intricate orchestration of T cell priming, a process in which antigen-presenting cells activate T cells by presenting specific antigens derived from cancer cells. However, this process is often disrupted in the complex landscape of advanced cancers, where immune evasive mechanisms can dampen the effectiveness of the immune response. To address this challenge in cancer treatment, chimeric Antigen Receptor T-cell (CAR-T) therapy has been developed to bypass the T cell priming step. This is achieved by expressing chimeric receptors that combine the antigen-recognition domain of an antibody with the activating machinery of a T cell. The CAR structure pre-equips T cells with the ability to recognize tumor cells in an antigen-specific manner (Dagar, Gupta et al. 2023).

Despite its success in treating certain hematologic malignancies (Maude, Laetsch et al. 2018), CAR-T therapy has shown limited efficacy in solid tumors. In the context of PDAC, numerous ongoing clinical trials are testing the efficacy of CAR-T therapy targeting MUC-1 (Posey, Schwab et al. 2016), HER-2 (Feng, Liu et al. 2018), B7-H3 (Du, Hirabayashi et al. 2019), among others. Unfortunately, none of these trials have yielded satisfying outcomes so far. The failure of CAR-T therapy in PDAC can be attributed to factors such as restricted tumor infiltration, exhaustion induced by the immunosuppressive TME, tumor antigen heterogeneity, and off-target effects (Sterner and Sterner 2021). While current efforts to enhance CAR-T therapy efficacy largely focus on optimizing CAR affinity to tumor antigens or disrupting T cells' intrinsic suppressive signaling to avoid exhaustion (Gumber and Wang 2022), there is a notable gap in research regarding the combination of CAR-T therapy with strategies aimed at reducing tumor cell

intrinsic immunosuppressive resistance to T cells. Exploring this neglected field may provide new insights and potential solutions to enhance the effectiveness of CAR-T therapy in the challenging landscape of PDAC.

In this study, we aimed to elucidate the mechanisms underlying the failure of CAR-T therapy in PDAC by establishing *in vitro* and *in vivo* platforms that mimic this therapeutic challenge. Our investigations revealed a pivotal mechanism employed by the TME to educate PDAC tumor cells, rendering them resistant to CD8 T cell-mediated killing. Specifically, we observed a robust activation of TNFα-NFκB signaling in PDAC tumor cells by the TME, leading to the induction of immunosuppressive gene expression, particularly of COX2 and LIF. Crucially, intervention strategies targeting either COX2 or LIF *in vivo* demonstrated a significant sensitization of PDAC tumors to antigen-specific CD8 T cell-mediated killing. This breakthrough not only unveils novel mechanisms through which the TME triggers immune evasion in tumor cells but also opens avenues for potential therapeutic interventions. Our findings hold promise for the enhancement of PDAC treatment by combining CAR-T therapy with targeted approaches aimed at disrupting the immunosuppressive signals induced by the TME. This integrated approach represents a step forward in comprehending and overcoming the challenges posed by the complex PDAC microenvironment in the context of immunotherapeutic strategies.

4.1 Pancreatic tumor cells are vulnerable to T cell-mediated killing without the support of TME

The ineffectiveness of therapies aimed at bypassing T cell priming and promoting the recognition of tumor cells, such as tumor vaccines and CAR-T therapy, in human patients underscores the existence of inherent resistance *in vivo*. To discern whether this resistance is intrinsically programmed into pancreatic cancer cells or is conferred by the supportive TME, we sought to establish an *in vitro* tumor cell-T cell coculture system. This system would allow us to study the response of tumor cells to T cell-mediated killing in the absence of TME influence. However, merely co-culturing tumor cells with random CD8 T cells is insufficient to trigger killing. CD8 T-cell mediated tumor killing necessitates the interaction between major histocompatibility complex type I (MHC-I)-bound tumor antigens displayed on the tumor cell surface and the cognate T-cell receptor (TCR) expressed on CD8 T cell surfaces. To simulate this interaction, we introduced a gene encoding a virus-derived antigen, gp33-41 (referred to as gp33), into the PDAC1245 parental mouse pancreatic cancer cell line, resulting in the PDAC1245-gp33-12 cell line. (Gairin, Mazarguil et al. 1995). This cell line constitutively expresses the antigen gp33 and can be specifically recognized and killed by gp33-peptide-activated P14 CD8 T cells but not by αCD3/αCD28 activated wild-type T cells *in vitro* (Figure 4.1). To assess the sensitivity of tumor cells to T-cell-mediated killing, PDAC1245-gp33-12 cells and P14 T cells were cocultured at different ratios. The results revealed that T cell-mediated killing occurred in a ratio-dependent manner, with a killing efficiency of >95% achievable at a T cell-to-tumor cell ratio of 6:1 or higher (Figure 4.2). In contrast, when transplanted into rag1-/- mice, where the adaptive immune system is disrupted, PDAC1245-gp33-12 cells developed tumors resistant to P14 T cell therapy (Figure 4.3), recapitulating the failure of T cell therapy observed in human patients. These findings suggest that in the absence of TME, PDAC tumor cells are susceptible to CD8 T cell-mediated antigen-

specific killing, emphasizing the potential role of TME in fostering immune resistance in pancreatic cancer.

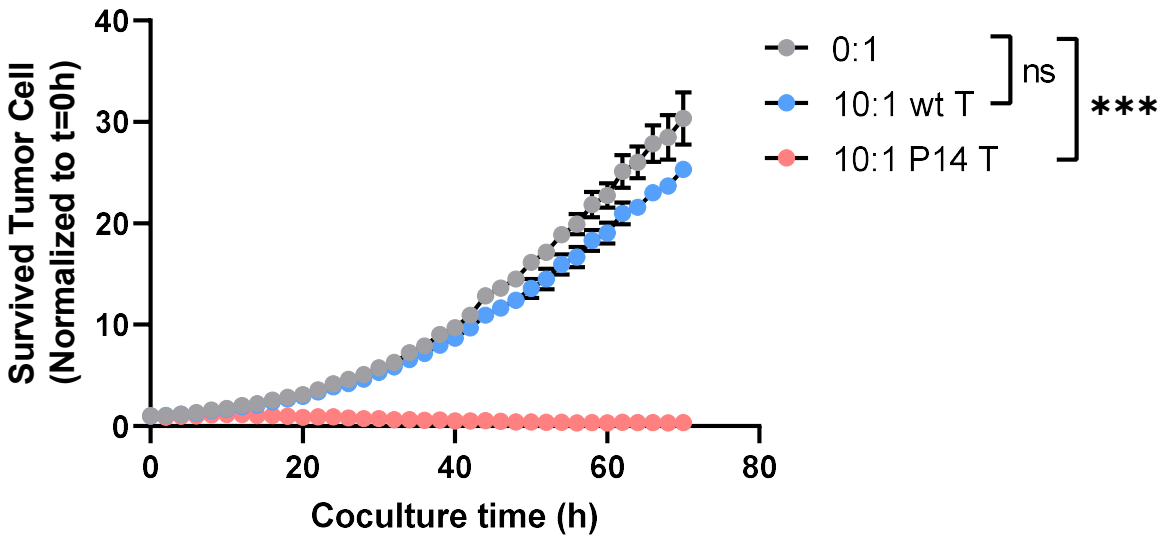

Figure 4.1 gp33-expressing tumor cells can be specifically killed with P14 CD8 T cells *in vitro*.

Killing efficiency comparing gp33 peptide-activated P14 T cells versus beads-activated wt T cells. Data were measured by Incucyte. Data are presented as connecting-dot plots, with each dot indicating means and error bars indicating SEMs. Data significance was analyzed by Ordinary one-way ANOVA in Prism. ***P<0.001.

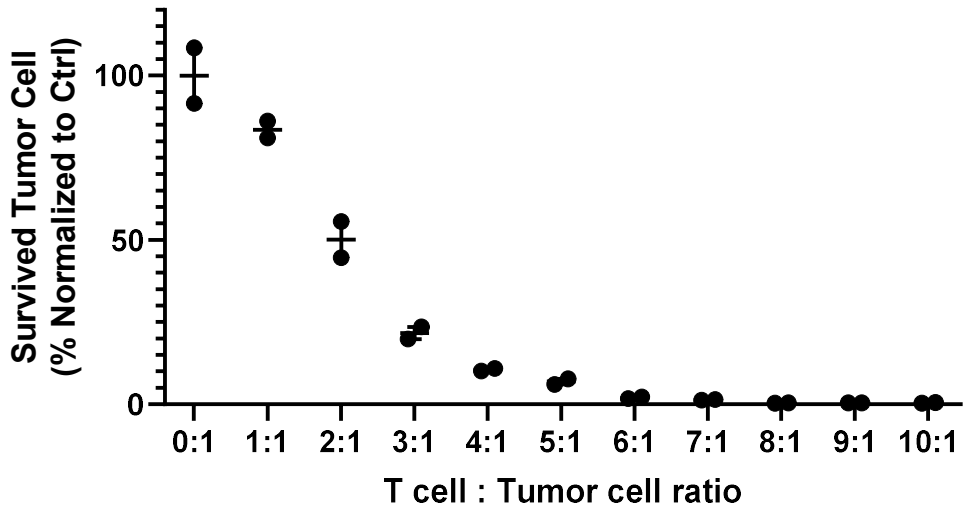

Figure 4.2 gp33-expressing tumor cells can be killed with P14 CD8 T cells in ratio-dependent manner *in vitro*.

Killing efficiency at different "T cell-to-tumor cell" ratio after 2 days of coculture. Data were measured by counting beads-based flow cytometry assay. Data are presented as dot plots, with each dot representing an individual value, horizontal lines indicating means and error bars indicating SEMs.

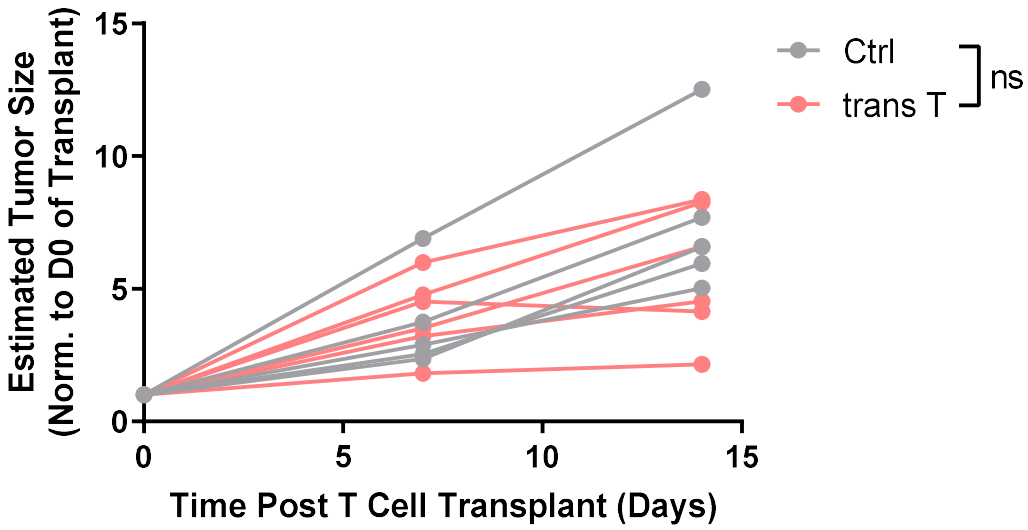

Figure 4.3 gp33-expressing tumor is resistant to P14 CD8 T cells *in vivo*.

Tumor growth rate of orthotopically transplanted PDAC1245-gp33-12 receiving P14 T cell therapy in rag1-/- mice. Tumor volume was measured by ultrasound imaging. Data are presented as connecting-dot plots, with each line of connected dots representing an individual tumor measured at different timepoints. Data significance was analyzed by Two-tailed Unpaired t-test in Prism.

4.2 Soluble factors enriched in TIF educate tumor cells to be resistant to T cell-mediated killing

In PDAC, the TME is known to harbor numerous secreted factors with immunosuppressive functions. However, it remains unclear whether these factors exert their effects by interacting with effector T cells, tumor cells, or other stromal cells. To address this question, we extracted tumor interstitial fluid (TIF) from orthotopically transplanted PDAC tumors, as it should contain most of the soluble factors (including proteins and metabolites) representing the PDAC TME. We introduced TIF into a coculture platform devoid of stromal cells. Interestingly, while TIF alone did not impact the growth of PDAC1245-gp33-12 cells in the absence of P14 CD8 T cells, it completely abolished tumor cell killing when T cells were present in the coculture (Figure 4.4). However, this result could be attributed to suppressive factors in TIF directly blocking P14 CD8 T cell function rather than rendering the tumor cells more resistant. To delve into the direct impact of TIF on PDAC tumor cells, we pretreated PDAC1245-gp33-12 cells with TIF for 2 days, then washed away the TIF and cocultured the cells with P14 CD8 T cells. Strikingly, we observed that TIF-pretreated tumor cells still exhibited partial resistance to T cell-mediated killing (Figure 4.5). To investigate whether the observed killing resistance phenotypes in the two TIF assays (TIF cotreatment of both cell types and TIF pretreatment of tumor cells) were due to P14 CD8 T cell exhaustion, we examined T cell activation (PD1) and exhaustion (Lag3) markers on P14 CD8 T cells from the coculture. We found that while the direct addition of TIF into the coculture led to P14 CD8 T cell exhaustion, pretreating tumor cells with TIF did not induce such phenotypes in T cells (Figure 4.6). Collectively, these findings suggest that while TIF contains factors capable of directly affecting CD8 T cell activation and exhaustion, it also simultaneously educates tumor cells and enhances their resistance to killing. This dual impact underscores the multifaceted nature of the TME in shaping immune responses in PDAC.

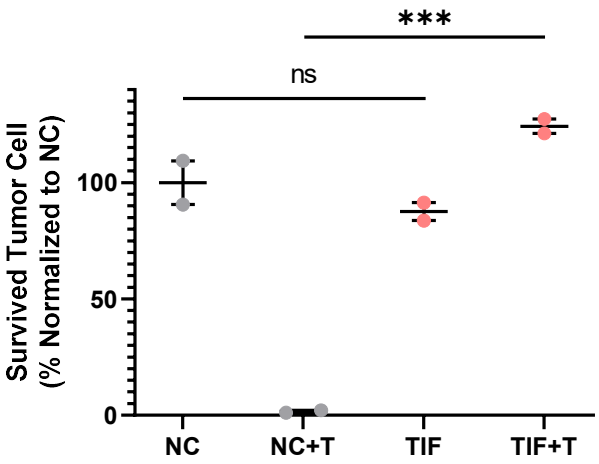

Figure 4.4 TIF treatment in coculture blocks T cell-mediated killing.

PDAC1245-gp33-12 tumor cell killing efficiency comparing 10% TIF treated cocultures versus control cocultures. T cell to tumor cell ratio is 6:1. Data were measured by counting beads-based flow cytometry assay. Data are presented as dot plots, with each dot representing an individual value, horizontal lines indicating means and error bars indicating SEMs. Data significance was analyzed by Ordinary one-way ANOVA in Prism. ***P<0.001.

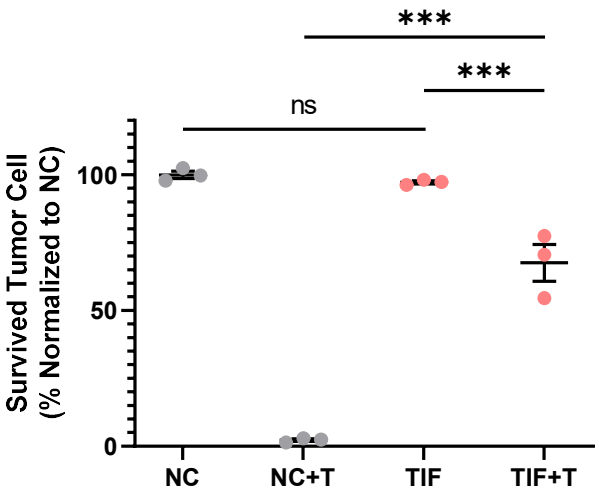

Figure 4.5 TIF pretreated tumor cells are partially resistant to T cell-mediated killing.

PDAC1245-gp33-12 tumor cell killing efficiency of tumor cells pretreated with 10% TIF. T cell to tumor cell ratio is 6:1. Data were measured by counting beads-based flow cytometry assay. Data are presented as dot plots, with each dot representing an individual value, horizontal lines indicating means and error bars indicating SEMs. Data significance was analyzed by Ordinary one-way ANOVA in Prism. ***P<0.001.

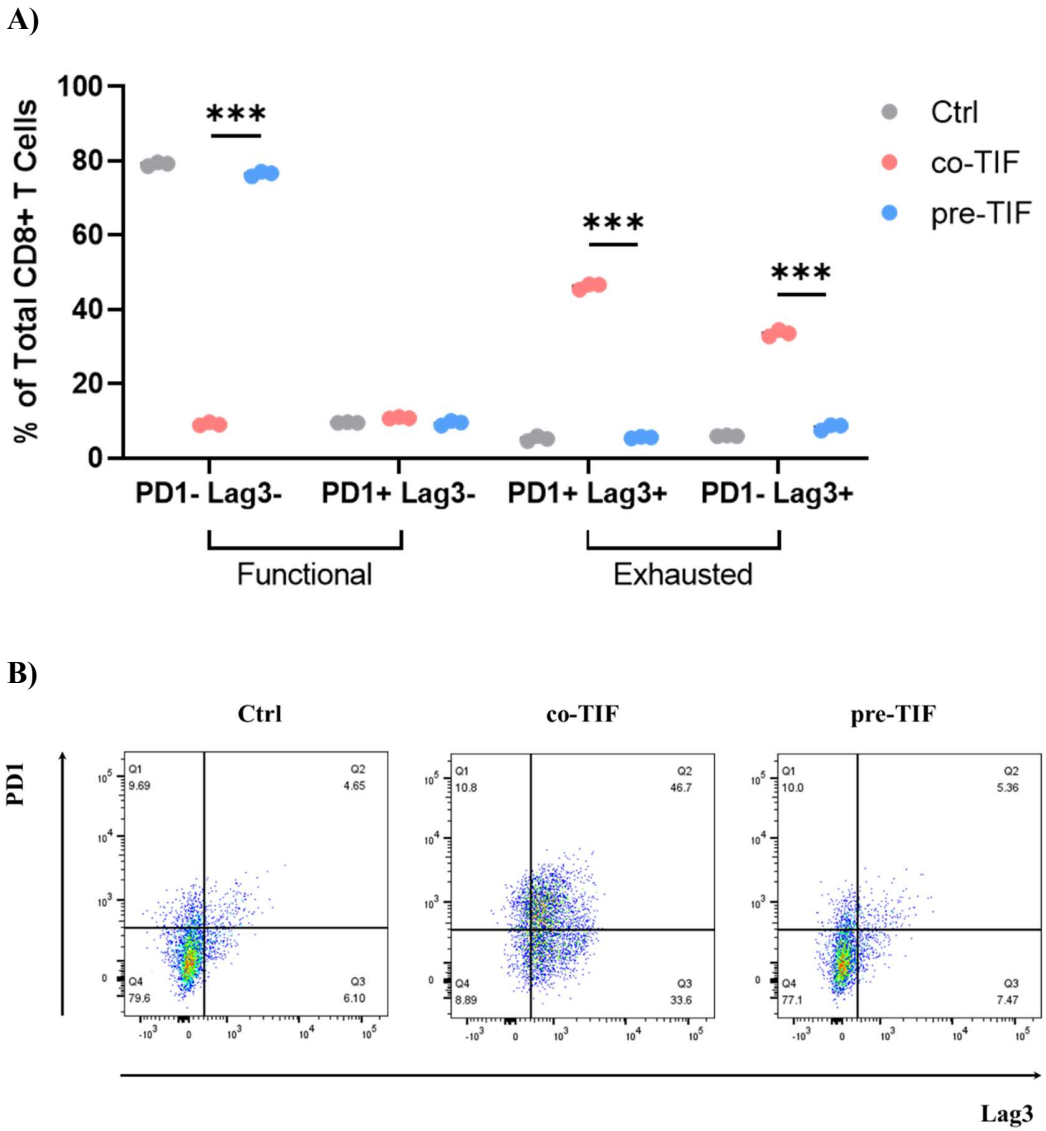

Figure 4.6 TIF treatment of CD8 T cells induces exhaustion phenotype.

A) P14 CD8 T cells in coculture were analyzed for functional (Lag3-), partially exhausted (PD1+ Lag3-) and terminally exhausted (PD1- Lag3-) phenotypes. Ctrl: tumor cell-T cell coculture, co-TIF: TIF added directly into tumor cell-T cell coculture, pre-TIF: tumor cells were pretreated with TIF before coculturing with T cells. Data were measured by flow cytometry assay. Data are presented as dot plots, with each dot representing an individual value, horizontal lines indicating means and error bars indicating SEMs. Data significance was analyzed by Ordinary one-way ANOVA in Prism. ***P<0.001.

B) Representative flow cytometry results from A). Ctrl: tumor cell-T cell coculture, co-TIF: TIF added directly into tumor cell-T cell coculture, pre-TIF: tumor cells were pretreated with TIF before coculturing with T cells. Data were analyzed by FlowJo. Data are presented as dot plots, with each panel representing an individual sample, and each dot within a panel represents an individual cell.

4.3 TIF treatment recapitulates functions of PDAC TME *in vivo*

To assess whether TIF-induced resistance to killing is under epigenetic control, we employed OTX, an epigenetic drug known for its capacity to bind to BET family proteins and impede their recognition of the H3K27Ac marker on histones. In the pretreatment phase of PDAC1245-gp33-12 cells, we co-administered OTX with TIF. Remarkably, our findings demonstrated that OTX effectively alleviated the killing-resistant phenotype induced by TIF in tumor cells (Figure 4.7). This suggests that the educational impact of TIF on tumor cells can be regulated through epigenetic mechanisms.

To identify key cellular alterations mediated by soluble factors in the TME, we conducted bulk RNA-seq analysis on PDAC1245-gp33-12 cells treated with TIF and OTX *in vitro*. Focusing on the gene set induced upon TIF treatment, 51% of the genes could be downregulated with the addition of OTX (Figure 4.8A), indicating a close relationship between the TIF-inducible gene set and epigenetically regulated gene set. Gene Ontology analysis on these overlapped genes identified TNFα-NFκB as the most significantly regulated signaling pathway activated by TIF treatment, and this activation could be blocked with epigenetic regulators (Figure 4.8B). Other significantly impacted cellular activities included unfolded protein response, hypoxia, senescence, and DNA damage repair, indicating that TIF treatment induces stress-related responses in PDAC tumor cells. Common oncogenic signaling pathways related to PDAC cells, such as KRAS, P53, and MYC, were also identified by gene ontology analysis (Figure 4.8B). Further exploration of the gene set blocked upon TIF treatment revealed a substantial 44% overlap with genes that could be reactivated with the addition of OTX treatment (Figure 4.9A). Gene ontology analysis on these genes identified significant suppressions in multiple metabolic pathways in PDAC tumor cells upon TIF treatment, including cholesterol homeostasis, fatty acid metabolism, glycolysis, and

oxidative phosphorylation (Figure 4.9B). Most of these pathways function in tumor cells grown in a culture dish where nutrients are generally considered to be sufficient. The addition of TIF, however, appears to induce stress responses in PDAC tumor cells, leading to their transition into a state with reduced metabolic activities. Although not further pursued in our research, this metabolic switch might play protective roles for PDAC tumor cells growing *in vivo* where a hypoxic, hypovascular, and nutrient-deficient microenvironment prevails. Apart from metabolic changes, mTOR and E2F-related pathways were significantly inhibited by TIF (Figure 4.9B), suggesting reduced cell growth in response to TIF-related stress.

To validate the *in vivo* relevance of the identified TIF-altered cellular responses, we cross-referenced our findings with previously performed bulk RNA-seq, where the differential gene expression between PDAC1245 parental cells isolated from orthotopic tumors and those grown in 2D culture was analyzed (Figure 4.10 and 4.11). Interestingly, pathways induced by TIF treatment, such as TNFα-NFκB, epithelial-mesenchymal transition (EMT), hypoxia, KRAS, and P53 responses, were significantly upregulated *in vivo*. Conversely, pathways blocked by TIF, such as E2F, mTOR, and oxidative phosphorylation pathways, were also significantly downregulated *in vivo*. These findings suggest that *in vitro* use of TIF can recapitulate TME-induced responses in PDAC tumor cells *in vivo*.

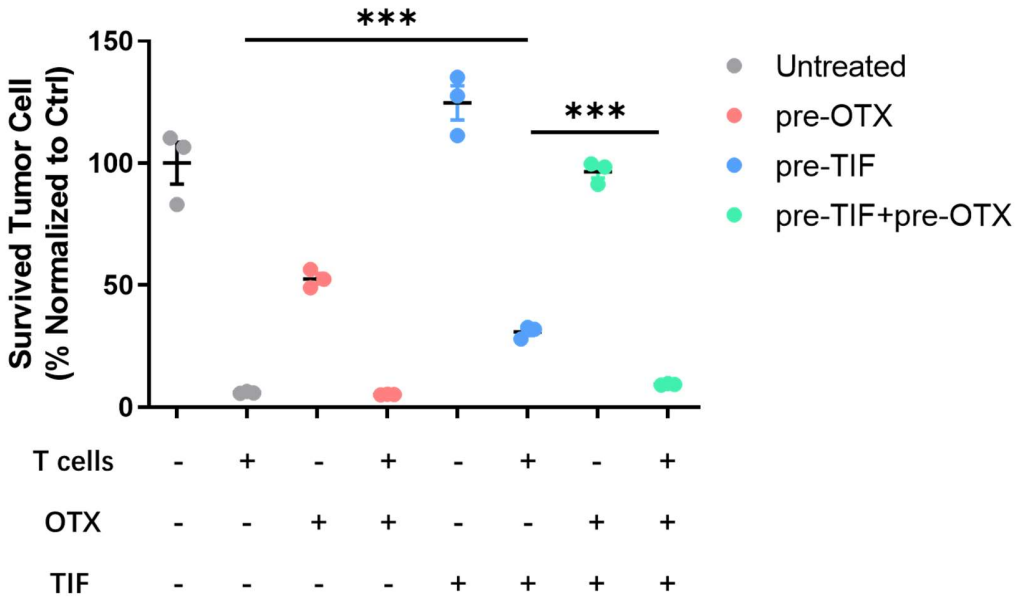

Figure 4.7 TIF-induced killing resistance in tumor cells can be blocked with BETi.

TIF education of killing resistance in tumor cells can be regulated with epigenetic regulator OTX. PDAC1245-gp33-12 cells were either untreated or pretreated with 1μM OTX, TIF and OTX+TIF before coculturing with P14 CD8 T cells. Data were measured by counting beads-based flow cytometry assay. Data are presented as dot plots, with each dot representing an individual value, horizontal lines indicating means and error bars indicating SEMs. Data significance was analyzed by Ordinary one-way ANOVA in Prism. ***P<0.001.

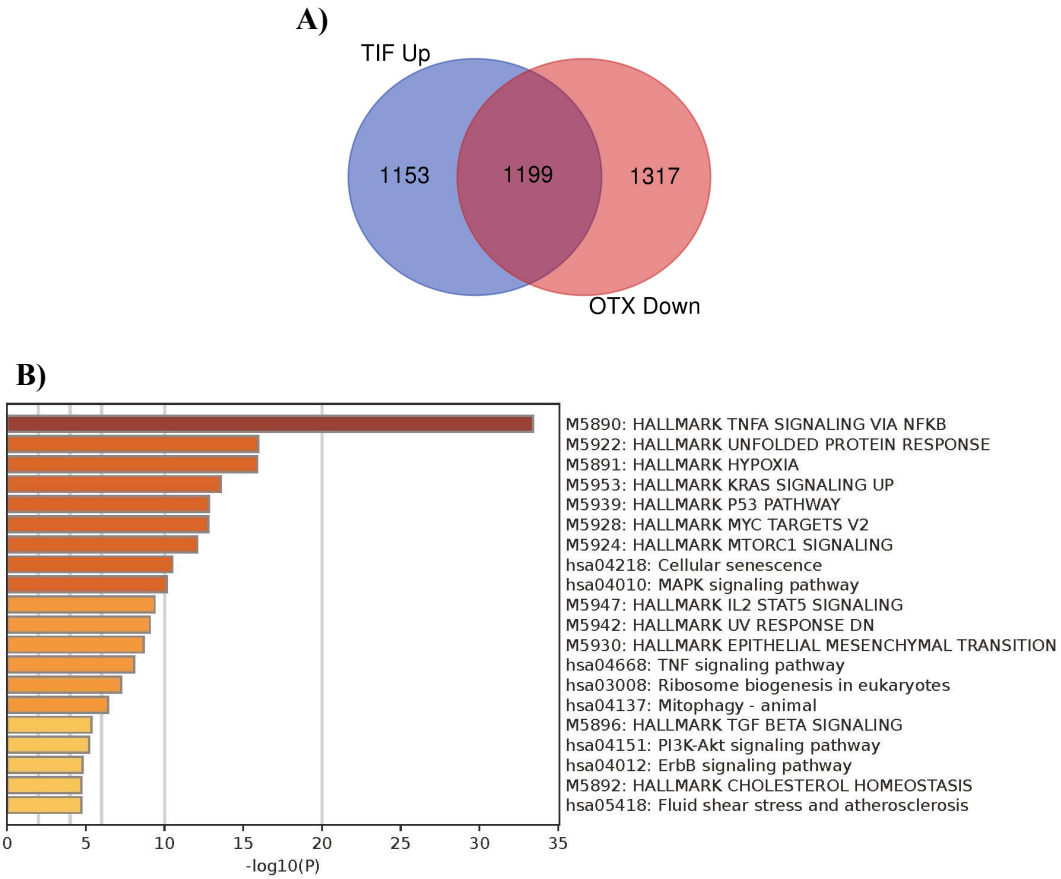

Figure 4.8 Pathways induced by TIF and inhibited by BETi in tumor cells.

A) Venn diagram showing number of genes with upregulation comparing untreated versus TIF treated arms and number of genes with downregulation comparing TIF treated versus TIF+OTX treated arms in PDAC1245-gp33-12 cells. Data were analyzed based of bulk RNA-seq results.
B) Gene Ontology (Pathway Enrichment) analysis of gene sets in PDAC1245-gp33-12 cells that were significantly upregulated by TIF and downregulated by OTX. Analysis was performed by Metascape, where gene list was referred to “HALLMARK” and “KEGG” database.

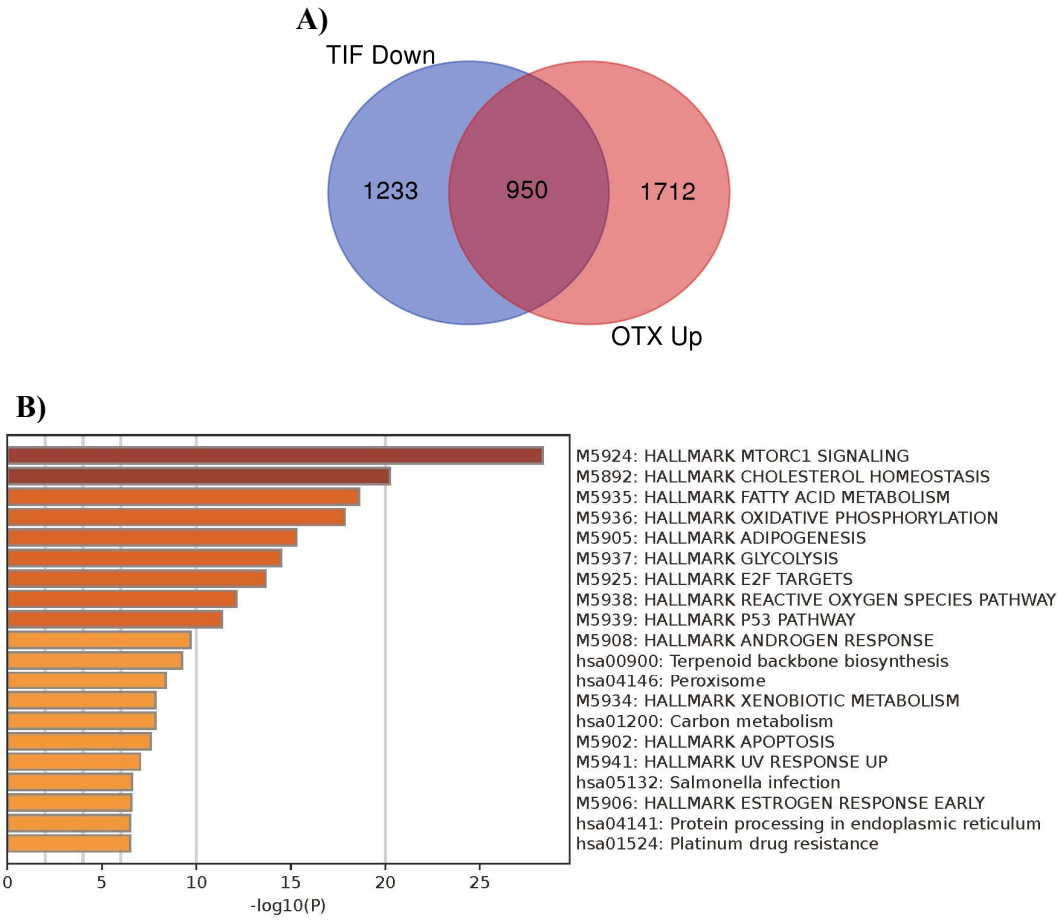

Figure 4.9 Pathways inhibited by TIF and induced by BETi in tumor cells.

A) Venn diagram showing number of genes with downregulation comparing untreated versus TIF treated arms and number of genes with upegulation comparing TIF treated versus TIF+OTX treated arms in PDAC1245-gp33-12 cells. Data were analyzed based of bulk RNA-seq results.
B) Gene Ontology (Pathway Enrichment) analysis of gene expression list that was found to be significantly downregulated by TIF and upregulated by OTX, i.e. overlapped genes in D). Analysis was performed by Metascape, where gene list was referred to “HALLMARK” and “KEGG” database.

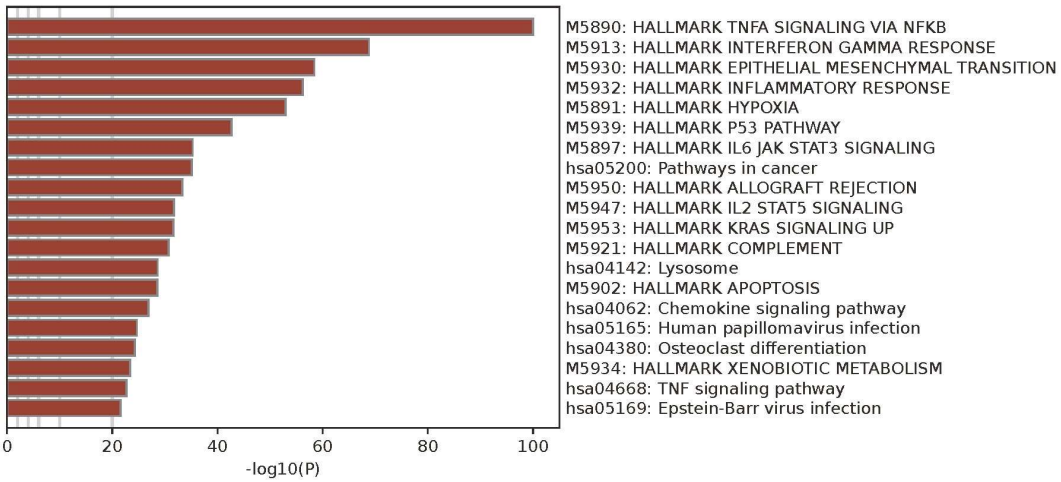

Figure 4.10 Pathways induced *in vivo* compared to *in vitro* in tumor cells.

Gene Ontology (Pathway Enrichment) analysis of gene expression list that was found to be significantly upregulated in PDAC1245 parental cells that were orthotopically transplanted into mouse (*in vivo*) comparing to those that were grown in 2D culture (*in vitro*). Analysis was performed by Metascape, where gene list was referred to “HALLMARK” and “KEGG” database.

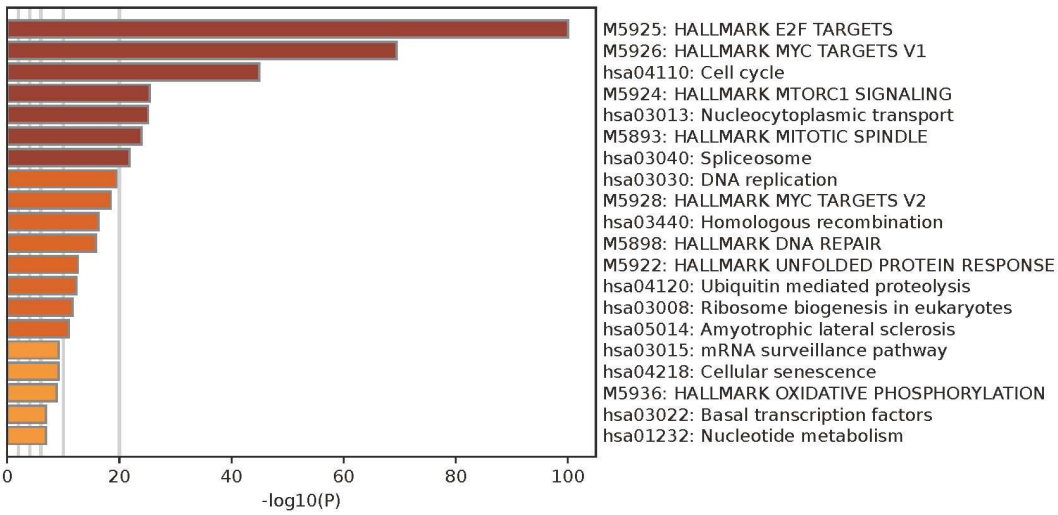

Figure 4.11 Pathways inhibited *in vivo* compared to *in vitro* in tumor cells.

Gene Ontology (Pathway Enrichment) analysis of gene expression list that was found to be significantly downregulated in PDAC1245 parental cells that were orthotopically transplanted into mouse (*in vivo*) comparing to those that were grown in 2D culture (*in vitro*). Analysis was performed by Metascape, where gene list was referred to “HALLMARK” and “KEGG” database.

4.4 Identification of TNFα-NFκB downstream targets promising for PDAC treatment

While TNFα signaling is extensively studied as one of the most commonly found cytokines mediating inflammation, its role in cancer development is complex and contradictory. To investigate whether the induction of TNFα-NFκB signaling by TIF treatment is crucial for tumor cell resistance against CD8 T cell-mediated killing, we depleted TNFα in TIF using a monoclonal TNFα neutralizing antibody (hereby referred to as αTNFα) before PDAC1245-gp33-12 cell treatment. The results showed that without activation of the TNFα signaling pathway, TIF-educated resistance of tumor cells was mostly abolished (Figure 4.12). This suggests that TNFα signaling is an effective pathway to target *in vivo* to sensitize PDAC tumors to CD8 T cell therapy. However, in our rag1-/- mouse model receiving PDAC1245-gp33-12 tumor cell transplants, αTNFα failed to promote P14 CD8 T cell therapy (data not shown). Considering that TNFα signaling also mediates inflammatory responses in multiple immune cell types such as macrophages, neutrophils, and immune effector cells, non-tumor-targeting blockade of TNFα may not lead to an overall anti-tumorigenic outcome.

To circumvent the dilemma of directly targeting TNFα signaling, we delved deeper into TNFα-NFκB-regulated genes identified from the bulk RNA-seq analysis described previously. We uncovered a list of genes that were significantly induced by TIF, suppressed by OTX, and upregulated *in vivo* compared to in 2D culture (Figure 4.13). Among these genes, ptgs2 (cox2) and lif have been documented to have immunosuppressive functions.

Prostaglandin-endoperoxide Synthase 2 (PTGS2, referred to as COX2) mediates the synthesis of prostaglandin E2 (PGE2), which, upon secretion and binding with prostaglandin receptors (EP) expressed on multiple stromal cell types and tumor cells, can impair anti-tumor immunity. Importantly, the crucial role of the COX2 (tumor cells)-PGE2 (microenvironment)-

EPHA2 (tumor cells) axis in mediating immune sensitivity of PDAC against T cell-mediated killing has previously been demonstrated (Markosyan, Li et al. 2019). The same study also demonstrated a synergistic effect combining the COX2 inhibitor Celecoxib with αPD1 and CD40 agonist on reducing PDAC tumor burden. On the other hand, Leukemia Inhibitory Factor (LIF), a key member of the IL-6 family of cytokines that mediates inflammation response, emerges as a significant factor in PDAC. Research indicates its capability not only to influence PDAC tumor cell differentiation and epithelial-mesenchymal transition (EMT) status (Shi, Gao et al. 2019), but also to impede intra-tumoral T cell recruitment by downregulating CXCL9 expression in tumor-associated macrophages (TAMs) via epigenetic mechanisms observed in glioblastoma and ovarian cancer (Pascual-Garcia, Bonfill-Teixidor et al. 2019). Furthermore, studies have highlighted LIF blockade as a strategy to enhance PDAC tumor sensitivity to gemcitabine (Wang, Fer et al. 2019). Nonetheless, its involvement in mediating PDAC tumor cell-intrinsic resistance to T cell-mediated cytotoxicity remains to be elucidated.

Importantly, our qPCR results confirmed Cox2 and Lif being downstream targets of TNFα signaling in TIF (Figure 4.14). These findings implicate that targeting COX2 and LIF, rather than their upstream regulator TNFα, can be promising strategies to treat PDAC tumors in combination with CD8 T cell therapy.

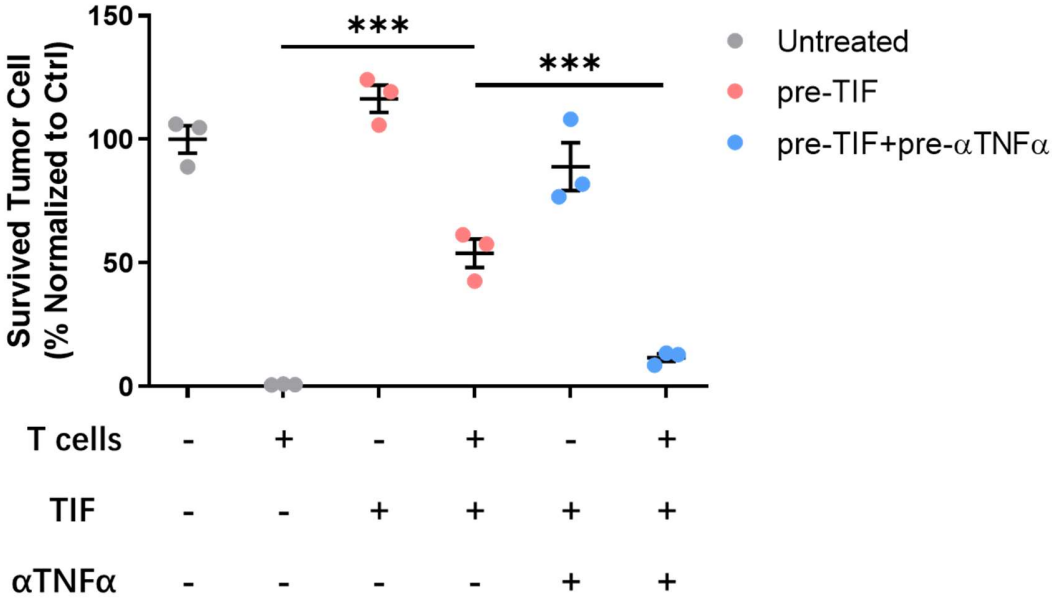

Figure 4.12 TNFα-depleted TIF reduces ability to induce killing resistance in tumor cells.

TIF education of killing resistance in tumor cells can be disrupted with TNFα neutralization in TIF. PDAC1245-gp33-12 cells were either untreated or pretreated with TIF and 5μg/ml αTNFα+TIF before coculturing with P14 CD8 T cells. Data were measured by counting beads-based flow cytometry assay. Data are presented as dot plots, with each dot representing an individual value, horizontal lines indicating means and error bars indicating SEMs. Data significance was analyzed by Ordinary one-way ANOVA in Prism. ***P<0.001.

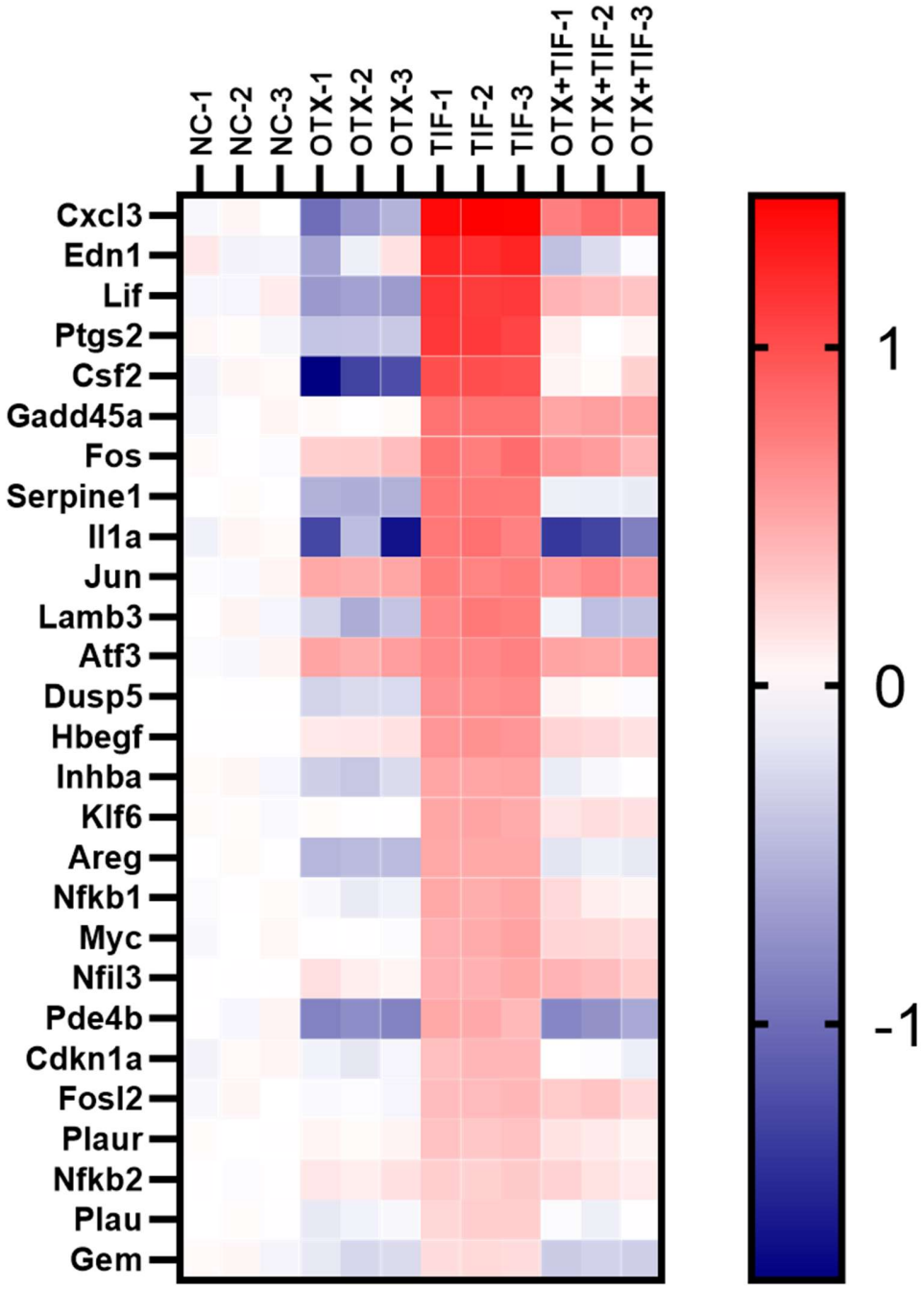

Figure 4.13 TNFα-NFκB downstream genes likely accounting for killing resistance in tumor cells.

Heatmap demonstrating a list of TNFα-NFκB downstream genes that are upregulated with TIF treatment, downregulated with OTX treatment, and upregulated *in vivo* compared to *in vitro*. Gene list was arranged based of average fold increase comparing TIF arm and NC arm. Heatmap was generated from bulk RNA-seq data using Metascape and Prism.

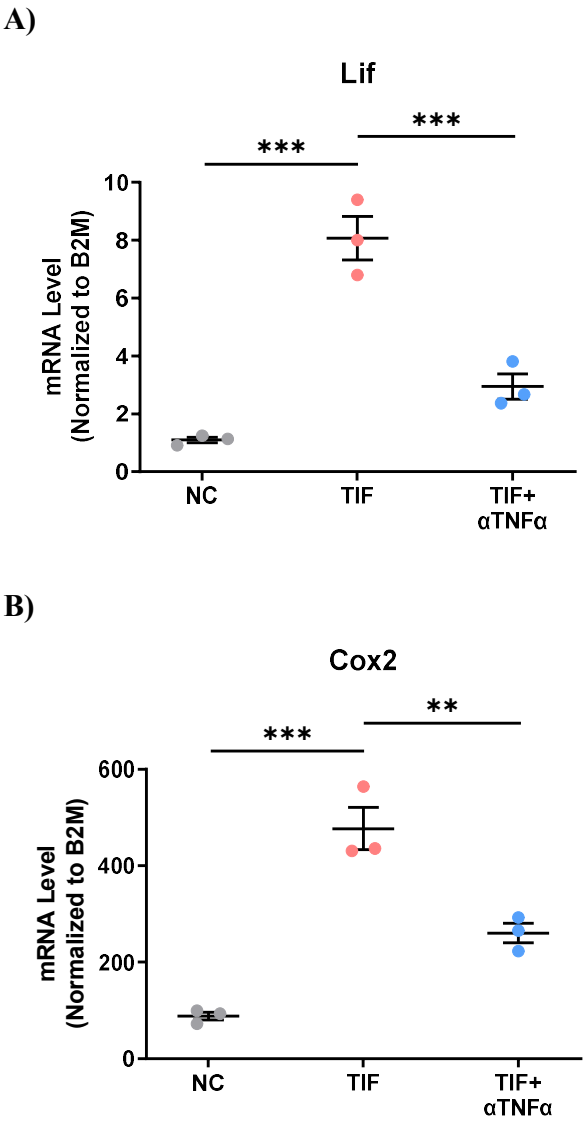

Figure 4.14 Lif and Cox2 expression in tumor cells is mediated partially by TNFα signaling in TIF.

qPCR analysis of A) Lif and B) Cox2 in PDAC1245-gp33-12 cells with treatment of TIF and 5μg/ml αTNFα. Data are presented as dot plots, with each dot representing an individual value, horizontal lines indicating means and error bars indicating SEMs. Data significance was analyzed by Ordinary one-way ANOVA in Prism. **P<0.01, ***P<0.001.

4.5 Targeting LIF and COX2 sensitize PDAC tumors to CD8 T cell-mediated killing

To assess the contribution of COX2 upregulation to the killing resistance phenotype in PDAC tumor cells, we introduced COX2 inhibitors (NS398, Celecoxib) or the COX2-synthesized product (PGE2) into the coculture system. Interestingly, PGE2 treatment alone resulted in a comparable killing-resistant outcome as TIF pre-treatment, while COX2 blockade with NS398 or Celecoxib resensitized PDAC1245-gp33-12 cells to P14 CD8 T cell-mediated killing (Figure 4.15). These results confirm that TIF induces PDAC tumor cells' killing resistance through the upregulation of COX2 in tumor cells. To assess whether COX2 inhibition could sensitize PDAC to CD8 T cell therapy *in vivo*, we administered Celecoxib to PDAC1245-gp33-12-bearing rag1-/- mice, with or without adoptive P14 CD8 T cell transfer. Our results showed that while Celecoxib alone did not affect tumor growth in the absence of T cells (Figure 4.16A), it significantly enhanced the killing efficiency of transferred P14 CD8 T cells, resulting in a further reduction in tumor burden after 3 weeks of treatment compared to P14 CD8 T cell transfer alone (Figure 4.16B). Notably, the survival benefit of Celecoxib+P14 CD8 T cell transfer over P14 CD8 T cell transfer alone was observed in rag1-/- mice bearing another PDAC1245-gp33 tumor line (Figure 4.17). These findings highlight the therapeutic potential of COX2 blockade, as identified through our *in vitro* coculture platform, in combination with adoptive CD8 T cell therapy in PDAC.

Additionally, we investigated the impact of blocking LIF, another downstream target of TNFα-NFκB signaling identified in tumor cells, on reducing CD8 T cell-mediated killing resistance. Apart from LIF produced by cancer associated fibroblasts (CAFs), here we showed that PDAC tumor cells can also be a source of LIF production, and that such production can be induced with TIF treatment. However, it remains unclear how tumor cell-produced LIF makes PDAC tumor cells resistant to killing, as it can work either by directly impacting CD8 T cell function or

activating tumor cells' intrinsic LIF signaling through autocrine or paracrine processes. To test these possibilities, we blocked LIF signaling with a neutralizing antibody either at the TIF pre-treatment stage or at the coculture stage, evaluating their impacts on CD8 T cell-mediated killing. Our results showed that LIF blockade in the coculture system did not restore T cell function for killing, indicating that tumor cell-produced LIF does not act directly on CD8 T cells. Alternatively, LIF signaling depletion during the TIF pre-treatment stage partially inhibited the acquisition of killing resistance in PDAC1245-gp33-12 cells (Figure 4.18), confirming the direct role of LIF on tumor cells. Taken together, our data demonstrated that tumor cell intrinsic LIF signaling, rather than the impact of secreted LIF on cocultured T cells, contributes to tumor cells' killing resistance phenotype. Next, we sought to investigate the impact of LIF blockade on CD8 T cell therapy *in vivo*. To achieve this, we administered αLIF to rag1-/- mice bearing PDAC1245-gp33-12 tumors, with or without adoptive P14 CD8 T cell transfer. Notably, we discovered that while LIF blockade alone did not affect tumor growth in the absence of CD8 T cells, just 1 week of αLIF treatment significantly enhanced CD8 T cell killing efficiency in tumor-bearing mice (Figure 4.19).

In summary, the inhibition of either COX2 or LIF in PDAC tumor cells disrupted TIF-educated killing resistance phenotype. While directly targeting TNFα signaling failed to impact tumor progression, targeting genes downstream of TNFα-NFκB holds promise for reducing PDAC tumor's immune resistance. Such an approach has the potential to serve as a therapeutic strategy in combination with CD8 T cell therapy.

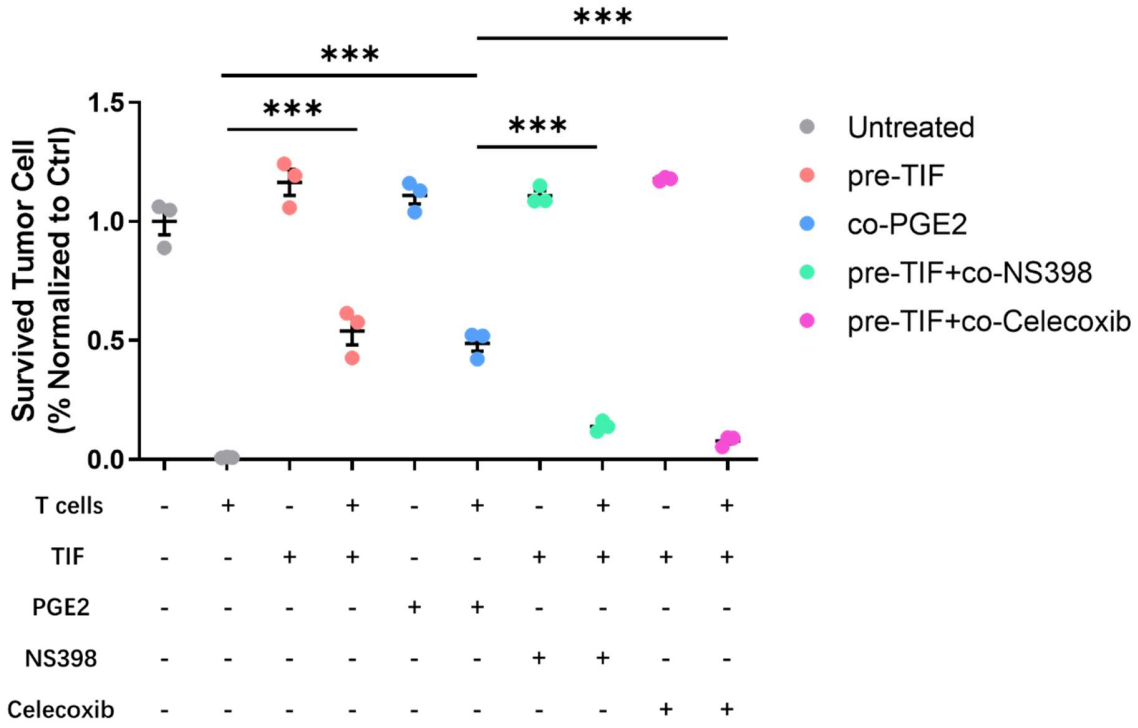

Figure 4.15 TIF-induced killing resistance in tumor cells is partially mediated by COX2.

TIF education of killing resistance in tumor cells can be mediated by COX2 function. PDAC1245-gp33-12 cells were either untreated or pretreated with TIF, and were then cocultured with P14 CD8 T cells. COX2-synthesized products (5μM PGE2) or COX2 inhibitors (10μM NS398 or 1μM Celecoxib) were added into the coculture. Data were measured by counting beads-based flow cytometry assay. Data are presented as dot plots, with each dot representing an individual value, horizontal lines indicating means and error bars indicating SEMs. Data significance was analyzed by Ordinary one-way ANOVA in Prism. ***P<0.001.

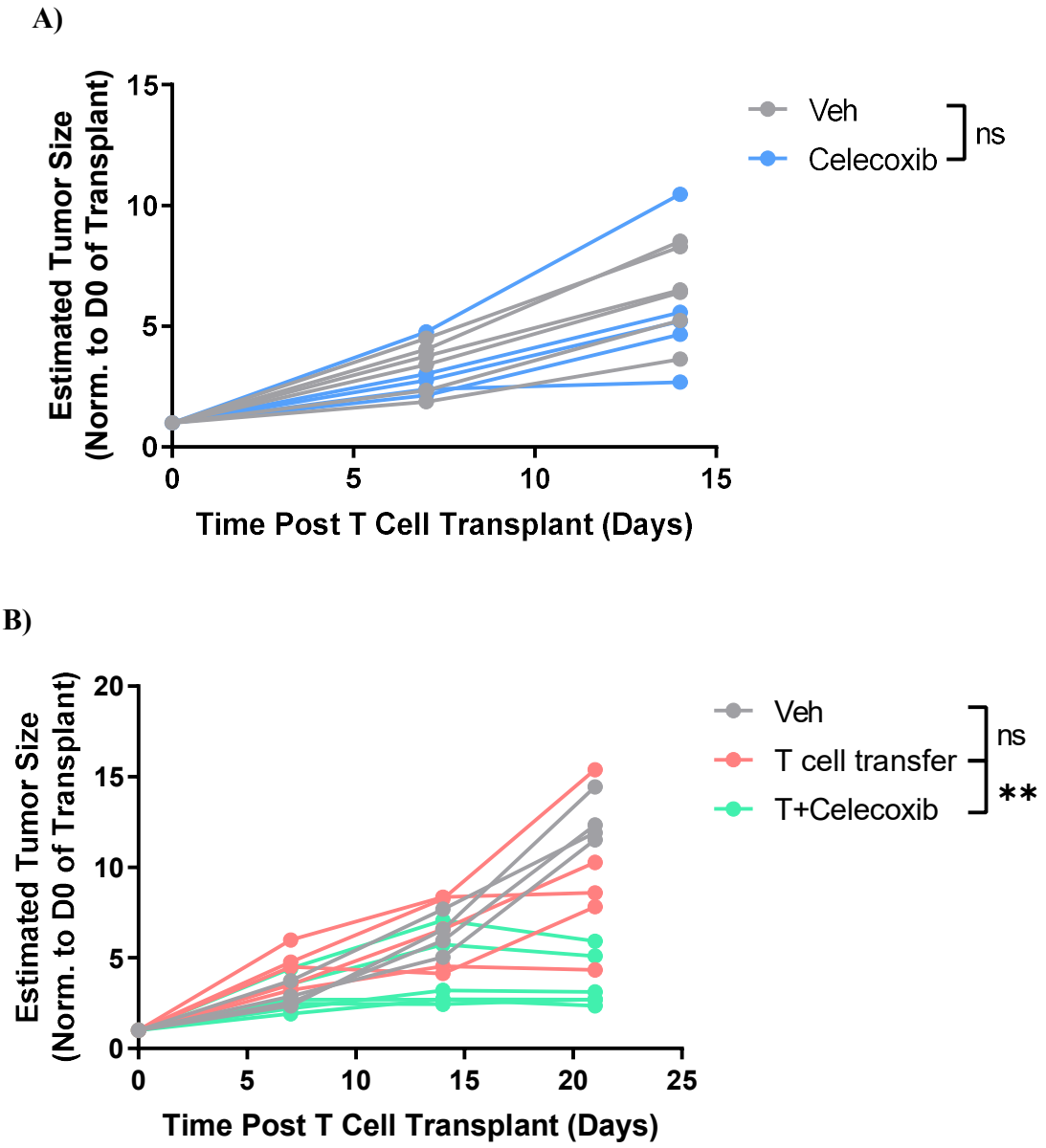

Figure 4.16 COX2 inhibition promotes sensitivity of PDAC tumor to T cell-mediated killing.

A) Tumor volume change over time in rag1-/- mice bearing orthotopically transplanted PDAC1245-gp33-12 tumor. Mice were treated daily with Veh or 200mg/kg Celecoxib o.g. for 2 weeks. Tumor volume was measured by ultrasound imaging. Data are presented as connecting-dot plots, with each line of connected dots representing an individual tumor measured at different timepoints. Data significance was analyzed by Two-tailed Unpaired t-test in Prism.
B) Tumor volume change over time in rag1-/- mice bearing orthotopically transplanted PDAC1245-gp33-12 tumor. Mice receiving adoptive CD8 T cell transfer were treated daily with Veh or 200mg/kg Celecoxib o.g. for 3 weeks. Tumor volume was measured by ultrasound imaging. Data are presented as connecting-dot plots, with each line of connected dots representing an individual tumor measured at different timepoints. Data significance was analyzed by Ordinary one-way ANOVA in Prism. **P<0.01.

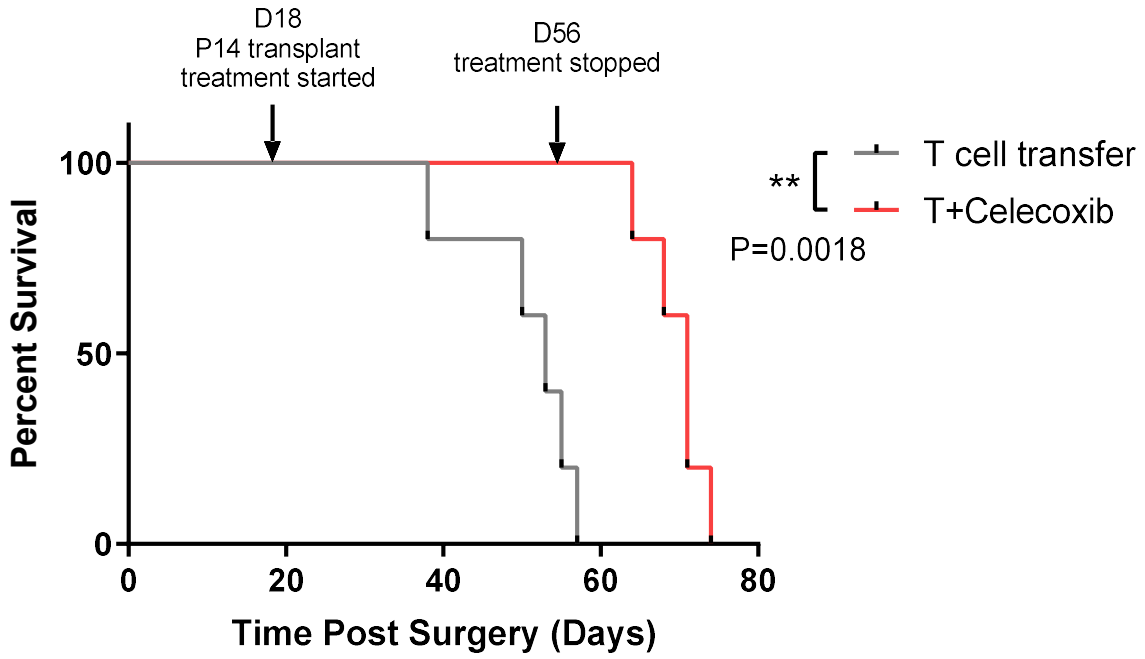

Figure 4.17 COX2 inhibition in combination with adoptive T cell therapy shows survival benefit in PDAC-bearing mouse.

Survival study of rag1-/- mice bearing orthotopically transplanted PDAC1245-gp33-05 tumor. Mice receiving adoptive CD8 T cell transfer were treated daily with Veh or 200mg/kg Celecoxib o.g. for 39 days. Data significance was analyzed by Log-rank test in Prism. **P<0.01.

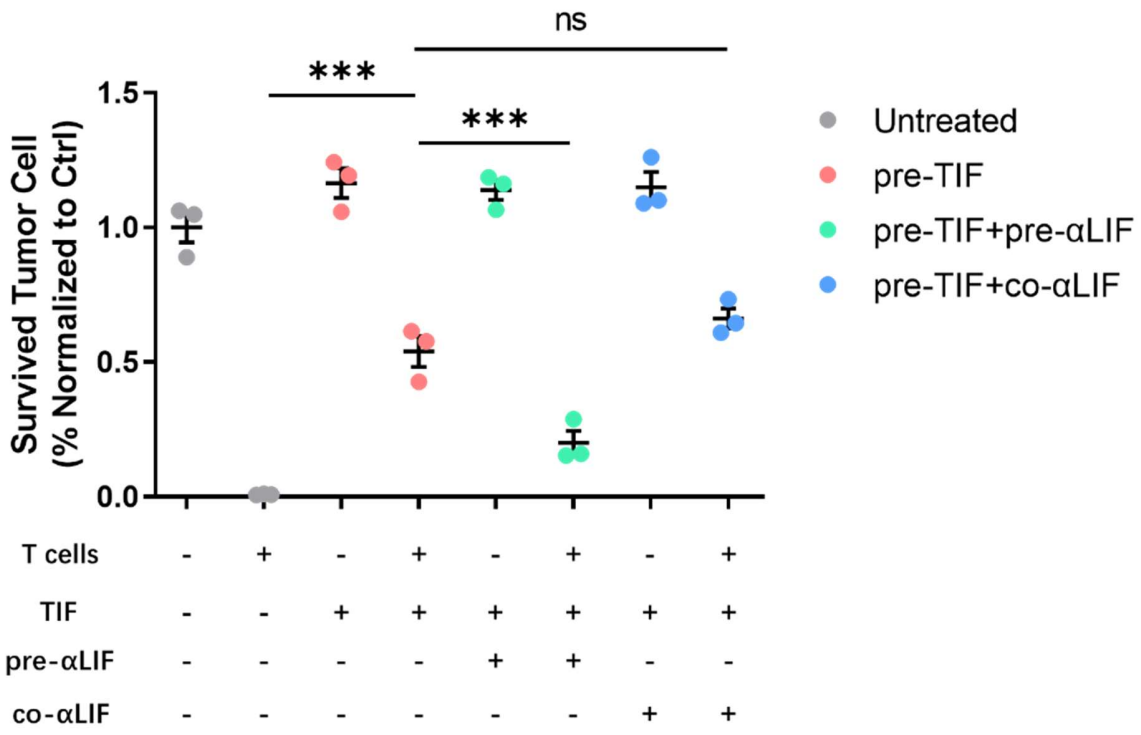

Figure 4.18 TIF-induced killing resistance is partially mediated by LIF signaling within tumor cells.

TIF education of killing resistance in tumor cells can be mediated by LIF signaling in tumor cells. PDAC1245-gp33-12 cells were either untreated or pretreated with TIF, and were then cocultured with P14 CD8 T cells. 5μg/ml of αLIF was added either during the pretreatment stage (pre-αLIF) or directly into the coculture (co-αLIF). Data were measured by counting beads-based flow cytometry assay. Data are presented as dot plots, with each dot representing an individual value, horizontal lines indicating means and error bars indicating SEMs. Data significance was analyzed by Ordinary one-way ANOVA in Prism. ***P<0.001.

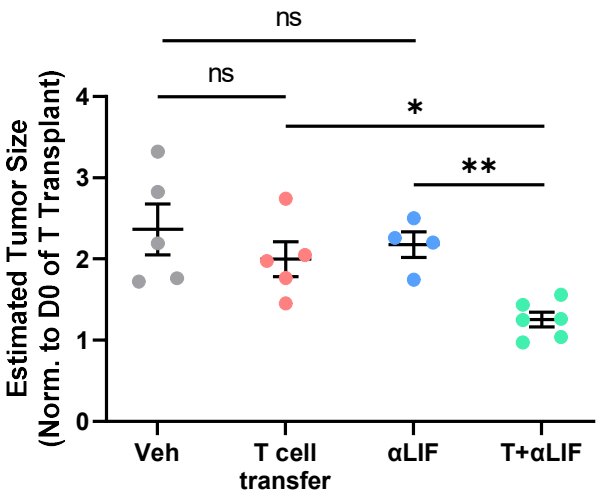

Figure 4.19 LIF blockade promotes sensitivity of PDAC tumor to T cell-mediated killing.

Tumor volume in rag1-/- mice bearing orthotopically transplanted PDAC1245-gp33-12 tumor. Mice with or without adoptive CD8 T cell transfer were treated once every 3 days with Veh or 10mg/kg αLIF i.p. for 1 week. Data were measured by Ultrasound imaging. Data are presented as dot plots, with each dot representing an individual tumor. Data significance was analyzed by Ordinary one-way ANOVA in Prism. *P<0.05, **P<0.01.

Discussion

The inherent resistance of pancreatic cancer, particularly PDAC, to immunotherapy is a well-documented challenge. This resistance is predominantly ascribed to the desmoplastic stroma of pancreatic cancer, which not only directly impedes immune effector cell function, as discussed earlier, but also imparts resistance to immune effector cell-mediated killing by educating tumor cells. In this study, we employed TIF *in vitro* to partially emulate the functions of the TME observed in PDAC tumors, establishing a platform to investigate antigen-specific CD8 T cell killing of PDAC tumor cells. Our results demonstrate that PDAC tumor cells exhibit efficient killing by antigen-specific CD8 T cells in the absence of TME. However, TIF treatment of tumor cells initiates a TNFα-NFκB signaling response, mirroring observations *in vivo*. This TNFα-NFκB response plays a crucial role in reinstating PDAC tumor cells' ability to resist CD8 T cell-mediated killing. Notably, the effects of TIF can be counteracted either through TNFα depletion or inhibition of downstream targets of TNFα-NFκB, such as COX2 and LIF. Our *in vivo* experiments further underscore that while direct targeting of TNFα may not be efficacious, independent blockade of COX2 with Celecoxib and LIF with αLIF can sensitize PDAC tumors to adoptive CD8 T cell therapy. These findings open avenues for the development of innovative therapeutic strategies in pancreatic cancer, utilizing TIF as a valuable tool for further exploration.

Historically, the focus of TIF studies has predominantly centered around its formation and the physical implications of its pressure on nutrient and drug delivery within solid tumors (Bockelmann and Schumacher 2019) (Stylianopoulos, Munn et al. 2018) (Heldin, Rubin et al. 2004). TIF in solid tumors is typically characterized as hypoxic, acidic (attributed to lactate accumulation), and exhibiting elevated pressure compared to plasma and subcutaneous interstitial fluid (Wagner and Wiig 2015). These features collectively create a stressful microenvironment in

solid tumors. Despite proteomic analyses dissecting TIF components (Baronzio, Parmar et al. 2014), limited efforts have been directed towards exploring the composition of TIF in pancreatic cancer, where stromal components significantly contribute to TIF formation alongside tumor cells. The contribution of stromal cell-secreted factors to the resistance of pancreatic tumors to treatment remains unexplored. Additionally, while our findings demonstrate the feasibility of using TIF to educate PDAC tumor cells to exhibit *in vivo*-like responses, it remains unexplored whether TIF elicits similar effects on stromal cells, such as macrophages and fibroblasts, grown in 2D culture. A parallel study in our laboratory indicates that TIF induces M2 marker expression in M0 macrophages cultured *in vitro* (data not shown), suggesting potential roles in supporting PDAC tumor cells observed *in vivo*. Further investigation is warranted to determine whether TIF treatment *in vitro* maintains *in vivo* features in cancer-associated fibroblasts (CAFs), as these cells tend to lose their subtype features (i.e., iCAF, myCAF, and apCAF) after isolation from tumors and cultivation on plastic plates. In addition, it is crucial to acknowledge that while TIF recapitulates many features of the TME in PDAC, some responses altered within PDAC tumor cells are uniquely observed *in vivo* but not replicated with TIF treatment. These disparities, such as the activation of IFNγ responses, enhanced IL6 signaling, downregulation rather than upregulation of Myc target genes, and reduced spliceosome function (Figure 4.10 and 4.11), may be attributed to the limitations of TIF representing only the soluble factors in PDAC tumors. Responses triggered by matrix-bound factors or direct cell-cell interactions cannot be fully captured by TIF. Despite these limitations, the use of TIF *in vitro* holds promise for providing a more comprehensive understanding of the TME in PDAC, which, when combined with drug screening and CRISPR screening, could lead to novel discoveries in the treatment of pancreatic cancer.

An outstanding revelation from our bulk RNA-seq analysis, comparing untreated *in vitro* conditions, TIF-treated *in vitro* conditions, and *in vivo* groups, underscores the hyperactive TNFα-NFκB signaling within PDAC tumor cells. Initially recognized as a pro-inflammatory cytokine, TNFα's dual roles in carcinogenesis hinge on its concentration, production source, interacting receptors, and the cell types it engages under different circumstances. In the context of PDAC, TNFα has been predominantly identified as a pro-tumorigenic factor, promoting PDAC cell growth (Egberts, Cloosters et al. 2008) and aggressiveness (Kali, Ostapchuk et al. 2017) *in vitro*. In immune-deficient mouse models of human PDAC tumors, Infliximab, but not Etanercept (both commercial TNFα-blocking antibodies), was effective in slowing tumor progression (Egberts, Cloosters et al. 2008). And despite TNFα expression levels in human PDAC tumors not correlating with tumor stage, higher TNFα levels were associated with poor responses to chemotherapies (Zhao, Fan et al. 2016). However, clinical trials have shown that αTNFα fails to improve chemotherapy efficacy in advanced PDAC-bearing patients (Wu, Fernandez et al. 2013). The contradictory findings between *in vitro* and *in vivo*, as well as between mouse models and human patients, underscore the complexity of direct and non-cell-type-specific TNFα targeting. While TNFα signaling triggered in PDAC tumor cells can be pro-tumorigenic, its pro-inflammatory effects on immune cells, such as macrophages and dendritic cells, suggest an anti-tumorigenic role. The unpredictable impact of systemic TNFα blockade on PDAC tumor progression, with functions on both sides muted, underscores the challenge of targeting TNFα directly. Although selective targeting of TNFα signaling in tumor cells remains promising, our approach delves deeper into PDAC cells on TNFα-NFκB downstream target genes. We hypothesize that the induction of immunosuppressive genes or pathways through TNFα-NFκB signaling contributes to tumor cells' resistance to CD8 T cell-mediated killing. This research identifies COX2 and LIF as factors that

directly empower tumor cells to resist CD8 T cells, while other TNFα-NFκB-regulated factors identified in our analysis may serve pro-tumorigenic roles through crosstalk with other stromal cell types. For example, PDAC tumor cells secreting CXCL3 have been identified to interact with CXCR2, an exclusive receptor expressed in cancer-associated fibroblasts (CAFs). This interaction triggers the formation of myofibroblastic CAFs (myCAFs) and facilitates metastasis (Sun, He et al. 2022). Conversely, the upregulation of Edn1 serves as a significant regulator in mediating drug infiltration through endothelial cells. The blockade of Endothelin receptor holds promise as a potential strategy to enhance the perfusion of therapeutic agents into PDAC tumors (Gautam, Dalal et al. 2022). Furthermore, Csf2, a gene expressing granulocyte-macrophage colony-stimulating factor (GMCSF), has the ability to recruit Gr1+ myeloid cells into tumors to inhibit anti-tumor immunity of PDAC (Bayne, Beatty et al. 2012). The identification of these TNFα-NFκB targets broadens our exploration into the diverse functions of TIF on various stromal cell types within pancreatic tumors.

In summary, this study reveals a novel TIF-induced immune evasion program in pancreatic cancer, providing potential strategies to overcome tumor cell resistance to T cell-mediated killing, including LIF blockade, COX2 inhibition, and BET inhibitor (BETi) treatment. These findings have broad implications not only for CAR-T therapies but also for various immunotherapy strategies reliant on T cells, such as immune checkpoint blockade, T cell-stimulatory cytokine treatment, and therapeutic cancer vaccines. Despite these promising discoveries, several outstanding questions persist. Beyond TNFα, there may be additional factors in TIF educating PDAC tumor cells, necessitating exploration for potential co-targets to enhance therapeutic efficacy. Furthermore, the extent to which the identified factors in mouse TIF are present in human PDAC tumors remains unclear and could be addressed through comparative mass spectrometry-

based profiling. In addition, the epigenetic control of resistance regulatory genes, such as COX2 and LIF, following BET inhibition raises intriguing questions about whether BETi could serve as a superior strategy over COX2 and LIF targeting. Super-enhancer profiling in PDAC tumor cells upon TIF treatment could provide insights to these questions. Additionally, the functional validation of identified therapeutic targets in human PDAC tumors remains an open question, which could be addressed through evaluating LIF and COX2 blockade in tissue-slice cultures of human PDAC tissues combined with exogenously added CAR-T cells. Ultimately, the future work proposed here could even lead to personalized medicine strategies where patient specific TIF and tumor slice cultures could be used to identify stromal immunosuppressive factors, model how their targeted inhibition impacts T cell mediated killing, and guide patient enrollment into CAR-T cell trials.

Acknowledgements

Chapter 4, in full, is currently being prepared for submission for publication of the material. Work in this chapter was done in collaboration with Morgan Truitt, who helped with experimental design and data analysis. Hanna Dhiyebi, Mariel Burquez, Daniel Cao and Christopher Liddle provided technical support. The dissertation author was the primary researcher and author of this material. This chapter was written under the guidance of Morgan Truitt, Michael Downes, Annette Atkins, Ruth Yu and Ronald Evans.

References

Baronzio, G., G. Parmar, M. Baronzio and M. Kiselevsky (2014). "Tumor interstitial fluid: proteomic determination as a possible source of biomarkers." Cancer Genomics Proteomics 11(5): 225-237.

Bayne, L. J., G. L. Beatty, N. Jhala, C. E. Clark, A. D. Rhim, B. Z. Stanger and R. H. Vonderheide (2012). "Tumor-derived granulocyte-macrophage colony-stimulating factor regulates myeloid inflammation and T cell immunity in pancreatic cancer." Cancer Cell 21(6): 822-835.

Bockelmann, L. C. and U. Schumacher (2019). "Targeting tumor interstitial fluid pressure: will it yield novel successful therapies for solid tumors?" Expert Opin Ther Targets 23(12): 1005-1014.

Dagar, G., A. Gupta, T. Masoodi, S. Nisar, M. Merhi, S. Hashem, R. Chauhan, M. Dagar, S. Mirza, P. Bagga, R. Kumar, A. S. A. Akil, M. A. Macha, M. Haris, S. Uddin, M. Singh and A. A. Bhat (2023). "Harnessing the potential of CAR-T cell therapy: progress, challenges, and future directions in hematological and solid tumor treatments." J Transl Med 21(1): 449.

Das, S., B. Shapiro, E. A. Vucic, S. Vogt and D. Bar-Sagi (2020). "Tumor Cell-Derived IL1beta Promotes Desmoplasia and Immune Suppression in Pancreatic Cancer." Cancer Res 80(5): 1088-1101.

Dixit, A., A. Sarver, J. Zettervall, H. Huang, K. Zheng, R. A. Brekken and P. P. Provenzano (2022). "Targeting TNF-alpha-producing macrophages activates antitumor immunity in pancreatic cancer via IL-33 signaling." JCI Insight 7(22).

Du, H., K. Hirabayashi, S. Ahn, N. P. Kren, S. A. Montgomery, X. Wang, K. Tiruthani, B. Mirlekar, D. Michaud, K. Greene, S. G. Herrera, Y. Xu, C. Sun, Y. Chen, X. Ma, C. R. Ferrone, Y. Pylayeva-Gupta, J. J. Yeh, R. Liu, B. Savoldo, S. Ferrone and G. Dotti (2019). "Antitumor Responses in the Absence of Toxicity in Solid Tumors by Targeting B7-H3 via Chimeric Antigen Receptor T Cells." Cancer Cell 35(2): 221-237 e228.

Egberts, J. H., V. Cloosters, A. Noack, B. Schniewind, L. Thon, S. Klose, B. Kettler, C. von Forstner, C. Kneitz, J. Tepel, D. Adam, H. Wajant, H. Kalthoff and A. Trauzold (2008). "Anti-tumor necrosis factor therapy inhibits pancreatic tumor growth and metastasis." Cancer Res 68(5): 1443-1450.

Feng, K., Y. Liu, Y. Guo, J. Qiu, Z. Wu, H. Dai, Q. Yang, Y. Wang and W. Han (2018). "Phase I study of chimeric antigen receptor modified T cells in treating HER2-positive advanced biliary tract cancers and pancreatic cancers." Protein Cell 9(10): 838-847.

Gairin, J. E., H. Mazarguil, D. Hudrisier and M. B. Oldstone (1995). "Optimal lymphocytic choriomeningitis virus sequences restricted by H-2Db major histocompatibility complex class I molecules and presented to cytotoxic T lymphocytes." J Virol 69(4): 2297-2305.

Gautam, S. K., V. Dalal, B. R. Sajja, S. Gupta, M. Gulati, N. V. Dwivedi, A. Aithal, J. L. Cox, S. Rachagani, Y. Liu, V. Chung, R. Salgia, S. K. Batra and M. Jain (2022). "Endothelin-axis antagonism enhances tumor perfusion in pancreatic cancer." Cancer Lett 544: 215801.

Glorieux, C., X. Xia, Y. Q. He, Y. Hu, K. Cremer, A. Robert, J. Liu, F. Wang, J. Ling, P. J. Chiao and P. Huang (2021). "Regulation of PD-L1 expression in K-ras-driven cancers through ROS-mediated FGFR1 signaling." Redox Biol 38: 101780.

Gumber, D. and L. D. Wang (2022). "Improving CAR-T immunotherapy: Overcoming the challenges of T cell exhaustion." EBioMedicine 77: 103941.

Heldin, C. H., K. Rubin, K. Pietras and A. Ostman (2004). "High interstitial fluid pressure - an obstacle in cancer therapy." Nat Rev Cancer 4(10): 806-813.

Hiraoka, N., Y. Ino, S. Hori, R. Yamazaki-Itoh, C. Naito, M. Shimasaki, M. Esaki, S. Nara, Y. Kishi, K. Shimada, N. Nakamura, T. Torigoe and Y. Heike (2020). "Expression of classical human leukocyte antigen class I antigens, HLA-E and HLA-G, is adversely prognostic in pancreatic cancer patients." Cancer Sci 111(8): 3057-3070.

Ireland, L., T. Luckett, M. C. Schmid and A. Mielgo (2020). "Blockade of Stromal Gas6 Alters Cancer Cell Plasticity, Activates NK Cells, and Inhibits Pancreatic Cancer Metastasis." Front Immunol 11: 297.

Ischenko, I., S. D'Amico, M. Rao, J. Li, M. J. Hayman, S. Powers, O. Petrenko and N. C. Reich (2021). "KRAS drives immune evasion in a genetic model of pancreatic cancer." Nat Commun 12(1): 1482.

Kali, A., Y. O. Ostapchuk and N. N. Belyaev (2017). "TNFalpha and TGFbeta-1 synergistically increase the cancer stem cell properties of MiaPaCa-2 cells." Oncol Lett 14(4): 4647-4658.

Li, T., T. Guo, H. Liu, H. Jiang and Y. Wang (2021). "Platelet-derived growth factor-BB mediates pancreatic cancer malignancy via regulation of the Hippo/Yes-associated protein signaling pathway." Oncol Rep 45(1): 83-94.

Lohr, M., C. Schmidt, J. Ringel, M. Kluth, P. Muller, H. Nizze and R. Jesnowski (2001). "Transforming growth factor-beta1 induces desmoplasia in an experimental model of human pancreatic carcinoma." Cancer Res 61(2): 550-555.

Malik, S., J. M. Westcott, R. A. Brekken and F. J. Burrows (2021). "CXCL12 in Pancreatic Cancer: Its Function and Potential as a Therapeutic Drug Target." Cancers (Basel) 14(1).

Markosyan, N., J. Li, Y. H. Sun, L. P. Richman, J. H. Lin, F. Yan, L. Quinones, Y. Sela, T. Yamazoe, N. Gordon, J. W. Tobias, K. T. Byrne, A. J. Rech, G. A. FitzGerald, B. Z. Stanger and R. H. Vonderheide (2019). "Tumor cell-intrinsic EPHA2 suppresses anti-tumor immunity by regulating PTGS2 (COX-2)." J Clin Invest 129(9): 3594-3609.

Maude, S. L., T. W. Laetsch, J. Buechner, S. Rives, M. Boyer, H. Bittencourt, P. Bader, M. R. Verneris, H. E. Stefanski, G. D. Myers, M. Qayed, B. De Moerloose, H. Hiramatsu, K. Schlis, K. L. Davis, P. L. Martin, E. R. Nemecek, G. A. Yanik, C. Peters, A. Baruchel, N. Boissel, F. Mechinaud, A. Balduzzi, J. Krueger, C. H. June, B. L. Levine, P. Wood, T. Taran, M. Leung, K. T. Mueller, Y. Zhang, K. Sen, D. Lebwohl, M. A. Pulsipher and S. A. Grupp (2018). "Tisagenlecleucel in Children and Young Adults with B-Cell Lymphoblastic Leukemia." N Engl J Med 378(5): 439-448.

Mutgan, A. C., H. E. Besikcioglu, S. Wang, H. Friess, G. O. Ceyhan and I. E. Demir (2018). "Insulin/IGF-driven cancer cell-stroma crosstalk as a novel therapeutic target in pancreatic cancer." Mol Cancer 17(1): 66.

Pascual-Garcia, M., E. Bonfill-Teixidor, E. Planas-Rigol, C. Rubio-Perez, R. Iurlaro, A. Arias, I. Cuartas, A. Sala-Hojman, L. Escudero, F. Martinez-Ricarte, I. Huber-Ruano, P. Nuciforo, L. Pedrosa, C. Marques, I. Brana, E. Garralda, M. Vieito, M. Squatrito, E. Pineda, F. Graus, C. Espejo, J. Sahuquillo, J. Tabernero and J. Seoane (2019). "LIF regulates CXCL9 in tumor-associated macrophages and prevents CD8(+) T cell tumor-infiltration impairing anti-PD1 therapy." Nat Commun 10(1): 2416.

Posey, A. D., Jr., R. D. Schwab, A. C. Boesteanu, C. Steentoft, U. Mandel, B. Engels, J. D. Stone, T. D. Madsen, K. Schreiber, K. M. Haines, A. P. Cogdill, T. J. Chen, D. Song, J. Scholler, D. M. Kranz, M. D. Feldman, R. Young, B. Keith, H. Schreiber, H. Clausen, L. A. Johnson and C. H. June (2016). "Engineered CAR T Cells Targeting the Cancer-Associated Tn-Glycoform of the Membrane Mucin MUC1 Control Adenocarcinoma." Immunity 44(6): 1444-1454.

Pylayeva-Gupta, Y., K. E. Lee, C. H. Hajdu, G. Miller and D. Bar-Sagi (2012). "Oncogenic Kras-induced GM-CSF production promotes the development of pancreatic neoplasia." Cancer Cell 21(6): 836-847.

Shi, Y., W. Gao, N. K. Lytle, P. Huang, X. Yuan, A. M. Dann, M. Ridinger-Saison, K. E. DelGiorno, C. E. Antal, G. Liang, A. R. Atkins, G. Erikson, H. Sun, J. Meisenhelder, E. Terenziani, G. Woo, L. Fang, T. P. Santisakultarm, U. Manor, R. Xu, C. R. Becerra, E. Borazanci, D. D. Von Hoff, P. M. Grandgenett, M. A. Hollingsworth, M. Leblanc, S. E. Umetsu, E. A. Collisson, M. Scadeng, A. M. Lowy, T. R. Donahue, T. Reya, M. Downes, R. M. Evans, G. M. Wahl, T. Pawson, R. Tian and T. Hunter (2019). "Targeting LIF-mediated paracrine interaction for pancreatic cancer therapy and monitoring." Nature 569(7754): 131-135.

Steele, C. W., S. A. Karim, J. D. G. Leach, P. Bailey, R. Upstill-Goddard, L. Rishi, M. Foth, S. Bryson, K. McDaid, Z. Wilson, C. Eberlein, J. B. Candido, M. Clarke, C. Nixon, J. Connelly, N. Jamieson, C. R. Carter, F. Balkwill, D. K. Chang, T. R. J. Evans, D. Strathdee, A. V. Biankin, R. J. B. Nibbs, S. T. Barry, O. J. Sansom and J. P. Morton (2016). "CXCR2 Inhibition Profoundly Suppresses Metastases and Augments Immunotherapy in Pancreatic Ductal Adenocarcinoma." Cancer Cell 29(6): 832-845.

Sterner, R. C. and R. M. Sterner (2021). "CAR-T cell therapy: current limitations and potential strategies." Blood Cancer J 11(4): 69.

Stylianopoulos, T., L. L. Munn and R. K. Jain (2018). "Reengineering the Physical Microenvironment of Tumors to Improve Drug Delivery and Efficacy: From Mathematical Modeling to Bench to Bedside." Trends Cancer 4(4): 292-319.

Sun, X., X. He, Y. Zhang, K. Hosaka, P. Andersson, J. Wu, J. Wu, X. Jing, Q. Du, X. Hui, B. Ding, Z. Guo, A. Hong, X. Liu, Y. Wang, Q. Ji, R. Beyaert, Y. Yang, Q. Li and Y. Cao (2022). "Inflammatory cell-derived CXCL3 promotes pancreatic cancer metastasis through a novel myofibroblast-hijacked cancer escape mechanism." Gut 71(1): 129-147.

Tape, C. J., S. Ling, M. Dimitriadi, K. M. McMahon, J. D. Worboys, H. S. Leong, I. C. Norrie, C. J. Miller, G. Poulogiannis, D. A. Lauffenburger and C. Jorgensen (2016). "Oncogenic KRAS Regulates Tumor Cell Signaling via Stromal Reciprocation." Cell 165(4): 910-920.

Vaish, U., T. Jain, A. C. Are and V. Dudeja (2021). "Cancer-Associated Fibroblasts in Pancreatic Ductal Adenocarcinoma: An Update on Heterogeneity and Therapeutic Targeting." Int J Mol Sci 22(24).

Wagner, M. and H. Wiig (2015). "Tumor Interstitial Fluid Formation, Characterization, and Clinical Implications." Front Oncol 5: 115.

Wang, M. T., N. Fer, J. Galeas, E. A. Collisson, S. E. Kim, J. Sharib and F. McCormick (2019). "Blockade of leukemia inhibitory factor as a therapeutic approach to KRAS driven pancreatic cancer." Nat Commun 10(1): 3055.

Wang, Z., P. Moresco, R. Yan, J. Li, Y. Gao, D. Biasci, M. Yao, J. Pearson, J. F. Hechtman, T. Janowitz, R. M. Zaidi, M. J. Weiss and D. T. Fearon (2022). "Carcinomas assemble a filamentous CXCL12-keratin-19 coating that suppresses T cell-mediated immune attack." Proc Natl Acad Sci U S A 119(4).

Waters, A. M. and C. J. Der (2018). "KRAS: The Critical Driver and Therapeutic Target for Pancreatic Cancer." Cold Spring Harb Perspect Med 8(9).

Wu, C., S. A. Fernandez, T. Criswell, T. A. Chidiac, D. Guttridge, M. Villalona-Calero and T. S. Bekaii-Saab (2013). "Disrupting cytokine signaling in pancreatic cancer: a phase I/II study of etanercept in combination with gemcitabine in patients with advanced disease." Pancreas 42(5): 813-818.

Yamamoto, K., A. Venida, J. Yano, D. E. Biancur, M. Kakiuchi, S. Gupta, A. S. W. Sohn, S. Mukhopadhyay, E. Y. Lin, S. J. Parker, R. S. Banh, J. A. Paulo, K. W. Wen, J. Debnath, G. E. Kim, J. D. Mancias, D. T. Fearon, R. M. Perera and A. C. Kimmelman (2020). "Autophagy promotes immune evasion of pancreatic cancer by degrading MHC-I." Nature 581(7806): 100-105.

Zhao, X., W. Fan, Z. Xu, H. Chen, Y. He, G. Yang, G. Yang, H. Hu, S. Tang, P. Wang, Z. Zhang, P. Xu and M. Yu (2016). "Inhibiting tumor necrosis factor-alpha diminishes desmoplasia and

inflammation to overcome chemoresistance in pancreatic ductal adenocarcinoma." Oncotarget 7(49): 81110-81122.

Methods

All procedures were conducted in compliance with relevant institutional and national ethical guidelines. All animal protocols were approved by the Institute of Animal Care and Use Committee (IACUC) at the Salk Institute.

Cancer cell lines

PDAC1245-parental cell line was derived from a *Kras*$^{LSL\text{-}G12D/+}$; *Trp53*$^{LSL\text{-}R172H/+}$; *Pdx1-Cre* mouse (KPC) mice (C57BL/6J) and was provided by David Tuveson at Cold Spring Harbor Laboratories. GFP-expressing cell line PDAC1245-GFP was derived from single cell clone of PDAC1245-parental transduced with lentivirus expressing GFP. Viral antigen gp33-41 (KAVYNFATC)-expressing cell lines PDAC1245-gp33-12 and PDAC1245-gp33-05 were derived from single cell clones of PDAC1245-parental transduced with retrovirus expressing fusion protein gp33-41-YFP.

Cell culture

All PDAC1245 tumor cell lines and pancreatic stellate cells were cultured in DMEM (Corning, Cat #10-013-CM) with 10% fetal bovine serum (FBS) (Corning, Cat #35-010-CV) and 1% Anti-Anti (Gibco, Cat #15240-062) except specified otherwise. P14 T cells and naïve T cells were cultured in RPMI (Corning, Cat #10-040-CM) with 10% FBS (Fisher Scientific, Cat #SH3039603), 1% Anti-Anti, 1% GlutaMAX (Gibco, Cat #35050-061), 1% sodium pyruvate (Gibco, Cat #11360-070), 1% HEPES (Gibco, Cat #15630-080), 1% non-essential amino acid (NEAA) (Gibco, Cat #11140-050) and 2-Mercaptoethanol (β-ME) (Gibco, Cat #21985-023) except specified otherwise.

Animals

Mice were housed at a temperature (22±1°C) and humidity (45–65%) controlled environment with a 12h light-dark cycle. Wild-type C57BL/6J mice (The Jackson Laboratory, Cat #000664) aged 8-12 weeks were used as hosts of orthotopic transplantation with PDAC1245-parental and PDAC1245-GFP cells. B6.129S7-Rag1tm1Mom/J (Rag1 KO) mice (The Jackson Laboratory, Cat #002216) aged 10-14 weeks were used as hosts of orthotopic transplantation with PDAC1245-gp33 cells, and as donors for P14 CD8 T cell transplantation. P14 Thy1.1+/+ mice were provided by Susan Kaech at the Salk Institute characterized before (Kaech and Ahmed 2001).

Orthotopic transplant of PDAC tumor cells

To prepare the tumor cell-Matrigel suspension for orthotopic injection, PDAC tumor cells grown in 2D culture plate were washed once with DPBS buffer (Corning, Cat #21-031-CM) and were treated with 0.25% trypsin (Gibco, Cat #25200-056) for 5-7min until single cell suspension formed. Equal volume of cell culture media was added to stop digestion, after which cells were harvested, centrifuged (330g 5min) and resuspended in culture media. Cells were counted and diluted to 1×104/ml with culture media, and were then mixed at 1:1 ratio by volume with cold Martigel (Corning, Cat #354230) on ice.

To perform the orthotopic transplantation, 20µl of tumor cell-Matrigel suspension (containing ~100 cells) was injected directly into the pancreatic parenchyma of mouse. About 2-3 weeks after transplantation, mice with successful injections would have a tumor with a diameter of 5-8 mm. They were then randomized and enrolled in therapeutic treatments for 2-3 weeks. In

some mouse studies, tumor volume was measured with ultrasound imaging for better arm enrollment.

Drug preparation and treatment

OTX-015 (MedKoo Bioscience, Cat #206116), JQ1 (Wuxi AppTec) and iBET-762 (Wuxi AppTec) were dissolved in dimethyl sulfoxide (DMSO) (Fisher, Cat #BP231-100) at 125mg/ml as stock solution and was stored at -20°C. To use, stocking solution was diluted 1:10 into corn oil (Sigma, Cat #C8267-500ML) and was administered to mice via oral gavage at 37.5mg/kg, 50mg/kg or 75mg/kg. DMSO dissolved in corn oil was used as Veh control.

αPDL1 (BioXCell, Cat #BE0101) was diluted in sterile saline and was administered to mice via intra intraperitoneal injection at 10mg/kg. Saline was used as Veh control.

αCXCR3 (BioXCell, Cat #BE0249) was diluted in sterile saline and was administered to mice via intra intraperitoneal injection at 10mg/kg. Saline was used as Veh control.

Gemcitabine (Torcis, Cat #3259) was diluted in sterile saline and was administered to mice via intra intraperitoneal injection at 10mg/kg. Saline was used as Veh control.

Celecoxib (MedKoo, Cat #200700) was dissolved in DMSO at 333mg/ml as stock solution and was stored at -20°C. To use, stocking solution was diluted 1:10 into corn oil (Sigma, Cat #C8267-500ML) and was administered to mice via oral gavage at 200mg/kg. DMSO dissolved in corn oil was used as Veh control.

αLIF mAb (synthesized by GenScript, the sequence was provided by Tony Hunter at the Salk Institute) was diluted in sterile saline and was administered to mice via intra intraperitoneal injection at 10mg/kg. Saline was used as Veh control.

αTNFα (BioXCell, Cat #BP0058) was diluted in sterile saline and was administered to mice via intra intraperitoneal injection at 10mg/kg. Saline was used as Veh control.

P14 CD8 T cell activation

Spleen and mesenteric lymph nodes were harvested from P14 Thy1.1+/+ mice aged 8-12 weeks. Tissues were minced, washed with DPBS and filtered through 100μm cell strainers. Flow-through lymphatic cells were centrifuged (400g 5min) and resuspended in 4ml 1×ACK lysis buffer (Miltenyi Biotec, Cat #130-094-183) and incubated at RT for 8min to remove red blood cells. Cells were centrifuged (400g 5min) and resuspended in 5ml T cell culture media. Cells were filtered through a 100μm cell strainer, and were plated in T cell culture media at 0.5M/ml supplied with gp33-41 peptides (provided by Susan Kaech at the Salk Institute) and IL2 (Peprotech, Cat #200-02). After 48h, cells were harvested (400g 5min) and washed once with pure RPMI, then replated in T cell culture media at 0.3M/ml supplied with IL2. After 24h, >95% of alive and proliferating cells in the cell suspension should be activated gp33-specific CD8 T cells. These cells can either be used directly or further purified with CD8 Positive Isolation Kit (Invitrogen, Cat #11333D) for downstream experiments such as *in vitro* tumor cell killing assay or adoptive T cell transfer in Rag1 KO mouse.

***In vitro* tumor cell killing assay**

To collect tumor interstitial fluid (TIF), PDAC1245 tumors were cut into thin slices, put on a 100μm filter, and were spun at 400g for 10min at 4℃. Flowthrough liquid was collected, pulled, and were spun again at 1000g for 5min at 4℃. Supernatant were collected, aliquoted and snap frozen for future use.

For TIF pretreatment of tumor cells, PDAC1245-gp33-12 cells were seeded at 100k/ml concentration in tumor cell culture media supplied with TIF (10%) and were cultured for 2 days. Other reagents added into the culture (specified in each experiment) include: OTX-015 (1μM), αTNFα (5μg/ml) and αLIF (5μg/ml).

For tumor cell-T cell coculture, both PDAC1245-gp33-12 cells and activated P14 CD8 T cells were harvested, washed and resuspended in T cell culture media. 10k PDAC1245-gp33-12 tumor cells and 60k P14 CD8 T cells were seeded in flat-bottom 96 well plate and were cultured for 2 days. Other reagents added into the coculture (specified in each experiment) include: TIF (10%), PGE2 (5μM), Celecoxib (1μM), NS398 (10μM) and αLIF mAb (5μg/ml). The killing efficiency was measured by counting the number of live tumor cells in each well using precision counting beads (BioLegend, Cat #B345814)-based flow cytometry.

Adoptive P14 T cell transfer

Activated P14 CD8 T cells were harvested, washed and resuspended in cold DPBS at 4M/ml. 50μl cell suspension (containing ~0.2M cells) was injected into Rag1 KO mice via retro-orbital injection.

Stromal cell isolation from PDAC tumor

100-300mg of tumor chunk was minced with razor blades on plastics and was transferred into a 50ml conical tube containing 20ml tumor digestion buffer. Components of the digestion buffer include DMEM, collagenase IV (1mg/ml) (Gibco, Cat #17104-019), soybean trypsin inhibitor (1mg/ml) (Gibco, Cat #17075-029), dispase (0.125mg/ml) (Gibco, Cat #17105-041), DNase (50U/ml) (Sigma, Cat #D5025-150KU), and hyaluronidase (600units/ml) (Sigma, Cat

#H3506-5G). Tumor samples were incubated with agitation at 37°C for 1h. After digestion, samples were neutralized with 20ml cold cell culture media, filtered through 100μm cell strainers and were then centrifuged (400g 5min) and resuspended in 1ml FACS buffer (0.5% Bovine serum albumin (BSA, Sigma, Cat #A7030-50G) in DPBS), and kept on ice for downstream assays.

Flow cytometry analysis

To perform fluorescence labeling, cell suspension samples were first blocked with Fc-block (Tonbo, Cat #70-0161-M001) 1:200 diluted in FACS buffer at 4°C for 25min, and were then incubated with surface-staining antibody diluted in FACS buffer at 4°C for 45min. After incubation, samples were washed and resuspended in FACS buffer for surface protein analysis or for Fluorescence-activated Cell Sorting (FACS). If intra-cellular proteins needed to be analyzed, after the last wash with FACS buffer, samples were fixed with fixation buffer (Invitrogen, Cat #00-5523-00) at room temperature (RT) for 40min. Samples were washed once with permeabilization buffer (Invitrogen, Cat #00-5523-00), and were then incubated with intracellular-staining antibody in permeabilization buffer 4°C for 1h (or overnight). After incubation, samples were washed once with permeabilization buffer and were resuspended in FACS buffer for flow cytometry analysis. LSR II or FACSymphony A3 flow cytometers (BD Biosciences) were used for data collection. FlowJo 10 software (BD Biosciences) was used for data analysis.

List of antibodies (anti-mouse): αTim3-BV421 (1:400, BioLegend, Cat #119723), αCD62L-BV605 (1:400, BioLegend, Cat #104438), αCD44-BV711 (1:400, BioLegend, Cat #103057), αPD1-BV785 (1:400, BioLegend, Cat #135225), αPD1-PerCP (1:400, BioLegend, Cat #135208), αCD45.2-Alexa Fluor 700 (1:200, BioLegend, Cat #109822), αLag3-APC (1:200, BioLegend, Cat #125210), αCD8a-APC/Cy7 (1:400, BioLegend, Cat #100714), αCD8a-BV711

(1:400, BioLegend, Cat #100748), αCD8a-BV510 (1:400, BioLegend, Cat #10075), αTCRβ-PE/Cy7 (1:200, BioLegend, Cat #109222), αTCRβ-PE (1:200, BioLegend, Cat #109208), αTCRβ-APC/Cy7 (1:200, BioLegend, Cat #109220), αCD4-BUV395 (1:400, Invitrogen, Cat #363-0042-82), αGranzyme B-Alexa Fluor 647 (1:200, BioLegend, Cat #515406), αKI67-PE/Cy7 (1:400, BioLegend, Cat #652426), αThy1.1-PerCP (1:400, BioLegend, Cat #202516), αVα2-PE (1:400, BioLegend, Cat #127808), αCD69-PE (1:400, BioLegend, Cat #104508).

Fluorescence-activated cell sorting (FACS)

As described previously, cell samples were blocked with Fc-block 1:200 diluted in FACS buffer at 4°C for 25min, and were then centrifuged and incubated with surface-staining antibody diluted in FACS buffer at 4°C for 45min. After staining, cell samples were washed once, resuspended in FACS buffer containing 1/1000 DAPI (BioLegend, Cat #422801) and filtered with 40μm cell strainers (Fisher, Cat #352340) right before loading onto the sorter. Cell sorting was performed on a FACSAria Fusion sorter (BD). Sorted immune cells (DAPI-, CD45+), CAFs (DAPI-, CD45-, Podoplanin+), tumor cells (DAPI-, CD45-, GFP+ or Epcam+), TAMs (DAPI-, CD45+, CD11b+, F4/80+) or CD8+ T cells (DAPI-, CD45+, TCRb+, CD8a+) were either put into cell culture or lysed in Trizol for RNA extraction.

List of antibodies (anti-mouse): αCD45-APC (BioLegend, Cat #109814), αCD45-BV510 (BioLegend, Cat #109838), Epcam-PerCP/Cy5.5 (BioLegend, Cat #118220), Podoplanin-PE/Cy7 (BioLegend, Cat #127408), F4/80-PE/Cy7 (BioLegend, Cat #123114), CD11b-PE (BioLegend, Cat #101208), Ly6G-APC/Cy7 (BioLegend, Cat #108424), Ly6C-PerCP/Cy5.5 (BioLegend, Cat #128012), MHCII-APC (BioLegend, Cat #107614).

Naïve T cell proliferation assay

Spleen and mesenteric lymph nodes were harvested from WT B6J mouse aged 6-8 weeks. Tissues were minced, washed with DPBS and filtered through 100μm cell strainers (Fisher, Cat #352360). Flow-through lymphatic cells were centrifuged (400g 5min) and resuspended in 4ml 1×ACK lysis buffer (Miltenyi Biotec, Cat #130-094-183) and incubated at RT for 8min to remove red blood cells. Cells were then centrifuged (400g 5min) and resuspended in MACS buffer (FACS buffer containing 2mM EDTA, pH=7.3).

To prepare CFSE labeled T cells, Naive CD8a+ T Cell Isolation Kit (Miltenyi Biotec, Cat #130-096-543) and Naïve CD4+ T Cell Isolation Kit (Miltenyi Biotec, Cat #130-104-453) were used to isolate naïve CD8 T cells and naïve CD4 T cells respectively according to manufacturer's protocols. Isolated naïve T cells were centrifuged (400g 5min) and resuspended in 5%FBS-DPBS at RT. CellTrace CFSE dye (Invitrogen, Cat #C34554) was dissolved in DMSO according to manufacturer's protocol, and further diluted in 5%FBS-DPBS to 50μM (10×working solution). To label the cells, 10×CFSE was added into T cell solution during low-speed vortexation to a final concentration of 5μM. Cells were incubated at RT for 5min in dark. Cells were then washed with 10 times volume of 5%FBS-DPBS, centrifuged (400g 5min), resuspended in T cell culture media and counted.

To prepare antigen-presenting cells (APCs), CD90.2 MicroBeads (Miltenyi Biotec, Cat #130-121-278) were used to get rid of pan-T cells from lymphatic cell suspension following manufacturer's protocol. To block proliferation, isolated APCs were centrifuged (400g 5min) and resuspended in pre-warmed RPMI containing 30μg/ml mitomycin C (Fisher, Cat #501632696). Cells were incubated at 37°C for 1h, then centrifuged (400g 5min) and washed with cold RPMI for 3 times. Cells were resuspended in T cell culture media and counted.

To set up the proliferation assay, 50k naïve CD4/8 T cells and 200k APCs were added into round-bottom 96 well plate supplied with 0.5μg/ml αCD3 (BioXCell, Cat #BE0261). 50-200k immunosuppressive cells were added into the coculture. Naïve T cells were let to proliferate for 3 days, after which the suppression efficiency was measured by analyzing the CFSE distribution within in naïve T cell population using flow cytometry.

Mouse PSC isolation

Isolation of PSCs from pancreata of wild-type C57BL/6J mice was carried out with a protocol adapted from previous reports (Apte, Haber et al. 1998). Briefly, pancreatic tissues from mice were incubated in Gey's balanced salt solution (GBSS, Sigma-Aldrich) with 0.05% Collagenase P (Roche), 0.02% Pronase (Roche) and 0.1% DNase I (Roche) at 37 °C with agitation for 20min. Digested tissue was filtered through a 100mm nylon mesh. Cells were subsequently pelleted, washed once with GBSS, and resuspended in 9.5ml GBSS containing 0.3% BSA and 8ml 28.7% Histodenz solution (Sigma) to reach an approximate density of 1.070. The cell suspension was layered beneath GBSS containing 0.3% BSA, and centrifuged at 1400g for 20 min at 4 °C. PSCs were retrieved at the interface of aqueous and Histodenz-containing solution. Harvested PSCs were washed with GBSS and resuspended in cell culture media.

***In vitro* proliferation/viability assay**

To test synergy between OTX-015 and Gemcitabine, PDAC1245-GFP cells were seeded into 384-well plates with 200 cells per well and applied with drugs of gradient concentrations using a D300e digital dispenser (HP). After 2 days of treatment, CellTiter-Glo assay (Promega, Cat # G9681) was performed and luminescent signals measured by an Envision plate reader (Perkin

Elmer). Relative cell numbers were calculated by normalizing luminescence signals from treated wells to untreated controls.

Bulk RNA sequencing

Total RNA from samples was isolated by RNeasy Mini or RNeasy Plus Micro Kit and controlled for quality with a 2100 Bioanalyzer (Agilent) prior to cDNA libraries construction. Libraries were prepared using 100–500 ng total RNA with TruSeq Stranded RNA Sample Preparation Kit (Illumina, v2) according to the manufacturer's protocol. Briefly, mRNA was purified, fragmented, and used for first-, then second-strand cDNA synthesis followed by adenylation of 3' ends. Samples were ligated to unique adapters and subjected to PCR amplification. Libraries were then validated by BioAnalyzer, normalized and pooled for sequencing. High-throughput single-end sequencing was performed on the HiSeq 2500 system (Illumina) with a 100-bp read length. Image analysis and base calling were performed with CASAVA (Illumina, v1.8.2). Short read sequences were mapped to mouse (GRCm38) or human reference genomes (GRCh37) using the RNA-seq aligner STAR (v2.5.1b) (Dobin, Davis et al. 2013). Known splice junctions from mouse (Ensembl) or human (UCSC) genome annotations were supplied to the aligner and de novo junction discovery was also permitted. Differential gene expression analysis and statistical testing were performed using Cuffdiff 2 (v2.2.1) (Trapnell, Hendrickson et al. 2013). Transcript expression was calculated as gene-level relative abundance in fragments per kilobase of exon model per million mapped fragments (FPKM) and employed correction for transcript abundance bias. Hierarchical clustering was carried out using Cluster software (v3.0) and visualized by Java Treeview (v3.0).

Single cell RNA sequencing

scRNA-seq was performed with Chromium single cell kit (10x Genomics, v3), following the manufacturer's instructions. Single cell suspensions prepared by FACS were added to Chromium RT mix to achieve the loading target of 7,000-10,000 cells. High-throughput sequencing was performed at a NovaSeq (Illumina) sequencer. Demultiplexed fastq files from were aligned to mouse reference genome (mm10) using Cell Ranger software (10x Genomics, v4.0) with default settings. The R package Seurat (v3) was used to detect cell clusters based on gene expression and to identify subpopulation-enriched markers (Stuart, Butler et al. 2019). Cells detected with lower than 500 and higher than 6,500 genes and those with mitochondrial genes higher than 15% were excluded from the analysis. For data normalization, a scale factor of 10,000 was used. Canonical correlation analysis (CCA) was performed to remove batch effects. Cell clustering was performed with 0.6 resolution and results visualized by UMAPs. Contamination cell clusters expressing well established tissuespecific markers other than those for fibroblasts were validated by bioinformatic tools (e.g., scMRMA, Enrichr) and excluded. scRNA-seq for each cell type from each treatment condition were performed with 3 biological replicates. Trajectory inference was performed with the Slingshot package (Street, Risso et al. 2018).

Quantitative reverse-transcription polymerase chain reaction (qPCR)

Total RNA (50–100 ng) was used for cDNA synthesis with iScript reagent (Bio-Rad, Cat #1708840). qPCR was performed using a CFX384 detection system (Bio-Rad) by mixing cDNAs, gene-specific primers and SsoAdvanced SYBR Green reagent (Bio-Rad, Cat #1725272). Expression was analyzed using Bio-Rad CFX Maestro 2.3 software (Bio-Rad) with normalization to B2m, Rplp0 or Gapdh expression.

Primer sequence list:

Cxcl9-F: 5’-TCCTTTTGGGCATCATCTTCC-3’

Cxcl9-R: 5’-TTTGTAGTGGATCGTGCCTCG-3’

Cxcl10-F: 5’-CCAAGTGCTGCCGTCATTTTC-3’

Cxcl10-R: 5’-GGCTCGCAGGGATGATTTCAA-3’

Rplp0-F: 5’-AGATTCGGGATATGCTGTTGGC-3’

Rplp0-R: 5’-TCGGGTCCTAGACCAGTGTTC-3’

Il6-F: 5’-TAGTCCTTCCTACCCCAATTTCC-3’

Il6-R: 5’-TTGGTCCTTAGCCACTCCTTC-3’

Il1β-F: 5’-GCAACTGTTCCTGAACTCAACT-3’

Il1β-R: 5’-ATCTTTTGGGGTCCGTCAACT-3’

Gapdh-F: 5’-AATGGTGAAGGTCGGTGTG-3’

Gapdh-R: 5’-GTGGAGTCATACTGGAACATGTAG-3’

Cox2-F: 5’-GCGACATACTCAAGCAGGAGCA-3’

Cox2-R: 5’-AGTGGTAACCGCTCAGGTGTTG-3’

Lif-F: 5’-TCAACTGGCACAGCTCAATGGC-3’

Lif-R: 5’-GGAAGTCTGTCATGTTAGGCGC-3’

B2m-F: 5’-ACAGTTCCACCCGCCTCACATT-3’

B2m-R: 5’-TAGAAAGACCAGTCCTTGCTGAAG-3’

Histology analysis

Whole pancreatic tumor specimens isolated from mouse were fixed by immersing in 10% buffered formalin overnight at 4°C. Samples were sequentially dehydrated with 30%, 50% and 70%

ethanol, and were sent to UCSD histology core for paraffin embedding and sectioning (5μM). For standard histology analysis, section slides were stained with hematoxylin and eosin (H&E) and Sirius Red (SR) according to standard protocols.

For immunohistochemistry (IHC), section slides were first dewaxed in Clear-Rite 3 (Fisher Scientific, Cat #6915SS) and rehydrated with gradient ethanol solution. Slides were then processed with a pressure cooker for 15min in citric acid-based antigen retrieval buffer (Vector, Cat #H-3300) prior to staining. After antigen retrieval, slides were washed with DPBS and were incubated with 0.6% H2O2 (Sigma, Cat #H1009-100ML) in methanol (Fisher, Cat #A412-4) for 20min to block endogenous peroxidase activity. After washing, slides were blocked with 2.5% goat serum blocking buffer (Vector, Cat #MP-7404-50) at RT for 1h. Slides were then incubated with αCD8a (Invitrogen, Cat #14-0195-82) primary antibody diluted 1:50 in blocking buffer at 4°C overnight. In the next day, slides were washed and incubated with HRP-conjugated goat anti-rat secondary antibody (Vector, Cat #MP-7404-50) at RT for 30min. After washing, slides were incubated with DAB solution (Sigma, Cat #D3939) for 3-5min. Slides were then washed and counterstained with Nuclear Fast Red (Vector, Cat #H-3403) for 10min. After this, slides were washed and dehydrated with gradient ethanol solution and Clear-Rite 3. Lastly, slides were mounted with VectaMount (Vector, Cat #H-5000) and scanned with VS-120 virtual slide system (Olympus). Quantifications on the whole tumor sections or representative fields were performed with OlyVIA software.

ELISA

Intra-tumoral CXCL9 and CXCL10 cytokine levels were measured with corresponding cytokine Elisa Kits (Abcam, Cat #ab203364 for CXCL9 and Cat #ab214563 for CXCL10) according to manufacturer's protocol.

Cyanine5.5-labeled polymer for biodistribution studies

Cyanine5.5-labeled polymer was dissolved in DPBS at 25 mg/ml. C57BL/6J mice bearing PDAC1245-parental tumor was injected with 200µl of polymer and wait for 1 day, after which tissues were harvested and imaged on IVIS for Cy5.5 fluorescence.

Reference

Apte, M. V., P. S. Haber, T. L. Applegate, I. D. Norton, G. W. McCaughan, M. A. Korsten, R. C. Pirola and J. S. Wilson (1998). "Periacinar stellate shaped cells in rat pancreas: identification, isolation, and culture." Gut 43(1): 128-133.

Dobin, A., C. A. Davis, F. Schlesinger, J. Drenkow, C. Zaleski, S. Jha, P. Batut, M. Chaisson and T. R. Gingeras (2013). "STAR: ultrafast universal RNA-seq aligner." Bioinformatics 29(1): 15-21.

Kaech, S. M. and R. Ahmed (2001). "Memory CD8+ T cell differentiation: initial antigen encounter triggers a developmental program in naive cells." Nat Immunol 2(5): 415-422.

Street, K., D. Risso, R. B. Fletcher, D. Das, J. Ngai, N. Yosef, E. Purdom and S. Dudoit (2018). "Slingshot: cell lineage and pseudotime inference for single-cell transcriptomics." BMC Genomics 19(1): 477.

Stuart, T., A. Butler, P. Hoffman, C. Hafemeister, E. Papalexi, W. M. Mauck, 3rd, Y. Hao, M. Stoeckius, P. Smibert and R. Satija (2019). "Comprehensive Integration of Single-Cell Data." Cell 177(7): 1888-1902 e1821.

Trapnell, C., D. G. Hendrickson, M. Sauvageau, L. Goff, J. L. Rinn and L. Pachter (2013). "Differential analysis of gene regulation at transcript resolution with RNA-seq." Nat Biotechnol 31(1): 46-53.